ORIGINAL ARTICLES

DEVELOPMENT OF THE TECHNOLOGY FOR OBTAINING PLGA AND DIPROPOXYBATERIOPURPURINIMIDE-BASED NANOPARTICLES. EVALUATION OF PHYSICOCHEMICAL AND BIOLOGICAL PROPERTIES OF THE OBTAINED DELIVERY SYSTEM

Sapelnikov M.D.[1], Nikolskaya E.D.[2], Morozova N.B.[3], Plotnikova E.A.[3], Efremenko A.V.[4, 5], Panov A.V.[1, 6], Grin M.A.[1], Yakubovskaya R.I.[3]
[1]Federal State Budget Educational Institution of Higher Education "MIREA – Moscow Technological University", Moscow, Russia
[2]Russian research center for molecular diagnostics and therapy (RCMDT), Moscow, Russia
[3]P.A. Herzen Moscow Oncology Research Center – branch of FSBI NMRRC of the Ministry of Health of Russia, Moscow, Russia
[4]Shemyakin & Ovchinnikov Institute of Bioorganic Chemistry of the Russian Academy of Sciences, Moscow, Russia
[5]Lomonosov Moscow State University, Moscow, Russia
[6]ZAO "Institute of pharmaceutical technologies", Moscow, Russia

Abstract

The article describes the process of developing a technology for producing nanoparticles based on a copolymer of lactic and glycolic acids (PLGA) containing dipropoxybacteriopurpurinimide (DPBPI) for photodynamic therapy of malignant tumors of various origins. Technological parameters for optimizing the method in order to obtain nanoparticles with specified characteristics are presented in this paper. As a result, the nanoparticles sample with an average particle diameter of 222.6±2.8 nm; ξ-potential 26.3±4.61 mV; polydispersity index 0.144; the total content of DPBPI in PLGA-DPBPI nanoparticles 13.6% were obtained. In accordance with the developed technique, the batch of PLGA-DPBPI nanoparticles was developed for further biological studies. In vitro experiments on A549 human non-small cell lung carcinoma for DPBPI, delivered as a part of PLGA-DPBPI nanoparticles, and an EL cremophor-based emulsion (CrEL-DPBPI) showed a similar intracellular distribution (concentrated in vesicular cell structures and diffusely distributed in cytoplasm), as well as high photo induced activity and the absence of dark cytotoxicity in case of PLGA-DPBPI nanoparticles. The study of the PLGA-DPBPI nanoparticles specific activity in vivo on the S37 mouse soft tissue sarcoma model showed the selective accumulation of DPBPI in tumor tissue and the almost complete elimination of DPBPI from the body within 48 hours, as well as significant antitumor efficacy in PDT.

Keywords: photodynamic therapy, nanoparticles, PLGA, photosensitizer, photoinduced activity, photoinduced antitumor efficacy, dipropoxybacteriopurpurinimide.

For citations: Sapelnikov M.D., Nikolskaya E.D., Morozova N.B., Plotnikova E.A., Efremenko A.V., Panov A.V., Grin M.A., Yakubovskaya R.I. Development of the technology for obtaining PLGA and dipropoxybateriopurpurinimide-based nanoparticles. Evaluation of physicochemical and biological properties of the obtained delivery system, *Biomedical Photonics*, 2019, vol. 8, no. 1, pp. 4–17. (in Russian) doi: 10.24931/2413–9432–2019–8–1-4–17.

Contacts: Sapelnikov M.D., e-mail: maxsapelnikov@gmail.com

РАЗРАБОТКА ТЕХНОЛОГИИ ПОЛУЧЕНИЯ НАНОЧАСТИЦ НА ОСНОВЕ PLGA И ДИПРОПОКСИБАКТЕРИОПУРПУРИНИМИДА. ОЦЕНКА ФИЗИКО-ХИМИЧЕСКИХ И БИОЛОГИЧЕСКИХ СВОЙСТВ ПОЛУЧЕННОЙ СИСТЕМЫ ДОСТАВКИ

М.Д. Сапельников[1], Е.Д. Никольская[2], Н.Б. Морозова[3], Е.А. Плотникова[3], А.В. Ефременко[4,5], А.В. Панов[1,6], М.А. Грин[1], Р.И. Якубовская[3]
[1]МИРЭА – Российский технологический университет, Москва, Россия

[2]Всероссийский научный центр молекулярной диагностики и лечения (ВНЦМДЛ), Москва, Россия
[3]МНИОИ им. П.А. Герцена – филиал ФГБУ «НМИЦ радиологии» Минздрава России, Москва, Россия
[4]Институт биоорганической химии им. академиков М. М. Шемякина и Ю. А. Овчинникова Российской академии наук, Москва, Россия
[5]МГУ им. М.В. Ломоносова, Москва, Россия
[6]ЗАО «Институт фармацевтических технологий», Москва, Россия

Резюме

В статье описан процесс разработки технологии получения наночастиц на основе сополимера молочной и гликолевой кислот (PLGA), включающих дипропоксибактериопурпуринимид (DPBPI) и предназначенных для фотодинамической терапии (ФДТ) злокачественных новообразований различного генеза. В работе подобраны технологические параметры, позволяющие оптимизировать метод получения наночастиц с заданными характеристиками, в результате был получен образец сферических частиц, обладающая средним диаметром частиц 222,6±2,8 нм; ξ-потенциалом –26,3±4,61 мВ; индексом полидисперсности 0,144; общее содержание DPBPI в частицах PLGA-DPBPI составило 13,6%. В соответствии с разработанной методикой была осуществлена наработка партии наночастиц PLGA-DPBPI для дальнейших биологических исследований. В экспериментах *in vitro* на клетках немелкоклеточной карциномы легкого человека A549 для DPBPI, доставленного в клетки с помощью наночастиц PLGA-DPBPI, и эмульсии на основе кремофора EL (CrEL-DPBPI) было показано сходное внутриклеточное распределение (концентрирование в везикулярных клеточных структурах и диффузное распределение в цитоплазме), а также была показана высокая фотоиндуцированная активность и отсутствие темновой цитотоксичности в случае использования частиц PLGA-DPBPI. Изучение специфической активности наночастиц PLGA-DPBPI *in vivo* на модели саркомы мягких тканей мыши S37 показало селективное накопление DPBPI в опухолевой ткани и практически полное выведение DPBPI из организма в течение 48 ч, а также выраженную противоопухолевую эффективность при ФДТ.

Ключевые слова: фотодинамическая терапия, наночастицы, PLGA, фотосенсибилизатор, фотоиндуцированная активность, фотоиндуцированная противоопухолевая эффективность, дипропоксибактериопурпуринимид.

Для цитирования: Сапельников М.Д., Никольская Е.Д., Морозова Н.Б., Плотникова Е.А., Ефременко А.В., Панов А.В., Грин М.А., Якубовская Р.И. Разработка технологии получения наночастиц на основе PLGA и дипропоксибактериопурпуринимида. Оценка физико-химических и биологических свойств полученной системы доставки // Biomedical Photonics – 2019. – Т. 8, № 1. – С. 4–17. doi: 10.24931/2413–9432–2019–8–1–4-17.

Контакты: Сапельников М.Д., e-mail: maxsapelnikov@gmail.com

Introduction

Today, one of the topical areas of research is the development and production of new dosage forms (DF) of hydrophobic substances with high pharmacological activity. One of the promising DFs used for these purposes is nanoparticles based on biodegradable copolymers of lactic and glycolic acids (PLGA). This form makes it possible to influence the processes of drugs delivery and deposition in the target organs and tissues [1, 2]. Particles with an average diameter of about 200 nm both effectively accumulate in organs and tissues with malignant tumors and are internalized by tumor cells [1]. The use of PLGA with a terminal carboxyl group and a 50:50 ratio of monomer units allows to obtain particles with a smaller diameter compared to other ratios of lactic and glycolic acid monomers, this effect is due to its physicochemical properties [3].

One of the groups of new compounds in which the use of the above DF is relevant is photosensitizers (PS) used for photodynamic therapy (PDT) of oncological diseases. Of particular interest are bacteriochlorins with their intense absorption in the near IR region of the spectrum, since their therapeutic absorption window (750–850 nm) expands the possibilities for diagnosing and treating malignant neoplasms by penetrating into tissues to a depth of 20–25 mm and makes it possible to apply the currently used methods for the treatment of larger and/or deeper tumors.

For most bacteriochlorins, common shortcomings can be identified that limit their use in clinical practice [2]:

- low solubility in water, which leads to the limitation of the dose administered;
- insufficient level of selectivity and accumulation of drugs in tumor tissues and, as a consequence, a decrease in the efficiency of PDT;
- short circulation time and low level of PS accumulation in target organs and target tissues.

Thus, when obtaining new forms for this group of substances, it is important to take into account the above disadvantages and to select the optimal delivery system

to overcome them and increase the effectiveness of the PDT method.

The idea of therapeutic use of PLGA-based nanoparticles containing dipropoxybacteriopurupurinimide (DPBPI) implies selective delivery and time-controlled release of the photoactive substance into the tumor tissue, thereby reducing the non-specific toxicity of the drug, as well as its antitumor efficacy. In addition, this DF can be stored for a long period of time and can be quickly and easily produced in its consumer form.

Materials and methods

The development of technology for producing PLGA-DPBPI nanoparticles

Materials used

The DPBPI sample used for the research was produced at the Department of Chemistry and Technology of Biologically Active Compounds, Medical and Organic Chemistry named after N.A. Preobrazhensky at the Russian University of Technology. The structural formula of DPBPI is shown in Fig. 1. The concentration of DPBPI in nanoparticle samples and cremophor-based emulsions was determined spectrophotometrically at the long-wavelength absorption maximum (λ = 802 nm) with the use of a molar extinction coefficient of 30,000 l/(mol-cm) [4].

Method for producing PLGA-DPBPI nanoparticles

3.0 mg of DPBPI and 50.0 mg of PLGA-COOH were dissolved in 2.0 ml of methylene chloride (viscosity: 0.17 dl/g in hexafluoroisopropanol, LACTEL® (Absorbable Polymers, USA)) with magnetic stirring for 15 minutes. The resulting solution was added dropwise to 10.0 ml of a 1% aqueous solution of polyvinyl alcohol (PVA) in a 150 ml Drexel bottle and stirred with Variomag Multipoint magnetic stirrer (Variomag, USA) at a speed of 1120 rpm with a 9*32 mm magnet for 10 min, with the stopper closed. Then the emulsion was subjected to treatment with an IKA Ultra Turrax T25 homogenizer (IKA, Germany) (25,000 rpm, 3 times for 1 min at 1 min intervals). The organic solvent was removed from the resulting emulsion on a rotary evaporator (LABOROTA 4000-EFFICIENT (Heidolph, Germany)) at a vacuum of 0.9–1.0 kgf/m^2 and a water bath temperature of 35°C until the complete removal of the organic solvent. Then the suspension was centrifuged at 14000 rpm for 30 min at +4°C in order to separate the excess amount of PVA. The supernatant liquid was decanted, and the precipitate containing the nanoparticles was suspended in 2 ml of distilled water. The sediment in the form of a suspension was subjected to ultrasonication (Transsonic T420 (Transsonic, USA)) for 1 min, then the cryoprotectant was added (D-mannitol, 5.0 mg) and lyophilised for 24 h, with subsequent freezing in a freezer (-20°C) and freezer unit (-70°C). The obtained particles were stored at +4°C in a place without exposure to light.

In accordance with this method, PLGA-DPBPI nanoparticles were produced for further biological studies.

The determination of dimensions and ξ-potential of PLGA-DPBPI nanoparticles

The particle size was determined by dynamic light scattering, and ξ-potential was found by electrophoretic

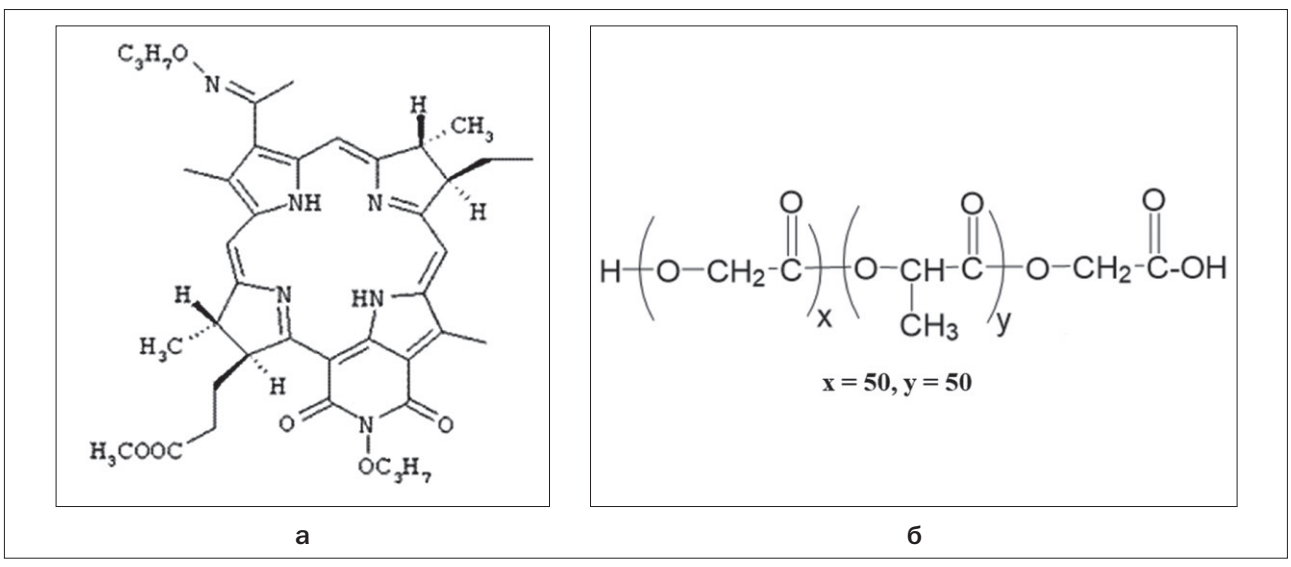

Рис. 1. Химические структуры:
а. Дипропоксибактериопурпуринимид (DPBPI);
б. Сополимер молочной и гликолевой кислот (PLGA-COOH 50/50)
Fig. 1. The chemical structures of:
a. Dipropoxybacteriopurpurinimide (DPBPI);
б. Copolymer of lactic and glycolic acids (PLGA-COOH 50/50)

method. The tested sample of PLGA-DPBPI nanoparticles was used to prepare an aqueous suspension with a concentration of 1 mg/ml. The measurements were performed with Zetasizer Nano ZS ZEN 3600 analyzer (Malvern Instruments, UK) under a standardized protocol (SOP).

The determination of water content in the lyophilisate of PLGA-DPBPI nanoparticles with K. Fisher method (semi-micromethod)

A test sample of the PLGA-DPBPI nanoparticles lyophilisate in an amount of 20.0 to 100.0 mg (exact sample weight) is placed in a titrator vessel (Metrohm 852 KF Titrando, Switzerland), and 5.0 ml of methyl alcohol is added. Titration is performed with a titrating solution (Fisher's reagent). Fisher's reagent is a solution of sulfur dioxide, iodine and pyridine in methanol. The instrument automatically sets the time of 10 seconds for the dissolving (or suspending) of the sample. Water content is determined with due account for the titer values. At least two parallel measurements were taken. The end of the titration was determined potentiometrically.The water content *X* (%) was calculated by formula 1:

$$X = [(a - b) \times T \times 100] / c, \quad (1)$$

where *a* is the volume of Fisher reagent consumed for titration in the main experiment, ml; *b* is the amount of Fisher reagent consumed for titration in the control experiment, ml; (c) the weight of the nanoparticles, g; T - Fisher reagent titer, g/ml.

The determination of total DPBPI content and its degree of incorporation into PLGA-DPBPI nanoparticles by a spectrophotometric method

A precise sample weight (4.0 mg) of the PLGA-DPBPI nanoparticle lyophilisate was dissolved in 5 ml of chloroform. The Helios α spectrophotometer (Thermo Electron, USA) was used to record the electronic absorption spectra of the solution obtained in the wavelength range of 200–1000 nm. The concentration of DPBPI was determined from the values of the absorption intensity of the solution at a wavelength of 802 nm. The calculation of the total DPBPI content in a sample of nanoparticles (m_{DPBPI}, mg) was carried out as follows.

According to formula 2, the molar concentration of DPBPI (in mol/l) in chloroform solution was calculated:

$$C_m = D_{802} / K, \quad (2)$$

where D_{802} is the optical density of the sample solution at a wavelength of 802 nm, *K* is the molar extinction coefficient of the substance, equal to 30,000 l/(mol · cm).

Then, taking into account the known molecular mass of DPBPI (696.84 g/mol), the mass concentration of DPBPI (in g/l) in the resulting solution was calculated under formula 3:

$$C = C_m \times M_{DPBPI}, \quad (3)$$

where C_m is the molar concentration of the substance in the solution, mol/l; M_{DPBPI} is the molar mass of the substance, g/mol.

With formula 4, the mass of DPBPI (mg) in chloroform solution was calculated.

$$m_{DPBPI} = C \times V, \quad (4)$$

where *C* is the mass concentration of the substance, mg/ml; *V* is the volume of chloroform solution, ml.

The total content of DPBPI (W_{DPBPI}, mg / g) in the resulting batch of particles (m_{NP}, mg) was determined by formula 5.

$$W_{DPBPI} = (m_{DPBPI} / m_{NP}) \times 1000, \quad (5)$$

where m_{DPBPI} is the mass of DPBPI in a solution of chloroform, mg, m_{NP} is the mass of the studied sample of PLGA-DPBPI nanoparticles, mg.

The number of included DPBPI or the degree of its inclusion (S, wt. %) in the nanoparticles was determined by formula 6.

$$S = (m_{DPBPI} / m_{loaded}) \times 100\%, \quad (6)$$

where m_{DPBPI} is the mass of DPBPI in chloroform solution, m_{loaded} is the mass of DPBPI initially loaded to produce nanoparticles.

The analysis of the morphology of PLGA-DPBPI nanoparticles by scanning electron microscopy

The tested sample of PLGA-DPBPI nanoparticles was used to prepare an aqueous suspension with a concentration of 1 mg/ml, which was applied with a microdosing device onto a double-sided adhesive carbon tape. It was left to dry for about 20 minutes. Images of the samples were obtained with JSM-7401F transmission electron microscope (JEOL, Japan).

The analysis of the morphology of PLGA-DPBPI nanoparticles by transmission electron microscopy

To carry out this analysis, 5–10 µl of an aqueous suspension of the studied samples of nanoparticles with a concentration of 1 mg/ml were applied onto freshly ionized carbon-form films, after 2 min the excess liquid was removed with filter paper and the preparations were contrasted with 1% aqueous uranyl acetate solution. The preparations were analyzed with an electron microscope (JEOL 100CX, Japan) at an accelerating voltage of 80 kV. The negatives (magnification of 20,000–50000 times) were scanned with a resolution of 1200 dpi (dots per inch).

In vitro studies

Materials used

The biological model used for *in vitro* experiments was non-small cell lung human carcinoma cells of the

A549 human line. Cell cultivation was performed in DMEM medium (PanEco, Russia) with the addition of 10% fetal bovine serum (Hyclone, Thermo Fisher Scientific, USA) and 2 mM glutamine (PanEco, Russia) at 37°C in 5% CO^2 atmosphere , hereinafter referred to as the complete medium. The cells were re-seeded twice a week. The viability of the cells used in the experiments was at least 95%.

Sample preparation for in vitro experiments

The nanoparticles loaded with DPBPI (PLGA-DPBPI) were suspended in 50 mM Na-phosphate buffer (pH 7.4) to achieve a concentration of 0.3 mM for the active substance, thus obtaining a suspension (test sample). The positive control was produced by trituration of dry DPBPI powder in polyethoxylated castor oil, Cremophor EL (CrEL), with further ultrasound treatment in a sonication bath for 20 minutes and subsequent dilution with 50 mM Na-phosphate buffer (pH 7.4) to 10% CrEL. DPBPI concentration in the composition of Cremophor EL emulsion (CrEL-DPBPI) was 0.6 mM. In the experiments, a freshly prepared suspension of PLGA-DPBPI and an emulsion of CrEL-DPBPI were used.

The study of the accumulation of PLGA-DPBPI in cells of human non-small cell lung carcinoma A549

To assess the intracellular internalization of PLGA-DPBPI and CrEL-DPBPI, cells of the A549 line, upon reaching the logarithmic growth phase, were seeded on coverslips in 24-well plates (concentration 7.5×10^4 cells/well) and incubated for 24 hours at + 37°C 5% atmosphere of CO^2 to achieve confluency of 70%. The cells were incubated for 2 h with the test sample and positive control at concentrations of 4 and 8 μM. The intracellular distribution (visualized by DPBPI fluorescence) was studied with LSM710META laser scanning confocal microscope (LSCM) (Zeiss, Germany). All confocal fluorescent images were obtained with an oil-immersion x63 lens (C-Apochromat, numerical aperture 1.46). The lateral resolution was 0.3 μm, and the axial resolution was 1.5 μm. The fluorescence of the samples was excited with a helium-neon laser (543 nm). For fluorescence registration, APD detection with a long-wavelength barrier filter with a 655 nm limit was used. The resulting images were processed with ImageJ application.

The study of photo-induced cytotoxicity pf PLGA-DPBPI in vitro

To study the photoinduced cytotoxicity of the PLGA-DPBPI sample, A549 cells were seeded into 96-well flat-bottom plates (seeding density was $2.0 \cdot 10^4$, $1.2 \cdot 10^4$ and $0.7 \cdot 10^4$ cells/well). The studied samples were introduced into the wells after 24 h with a range of concentrations of samples from 14.0 μM to 0.010 μM, obtained by two-fold dilution. The dark cytotoxicity of PLGADPBPI particles was evaluated 72 hours after the sample was introduced to A549 cells with the density of $0.7 \cdot 10^4$ cells/well. For CrEL-DPBPI, the assessment of dark cytotoxicity was carried out in a similar way after 5 and 8 hours.

Photoinduced cytotoxicity of the samples at different A549 cell seeding densities was evaluated after incubating the cells with the samples in complete medium in the tested concentration ranges for 2 h, followed by irradiation for 15 min with a 500 W halogen lamp through a 5 cm water filter and a broadband filter (the transmittance was 680–1000 nm, the light dose was 13.5 J/cm^2).

To evaluate the photoinduced cytotoxicity of the samples under study as dependant on the light irradiation dose, cells with a density of $0.7 \cdot 10^4$ cells/well were incubated with the samples in complete medium for 2 h, then they were washed three times with DMEM medium without serum, fresh complete medium was added to the cells, and they were irradiated with a 500 W halogen lamp through a 5 cm thick water filter and a broadband filter (transmission 680–1000 nm) for 15 (13.5 J/cm^2), 30 (27.0 J/cm^2) or 45 (40.5 J/cm^2) minutes.

After irradiation, cells were incubated under standard conditions for 3 hours, and then stained with Hoechst 33342 (Sigma-Aldrich, USA) and propidium iodide (PI) (Sigma-Aldrich, USA). Hoechst 33342 (4 μM) and PI (6 μM) were added to the cells 15 minutes before the completion of incubation. The result of photodynamic exposure was analyzed with epi-fluorescence microscopy with the use of an Axio Observer fluorescence microscope (Zeiss, Germany). Stained cells were placed in a tablet on an object table of an inverted microscope and fluorescent images of Hoechst 33342 luminescence (λ_{exc} 359–371 nm, λ_{reg}> 397 nm) and PI (λ_{exc} 530–585 nm, λ_{reg}> 615 nm) in cells were recorded with the use of a digital camera. The resulting images were processed in ImageJ application, and the total number of cells and the number of dead cells were obtained for each sample. In each sample, 300–400 cells were subjected to calculation. According to the measurement results, a graph of the dependence of the percentage of surviving cells versus sample concentration was plotted. For the comparison of the photoinduced cytotoxicity of the samples, LC_{50} and LC_{90} values were calculated, which corresponded to the concentrations of PLGA-DPBPI and CrEL-DPBPI, by active substance, at which 50% and 90% cell death is observed, respectively.

In vivo studies

Materials used

For *in vivo* experiments, the first generation (F1) hybrid mice were used (CBA x C57Bl/6J), females (7–9 weeks old, body weight: 18–22 g) supplied by Andreevka laboratory animals breeding center of FSBRI NTsBMT of FMBA of Russia. The animals were kept in separate rooms, under controlled environmental conditions. For

the experiments, mice were inoculated with tumor cells of mouse soft tissue sarcoma, S37 line, with $1 \cdot 10^6$ cells subcutaneously in the region of the sural muscle on the outer side of the thigh. Strain S37 was maintained in ascites form in male mice of the ICR (CD-1) line. Studies were performed on day 7 after tumor inoculation, when its volume reached 130–160 mm^3.

All manipulations were carried out in accordance with national and international rules on humane treatment of animals [5, 6].

Sample preparation for in vivo experiments

To assess the distribution of PS in nanoparticles in organs and tissues of mice, as well as to study photoinduced antitumor activity, a PLGA-DPBPI sample with an active substance content of 13.6 mg/g was used. To obtain a consumer form, a weighted sample was added to a 0.9% sodium chloride solution to produce a stable pink suspension.

Assessment of the distribution of PLGA-DPBPI in animal tissues and organs

A study of the biodistribution of DPBPI, which is part of PLGA-DPBPI nanoparticles (7.5 mg/kg dose by DPBPI, intravenous administration), was carried out ex vivo in mice with developed tumor with the use of local fluorescence spectroscopy. Fluorescence was recorded by contact method on LESA laser spectral analyzer for fluorescent diagnosis of tumors (OOO "Biospec", Russia).

The objects of study were tumor tissue, skin and muscle, liver, kidneys, spleen, omentum and blood obtained from three animals for each observation interval (0.25, 2, 4, 24, and 48 hours). When fluorescence was excited in the red region of the spectrum (632.8 nm), the integrated fluorescence intensity in the spectral range of measurements (640–900 nm) was normalized by the integrated intensity of the back diffuse scattering of exciting laser radiation signal in the tissue, determining the normalized fluorescence (FN) in the tissues. The accumulation of PLGA-DPBPI in tissues was assessed by the maximum values of FN at a wavelength corresponding to the maximum fluorescence of DPBPI. During the study, the fluorescent contrast (FC) was calculated as the ratio of PN in the tumor to PN in the skin.

The study of the efficiency of photodynamic therapy with the use of PLGA-DPBPI nanoparticles

Photodynamic therapy was performed remotely on the seventh day of tumor growth of S37 sarcoma in mice with injected PLGA-DPBPI particles at a dose of 2.5 mg/kg with the active component of DPBPI. The control animals were injected isotonic 0.9% sodium chloride solution intravenously. Droperidol (solution for injections, 2.5 mg/ml, FSUE Moscow Endocrine Plant, Russia) was used as anesthesia at a dose of 0.25 mg/mouse intraperitoneally. By the time of PDT, the volume of tumors varied from 130 to 160 mm^3. For irradiation, a LED source with a wavelength of 810 ± 21 nm was used (FSUE SSC NIOPIK, Russia): power density of 100 mW/cm^2 and energy density of 150 J/cm^2. The interval between the introduction of PS and the irradiation was 2 hours. The animals that did not have continued tumor growth were observed for 90 days after treatment. The antitumor effect was evaluated according to the average values of the tumor volume, the inhibition of tumor growth, the increase in life expectancy and the recovery criterion in the control and experimental groups [7]. The tumor volume (in mm^3) was calculated by formula 7,

$$V = a \times b \times c, \quad (7)$$

where *a* is the length, *b* is the width and *c* is the height of the tumor nodule.

Statistic analysis

The statistical processing of results was performed with Student's t-test. The construction of graphs and statistical processing was done with OriginPro 8 SRO (OriginLab Corporation, USA), Excel (Microsoft) and Statistica 8 (StatSoft) software.

Results and discussion

The development of technology for PLGA-DPBPI nanoparticles production and their physico-chemical properties

Particles containing DPBPI were produced by single emulsions method [2]. As part of the development of the technology, the optimal polymer composition was determined: the concentration of surfactant and the ratio of the organic phase to the aqueous phase (O/A). The parameters of the technological process of obtaining particles and their characteristics are presented in Table 1. Within the framework of the development, technological parameters were also selected, such as the type of homogenization (with the use of an immersion homogenizer or with ultrasound (US)), the method of removing organic solvent (diffusion or vacuum), the time of centrifuging the particles suspension.

As can be seen from Table 1, an increase in PVA concentration leads to an increase in the average particle size and polydispersity index (PDI) (samples 3, 9). The reduction of PVA concentration, on the contrary, leads to the reduction of the average particle size (samples 4, 10), but results in particles with a lower content of DPBPI due to an increase in the total sample mass of PLGA-DPBPI nanoparticles, and, therefore, 1% PVA was chosen, as it made it possible to obtain particles of smaller diameter without a visible decrease in the total content of the chemical. The most optimal O/W ratio is 1: 5, since a decrease in the ratio to 1: 2.5 led to a sharp increase in size and an increase in the polydispersity of the system

(sample 6), while an increase in the ratio to 1:10 (sample 5) did not contribute to a significant decrease in size, but reduced the total content of DPBPI in the particles. The use of an ultrasonic homogenizer contributed to a slight increase in particle size (sample 8), however, the degree of inclusion of the drug was much lower, and, therefore, the use of a submersible homogenizer was the most relevant. Solvent was removed from all particles with the use of vacuum, since the use of diffusion at atmospheric pressure resulted in broad size distribution peaks of the particles and the formation of a polydisperse system (sample 1). An increase in the time of particle suspension centrifuging from 15 to 30 min, in its turn, also made it possible to reduce the average particle size in a sample with a simultaneous decrease in PDI, which suggests that the optimal conditions for obtaining particles with the given characteristics have been found.

As a result, the optimal parameters of the method of obtaining particles PLGA-DPBPI (sample 7) were selected, making it possible to produce particles with improved physicochemical characteristics, such as the maximum values of the total substance content and the degree of sorption, monodisperse particle size distribution (PDI below 0.250), the average particle diameter of less than 250 nm, which was the reason for their selection for further experiments. The water content in the resulting PLGA-DPBPI nanoparticle lyophilisate (sample 7) was determined to be no more than 1.5%, and this value was taken into account in all the calculations. The total DPBPI content values obtained are given for anhydrous substance.

The particle size and their spherical shape were confirmed with the use of transmission electron microscopy and scanning electron microscopy (Fig. 2).

In this way, further experiments on the study of the efficiency of internalization of the particles obtained by

Таблица 1
Влияние технологических параметров на основные физико-химические характеристики полученных частиц PLGA-DPBPI

Table 1
The influence of technological parameters on the major physico-chemical characteristics of the obtained PLGA-DPBPI NPs

№ образца PLGA-DPBPI PLGA-DPBPI sample №	ПВС, % PVA, %	О/В O/W	Удаление растворителя Evaporation of organic solvent	Тип гомогенизатора Homogenizer type	t, мин t, min	W_{DPBPI}, мг/г W_{BPP}, mg/g	S, % масс. S, % w.	Средний диаметр, нм Mean diameter, nm	ξ-потенциал, мВ ξ-potential, mV	ПДИ PDI
1	1	1:5	Диффузия Diffusion	Погружной гомогенизатор Immersion homogenizer	15	9,6	28,7	485,1±2,3	–23,8±4,09	0,392
2	1	1:5	Вакуум Vacuum		15	9,5	26,3	490,1±3,0	–24,6±2,87	0,230
3	2	1:5			15	13,4	35,1	761,3±4,5	–27,4±2,65	0,354
4	0,5	1:5			15	10,2	46,8	540,8±2,4	–20,1±3,42	0,325
5	1	1:10			15	8,1	72,6	523,2±2,2	–17,2±3,21	0,263
6	1	1:2.5			15	10,4	63,4	834,3±1,7	–14,4±2.86	0,368
7	**1**	**1:5**			**30**	**13,6**	**86,1**	**222,6±2,8**	**–26,3±4,61**	**0,144**
8	1	1:5		УЗ-гомогенизатор US-homogenizer	30	16,9	36,4	261,5±3,2	–23,2±3,92	0,205
9	2	1:5		Погружной гомо-гениза-тор Immersion homogenizer	30	15,6	25,2	340,2±2,4	–20,3±2,47	0,356
10	0.5	1:5			30	12,4	30,3	245,1±3,6	–19,2±4,06	0,232

О/В – соотношение органической фазы к водной; t – время центрифугирования
ПДИ – индекс полидисперсности
O/W – ratio of organic phase to water; t– centrifugation time
PDI – polydispersity index

tumor cells and their photodynamic activity in *in vitro* and *in vivo* models were performed with the use of PLGA-DPBPI-7.

Biological properties of PLGA-DPBPI. In vitro studies

Study of the accumulation of PLGA-DPBPI in A549 lung adenocarcinoma cells

With the use of laser scanning confocal microscopy (LSCM), it was found that DPBPI in the PLGA-DPBPI particles accumulates in the cytoplasmic region of A549 cells. At the same time, DPBPI concentration is observed in vesicular cell structures of submicron size, as well as diffuse staining of the cytoplasm (Fig. 3 II). Partial co-localization of nanoparticles with lipid droplets is observed (Fig. 3 ж, з), which is characteristic of cycloimide derivatives of bacteriochlorin p [8].

Since DPBPI has hydrophobic properties, in the control group, Cremophor EL (CrEL) was chosen as a solubilizer, which is able to stabilize non-aggregated forms of tetrapyrrole compounds in aqueous solutions and is not toxic to cells *in vitro* at low concentrations [8–10]. It is important to note that CrEL is used in clinical practice [11].

By the use of LSCM method, it was discovered that the cells incubated with CrEL-DPBPI have an intracellular distribution of DPBPI similar to that of nanoparticles. (Fig.3 I). Thus, the inclusion of DPBPI in the composition of nanoparticles does not block its penetration into cells and does not affect the nature of the intracellular distribution of DPBPI.

PLGA-DPBPI photoinduced cytotoxicity study

In experiments on the study of the cytotoxicity of PLGA-DPBPI, it was found that the PLGADPBPI sample did not show toxicity to A549 cells at high concentrations and long incubation times (more than 8 hours), whereas the use of DPBPI, which is part of CrEL-DPBPI (positive control), was limited by CrEL cytotoxicity. The maximum indicators for its use are no more than 5 hours with a concentration not higher than 14 μM (Fig. 4).

In the study of photoinduced cytotoxicity, it was shown that PLGA-DPBPI particles cause concentration-dependent death of A549 cells (Fig. 5). At different cell seeding densities ($0.7 \cdot 10^4$ cells/well; $2 \cdot 10^4$ cells/well, Fig. 5a), the ratio of the parameters LC_{50} and LC_{90} (the concentrations causing the death of 50% and 90% of the cells, Table 2) of PLGA-DPBPI to CrELDPBPI remains the same, at 1.6±0.1 (Table.3). An increase in the light dose leads to an increase in the photodynamic activity of both forms of DPBPI (Fig. 5, Table. 2). The washing of A549 cells after 2 hours of incubation with PLGA-DPBPI or CrEL-DPBPI before irradiation did not lead to a decrease in the photodynamic effect (Fig. 5b). Consequently, photoinduced cell death occurs due to the activation of the intracellular concentration of PLGA-DPBPI or the positive control (Fig. 5, Table 2). The photodynamic effect of PLGA-DPBPI can be limited by the rate of intracellular release of the active substance from nanoparticles, and, therefore, the photoinduced cytotoxicity of compounds was studied at different irradiation times. The samples were preliminarily removed from the cell medium (the cells were washed after 2 h of incubation with the samples). An increase in the irradiation time and, consequently, the light dose of irradiation led to an increase in the photodynamic effect for both PLGA-DPBPI and CrEL-DPBPI (Fig. 5b, Table 2). The ratio of LC_{50} and LC_{90} parameters of PLGA-DPBPI to CrEL-DPBPI varies within the range of 1.6÷2.4 (table 3).

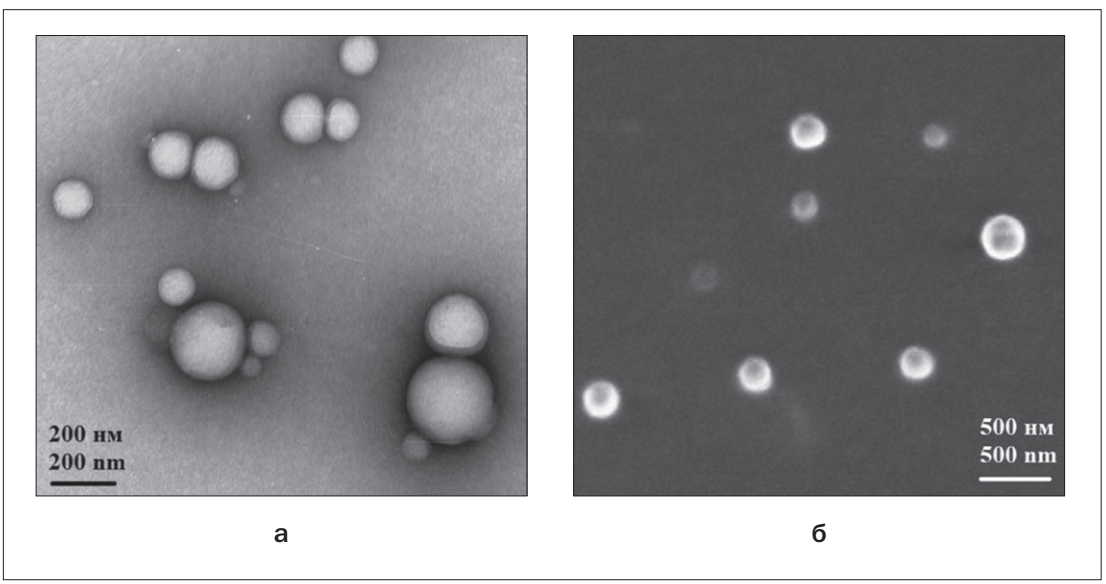

Рис. 2. Микрофотографии частиц PLGA-DPBPI, полученных методом просвечивающей электронной микроскопии (*а*) и сканирующей электронной микроскопии (*б*)
Fig. 2. TEM (*а*) and SEM (*б*) microphotographs of PLGA-DPBPI NPs

At the same time, a twofold increase in the dose (and a twofold increase in the exposure time) resulted in the decrease in LC_{50} by 2.53 times for positive control and 1.75 times for PLGA-DPBPI. A further x1.5 increase in dose (irradiation time) reduced the LC_{50} by a factor of 1.49 for a positive control, whereas in the sample under study the LC_{50} value decreased by a factor of 1.7.

Thus, the use of DPBPI in the composition of PLGA-DPBPI nanoparticles contributes to the accumulation of DPBPI in the cytoplasm of A549 tumor cells and causes photo-induced cytotoxicity, which is confirmed by the preservation of the photodynamic properties of DPBPI after its inclusion into the composition of the polymeric form.

With increasing exposure time and light dose, the photo-induced cytotoxicity of PLGA-DPBPI increases linearly, whereas CrELDPBPI tends to decrease.

Biological properties of PLGA-DPBPI. In vivo studies

Distribution of PLGA-DPBPI in animal tissues and organs

The analyzis of the fluorescence spectra obtained ex vivo after intravenous administration of DPBPI to mice showed that the maximum fluorescence for the dye in the organs and tissues of animals was recorded at 817±3 nm.

The studied PLGA-DPBPI nanoparticle preparation, when administered intravenously, entered the tumor tissue S37 relatively quickly, with the FN level reaching a maximum value 2 hours after the injection, at the level of 7.1±1.1 relative units (table 4). After 48 h, the mean FN level in the tumor was 9.8% of the maximum recorded value.

In normal skin, the maximum accumulation of DPBPI was determined in the time interval from 0.25 to 2 h after intravenous administration of the dye (the FN value was 2.6±0.3 - 3.5±0.3 relative units), and after 24 hours DPBPI was no longer determined. The maximum value of FC relative to the skin was recorded in the time interval from 2 to 4 h after the dye injection and amounted to 2.7–3.0 relative units.

Therefore, with PDT, irradiation has to be performed 2 hours after the introduction of PLGA-DPBPI nanoparticles, when the accumulation in the tumor and the fluorescent contrast reach their maximum value.

DPBPI was determined in the bloodstream within 24 hours after its administration. Low values of normalized fluorescence (4.3±0.4 relative units and 4.8±0.6 relative

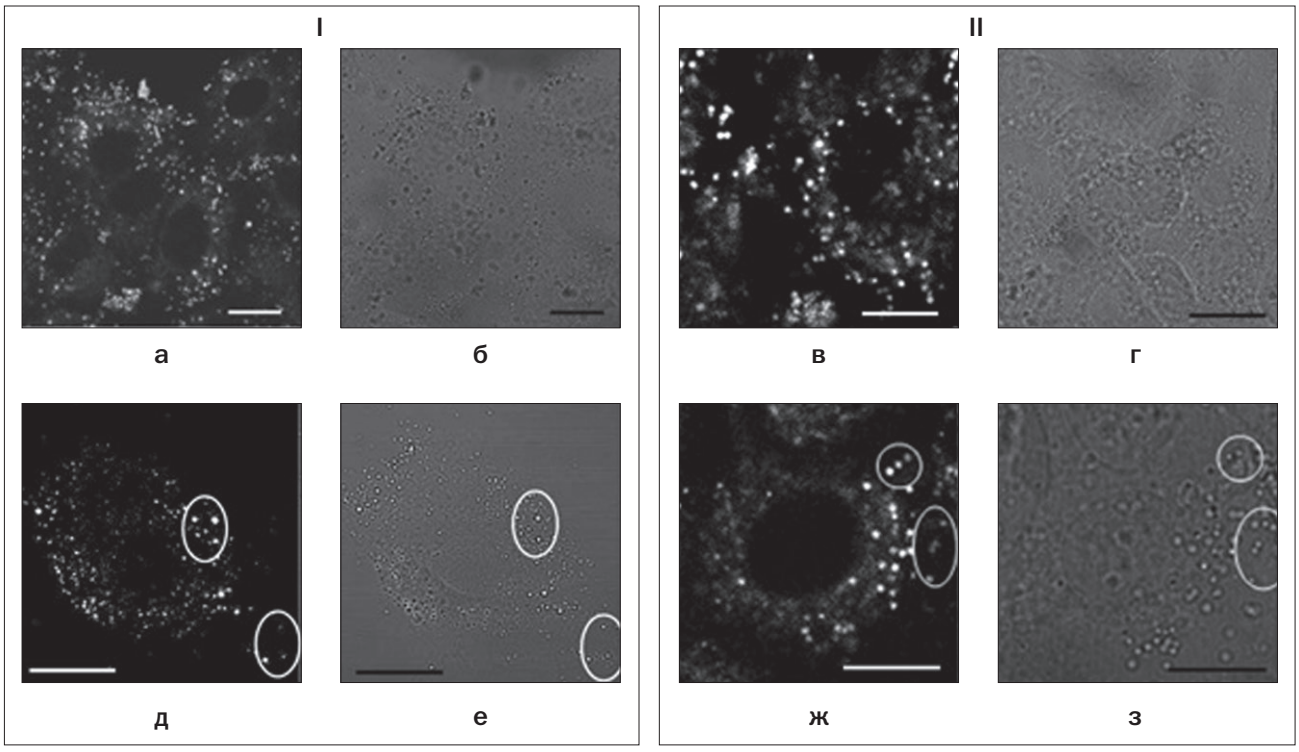

Рис. 3. Типичное внутриклеточное распределение DPBPI, входящего в состав CrEL-DPBPI (I) и PLGA-DPBPI (II), в клетках немелкоклеточной карциномы легкого человека линии A549, полученные методом ЛСКМ *(а, в, д, ж)* и в проходящем белом свете *(б, г, е, з)* после инкубации клеток с образцами в концентрации 4 мкМ в течение 2-х ч. На изображениях *д-з* показана со-локализация DPBPI с липидными каплями (области обведены овалами). Масштаб соответствует 15 мкм

Fig. 3. Typical intracellular distribution of DPBPI in CrEL-DPBPI (I) and PLGA-DPBPI (II) complexes inside A549 human non-small lung cancer cells. Images were obtained by LSCM *(а, в, д, ж)* and in transmitted white light *(б, г, е, з)* after incubation of cells with samples at the concentration of 4 μm for 2 h. The co-localization of DPBPI with lipid drops (the areas are circled ovals) is shown in the images *д-з*. Scale bar is equal to 15 μm

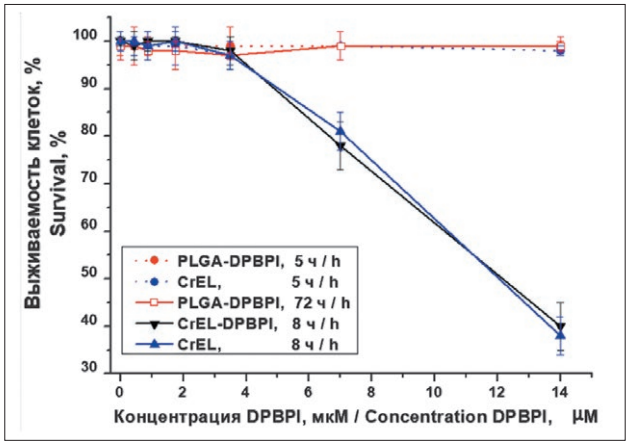

Рис. 4. Выживаемость клеток немелкоклеточной карциномы легкого человека линии A549 от концентрации PLGA-DPBPI, CrEL-DPBPI и CrEL при различном времени инкубации при изучении темновой цитотоксичности
Fig. 4. Survival of non-small cell lung carcinoma cells of the A549 line from the concentration of PLGA-DPBPI, CrEL-DPBPI and CrEL at different times of incubation in the study of dark cytotoxicity

units, respectively) were recorded in the muscle tissue and omentum, which decreased by 71.4% and 83.3% of the maximum recorded value, respectively. After 48 h, FN measured in the skin and in the omentum was at the background level. In the main internal organs, the maximum accumulation of DPBPI was registered in the liver and spleen 15 minutes after the administration, with FN of 31.3 ± 1.4 relative units and 25.9 ± 1.8 relative units, respectively. 24 hours after the intravenous administration of the dye, the level of normalized fluorescence in the liver and spleen decreased by 88.5% and 89.7% of the maximum value, respectively, and after 48 hours only background values were observed. In the kidneys, the maximum values of the normalized fluorescence of DPBPI were recorded 2 h after injection (12.0±0.2 relative units), and after 48 h the kidney fluorescence was found to be at the background level. The data obtained indicate rapid elimination of the photosensitizer from the body of mice and the predominant removal of the chemical through the excretory system of the liver.

Photo-induced antitumor activity of PLGA-DPBPI in mice with S37 sarcoma

Upon the performance of PDT with PLGA-DPBPI, the irradiated animals with S37 sarcoma developed an edema within 2 hours, which persisted for 4 days. No lethality of animals from phototoxic shock after a PDT session was observed.

The data presented in Fig. 6 and 7 show that the photosensitizer has an antitumor effect. With the use of PLGA-DPBPI at a dose of 2.5 mg/kg (by active substance) and a two hour interval between irradiation and administration, the average tumor volume in the experimental group increased slowly relative to the tumor volume in the control group, the tumor growth inhibition (TGI) on day 22 after the PDT session being 71%. The maximum TGI value was 78% on day 11. For 90 days, 33% of the mice did not demonstrate continued tumor growth.

Thus, the effect of PDT on the S37 transplanted tumor with the use of PLGA-DPBPI made it possible to achieve a pronounced antitumor effect in this experiment (life expectancy increase: 83%, recovery coefficient: 33%).

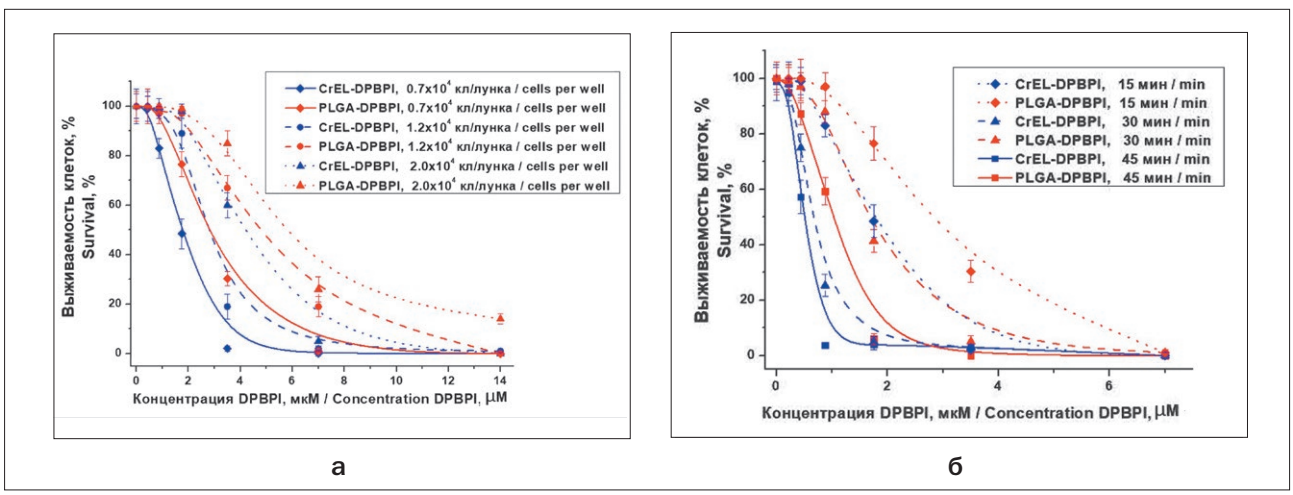

Рис. 5. Выживаемость клеток немелкоклеточной карциномы легкого человека линии A549 от концентрации CrEL-DPBPI и PLGA-DPBPI при изучении фотоиндуцированной цитотоксичности, где (*а*) – после 2 ч инкубации и облучения галогенной лампой в течение 15 мин (13,5 Дж/см^2) при различной плотности клеток; (*б*) – после 2 ч инкубации, отмывки клеток от соединений во внешней среде и облучения галогенной лампой в течение различного времени облучения. Плотность клеток 0,7·10^4 кл/лунка
Fig. 5. Survival of non-small cell lung carcinoma cells of the A549 line from the concentration of CrEL-DPBPI and PLGA-DPBPI in the study of photoinduced cytotoxicity. (*a*) – after 2 hours of incubation and irradiation with a halogen lamp for 15 minutes (13.5 J/cm^2) at different cell densities; (*б*) – after 2 hours of incubation, washing cells from compounds in the environment and irradiation with a halogen lamp for various irradiation times. The density of cells was 0.7·10^4 cells/well

Таблица 2
Значения LC_{90} и LC_{50} для CrEL-DPBPI и PLGA-DPBPI при различной концентрации клеток (облучение галогенной лампой в течение 15 мин, 13,5 Дж/см^2) и времени облучения (плотность клеток 0,7·10^4 кл/лунка, с проведением отмывки)

Table 2
The values of LC_{90} and LC_{50} for CrEL-DPBPI and PLGA-DPBPI at various cells concentrations (halogen lamp exposure for 15 minutes (13.5 J/cm^2)) and irradiation time (cell density of 0.7·10^4 cells / well, with washing)

Концентрация клеток, кл/лунку Cells concentration, cells/well	LC_{90}, мкМ LC_{90}, μM		LC_{50}, мкМ LC_{50}, μM	
	PLGA-DPBPI	CrEL-DPBPI	PLGA-DPBPI	CrEL-DPBPI
0,7·10^4	4,7±0,1	2,9±0,1	2,8±0,1	1,7±0,1
1,2·10^4	8,0±0,1	3,9±0,1	4,7±0,1	2,8±0,1
2·10^4	8,5±0,1	5,3±0,1	5,6±0,1	3,7±0,1
Время облучения, мин (световая доза, Дж/см^2) Exposure time, min (light dose, J/cm^2)	LC_{90}, мкМ LC_{90}, μM		LC_{50}, мкМ LC_{50}, μM	
	PLGA-DPBPI	CrEL-DPBPI	PLGA-DPBPI	CrEL-DPBPI
15 (13,5)	4,7±0,1	2,9±0,1	2,8±0,1	1,7±0,1
30 (27)	2,5±0,1	1,1±0,05	1,6±0,1	0,67±0,05
45 (40,5)	1,6±0,1	0,67±0,05	0,96±0,05	0,45±0,03

Таблица 3
Отношения $(LC_{90})_2/(LC_{90})_1$* и $(LC_{50})_2/(LC_{50})_1$* для CrEL-DPBPI (1) и PLGA-DPBPI (2) при различной концентрации клеток (облучение галогенной лампой в течение 15 мин (13,5Дж/см^2)) и времени облучения (плотность клеток 0,7·10^4 кл/лунка, с проведением отмывки)

Table 3
$(LC_{90})_2/(LC_{90})_1$* and $(LC_{50})_2/(LC_{50})_1$* rates for CrEL-DPBPI (1) and PLGA-DPBPI (2) at various cell concentrations (halogen lamp exposure for 15 minutes (13.5 J/cm^2)) and irradiation time (cell density of 0,7·10^4 cells / well, with washing)

Концентрация клеток, кл/лунка Cells concentration, cells/well	$(LC_{90})_2/(LC_{90})_1$	$(LC_{50})_2/(LC_{50})_1$
0,7·10^4	1,62	1,65
1,2·10^4	2,05	1,68
2,0·10^4	1,60	1,51
Время облучения, мин (световая доза, Дж/см^2) Exposure time, min (light dose, J/cm^2)	$(LC_{90})_2/(LC_{90})_1$	$(LC_{50})_2/(LC_{50})_1$
15 (13,5)	1,62	1,65
30 (27)	2,27	2,39
45 (40,5)	2,39	2,13

*(1) – CrEL-DPBPI; (2) – PLGA-DPBPI

Таблица 4
Интенсивность нормированной флуоресценции DPBPI в органах и тканях мышей с саркомой S37 после введения наночастиц PLGA-DPBPI в дозе 7,5 мг/кг

Table 4
The intensity of the normalized fluorescence of DPBPI in organs and tissues of mice with S37 sarcoma after administration of PLGA-DPBPI polymer particles at a dose of 7.5 mg / kg

Органы и ткани Organs and tissues	Контроль* (Фон) Control* (Background)	Нормированная флуоресценция (ФН), отн. ед. Normalized fluorescence (FN), rel.units				
		Сроки измерения нормированной флуоресценции после введения образца, ч The timing of the measurement of normalized fluorescence after the introduction of the sample, h				
		0,25	2	4	24	48
Опухоль Tumor	3,0±0,2	4,5±0,4	7,1±1,1	5,4±0,7	3,9±0,1	3,4±0,1
Кожа Skin	1,5±0,1	3,5±0,3	2,6±0,3	1,8±0,2	1,6±0,1	1,6±0,1
Мышца Muscle	2,7±0,1	4,1±0,5	4,3±0,4	3,9±0,3	3,1±0,4	2,8±0,1
Сальник Adipose tissue	3,0±0,3	4,2±0,2	4,8±0,6	3,2±0,2	3,2±0,2	3,1±0,1
Печень Liver	7,8±0,2	31,2±1,4	23,4±1,0	18,3±0,1	10,5±0,3	8,6±0,6
Почки Kidneys	7,6±0,2	10,8±0,2	12,0±0,2	9,8±1,2	8,3±0,1	7,8±0,2
Селезенка Spleen	9,4±0,3	25,9±1,8	20,7±1,0	17,0±0,9	11,1±0,6	10,2±0,5
Кровь Blood	4,0±0,5	22,3±0,2	7,7±0,1	6,1±0,1	4,2±0,1	3,9±0,1
ФК** FC**	-	1,3	2,7	3,0	2,4	2,1

*Контроль – мыши без воздействия (фон);
**ФК (флуоресцентная контрастность) = $ФН_{опухоль}$ / $ФН_{кожа}$
*Control – mice without exposure (background);
**FK (fluorescent contrast) = FN_{tumor} / FN_{skin}, rel. units.

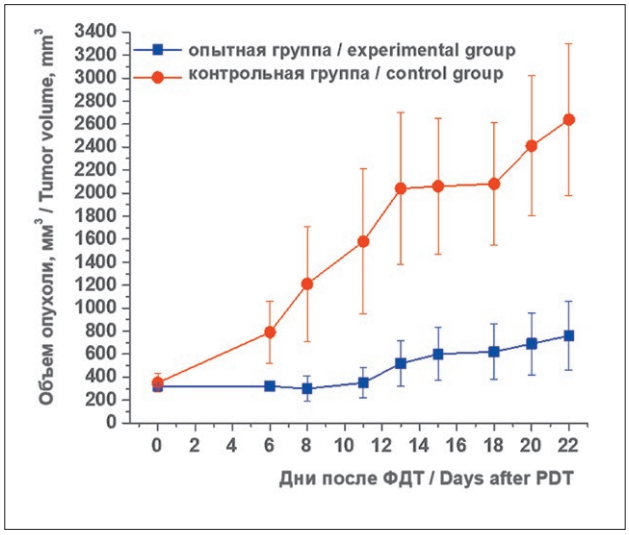

Рис. 6. Объем опухоли S37 у мышей после проведения ФДТ (150 Дж/см², время экспозиции 2 ч) после введения PLGA-DPBPI (в дозе 2,5 мг/кг) в контрольной и опытной группах
Fig. 6. S37 tumor volume in mice after PDT (150 J/cm², exposure time 2 h) after administration of PLGA-DPBPI (at a dose of 2.5 mg/kg) in the control and experimental groups

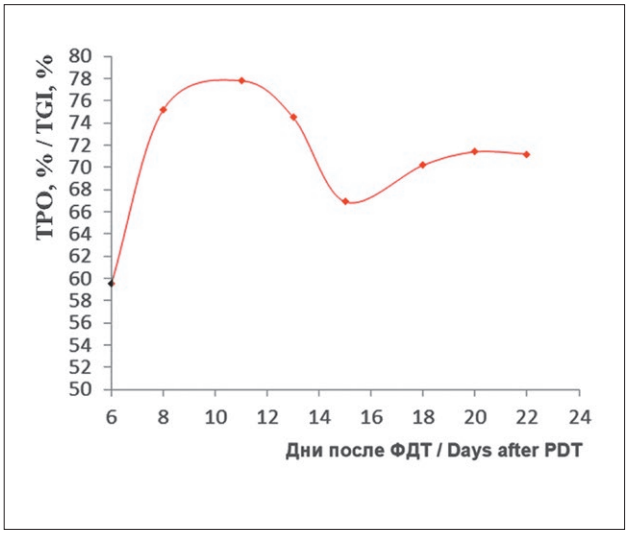

Рис. 7. Торможение роста опухоли (TPO, %) на 6–22 сут после проведения ФДТ (150 Дж/см², время экспозиции 2 ч) с использованием PLGA-DPBPI (в дозе 2,5 мг/кг)
Fig. 7. Inhibition of tumor growth (TGI, %) on days 6–22 after PDT (150 J/cm², exposure time 2 hours) using PLGA-DPBPI (2.5 mg/kg)

Conclusion

The authors developed a technology for producing PLGA-based nanoparticles containing DPBPI and possessing optimal physicochemical characteristics, such as average particle size, ξ-potential value, the degree of inclusion and the substance content in particles. *In vitro* experiments recorded intracellular accumulation and distribution of DPBPI in the composition of PLGA-DPBPI particles in A549 cells, the nature of which coincided with the distribution of DPBPI in the control composition (CrEL-DPBPI). It was shown that high concentrations of the particles and long incubation times do not lead to dark cytotoxicity. The antitumor efficacy of PLGA-DPBPI particles was comparable to the effect of CrEL-DPBPI, which is confirmed by the preservation of the photo-induced DPBPI activity after its incorporation into the polymer matrix. *In vivo* experiments showed accumulation of particles in tumor tissue with PC of up to 3.0 relative units, as well as the almost complete elimination of DPBPI from the body after 48 h. For skin, this value was 24 hours, which is important given the specific nature of the photodynamic therapy procedure. A photoinduced antitumor activity of the use of PLGA-DPBPI was also shown when performing PDT on the S37 soft tissue sarcoma model, with the cure rate of the animals reaching 33%. The data produced make it possible to conclude that the further study of PLGA-DPBPI particles may produce valuable results.

REFERENCES

1. Rejman J., Oberle V., Zuhorn I.S., Hoekstra D. Size-dependent internalization of particles via the pathways of clathrinand caveolae-mediated endocytosis, *Biochem. J.*, 2004, no. 377, pp. 159–169.
2. Sapelnikov M.D., Panov A.V., Nikolskaya E.D., Grin M.A. Development of delivery systems for highly effective photosensitizers applicable for photodynamic therapy of cancer, *Biopharmatsevticheskiy jurnal*, 2018, vol. 10, no 1, pp. 14–25. (in Russian)
3. Nikolskaya E., Sokol M., Faustova M., Zhunina O., Mollaev M., Yabbarov N., Tereshchenko O., Popov R., Severin E. The comparative study of influenceof lactic and glycolic acids copolymers type on propertiesof daunorubicin loaded nanoparticles and drug release, *Acta of Bioeng. and Biomech.*, 2018, vol. 20, no. 1, pp. 65–77.
4. Pantyushenko I.V., Grin M.A., Yakubovskaya R.I., Plotnikova E.A., Morozova N.B., Tsygankov A.A., Mironov A.F. A novel highly effective IR photosensitizer in the bacteriochlorophyll A series for photodynamic therapy of cancer, *Vestnik MITHT*, 2014, vol. 9, no. 3, pp. 3–10. (in Russian)
5. *Prilozhenie A k Evropeyskoy konventsii ob ohrane pozvonochnyh zhivotnyh, ispol'zuemyh dlya eksperimentov i v drugih nauchnyh tselyah (ETS 123)* [Appendix A of the European convention for the protection of vertebrate animals used for experimental and other scientific purposes (ETS No. 123)], 13 p. Available at: https://rm.coe.int/168007a6a8 (accessed 26.02.2019)
6. *Rukovodstvo po soderzhaniyu i uhodu za laboratornymi zhivotnymi (stat'ya №5 konventsii)* [Guidelines for the maintenance and care of laboratory animals (Article 5 of the Convention)], transl. by Krasilnischikova M.S., Belozertseva I.V. Saint-Petersburg, 2014. 102 p. Available at: http://ruslasa.ru/wp-content/uploads/2017/06/Приложение-А-к-ETS.pdf (accessed 26.02.2019)
7. Yakubovskaya R.I., Kazachkina N.I., Karmakova T.A., et al. *Methodical recommendations on the study of photoinduced antitumor properties of drugs*. In: Guide to conducting preclinical studies of medicines. Edited by A.N. Mironov. Moscow, Grif & Ko Publ., 2012, pp. 657–71. (in Russian)
8. Feofanov A., Grichine A., Karmakova T., Plyutinskaya A., Lebedeva V., Filyasova A., Yakubovskaya R., Mironov A., Egret-Charlier M., Vigny P. Near-infrared photosensitizer based on a cycloimide derivative of chlorin p6: 13,15-N-(3′-hydroxypropyl)cycloimide chlorin p6, *Photochem. Photobiol.*, 2002, no. 75, pp. 633–643.
9. Nazarova A., Ignatova A., Feofanov A., Karmakova T., Pljutinskaya A., Mass O., Grin M., Yakubovskaya R., Mironov A., Maurizot J-C. 13,15-N-cycloimide derivatives of chlorin p6 with isonicotinyl substituent are photosensitizers targeted to lysosomes, *Photochem. Photobiol. Sci.*, 2007, no. 6, pp. 1184–1196.

ЛИТЕРАТУРА

1. Rejman J., Oberle V., Zuhorn I.S., Hoekstra D. Size-dependent internalization of particles via the pathways of clathrinand caveolae-mediated endocytosis // Biochem. J. – 2004. – No. 377. – P. 159–169.
2. Сапельников М.Д., Панов А.В., Никольская Е.Д., Грин М.А. Разработка систем доставки высокоэффективных фотосенсибилизаторов для фотодинамической терапии рака // Биофармацевтический Журнал – 2018. – Т. 10, № 1. – С. 14–25.
3. Nikolskaya E., Sokol M., Faustova M., et al. The comparative study of influenceof lactic and glycolic acids copolymers type on propertiesof daunorubicin loaded nanoparticles and drug release // Acta of Bioeng. and Biomech. – 2018. – Vol. 20, No. 1. – P. 65–77.
4. Пантюшенко И.В., Грин М.А., Якубовская Р.И. и др. Новый высокоэффективный ИК-фотосенсибилизатор в ряду бактериохлорофилла А для фотодинамической терапии рака // Вестник МИТХТ. – 2014. – Т. 9, № 3. – С. 3–10.
5. Приложение А к Европейской конвенции об охране позвоночных животных, используемых для экспериментов и в других научных целях (ETS 123). – 13 с. Адрес доступа: https://rm.coe.int/168007a6a8 (дата обращения 26.02.2019)
6. Руководство по содержанию и уходу за лабораторными животными (статья №5 конвенции) / пер. с англ. М.С. Красильщиковой и И.В. Белозерцевой. – Санкт-Петербург, 2014. – 102 с. Адрес доступа: http://ruslasa.ru/wp-content/uploads/2017/06/Приложение-А-к-ETS.pdf (дата обращения 26.02.2019)
7. Якубовская Р.И., Казачкина Н.И., Кармакова Т.А. и др. Методические рекомендации по изучению фотоиндуцированных противоопухолевых свойств лекарственных средств // Руководство по проведению доклинических исследований лекарственных средств. Под ред. А.Н. Миронова и др. – М.: Гриф и К, 2012. – С. 657–71.
8. Feofanov A., Grichine A., Karmakova T., Pljutinskaya A., Lebedeva V., Filyasova A., Yakubovskaya R., Mironov A., Egret-Charlier M., Vigny P. Near-infrared photosensitizer based on a cycloimide derivative of chlorin p6: 13,15-N-(3′-hydroxypropyl)cycloimide chlorin p6 // Photochem. Photobiol. – 2002. – No. 75. – P. 633–643.
9. Nazarova A., Ignatova A., Feofanov A., et al. 13,15-N-cycloimide derivatives of chlorin p6 with isonicotinyl substituent are photosensitizers targeted to lysosomes // Photochem. Photobiol. Sci. – 2007. – No. 6. – P. 1184–1196.
10. Efremenko A.V., Ignatova A.A., Borsheva A.A., et al. Cobalt bis(dicarbollide) versus closo-dodecaborate in boronated chlorin e6 conjugates: implications for photodynamic and boron-neutron capture therapy // Photochem. Photobiol. Sci. – 2012. – Vol. 11, No. 4. – P. 645–652.

10. Efremenko A.V., Ignatova A.A., Borsheva A.A., Grin M.A., Bregadze V.I., Sivaev I.B., Mironov A.F., Feofanov A.V. Cobalt bis(dicarbollide) versus closo-dodecaborate in boronated chlorin e6 conjugates: implications for photodynamic and boron-neutron capture therapy, *Photochem. Photobiol. Sci.*, 2012, vol. 11, no. 4, pp. 645–652.
11. Loi S., Rischin D., Michael M., Yuen K., Stokes K.H., Ellis A.G., Millward M.J., Webster L.K. A randomized cross-over trial to determine the effect of Cremophor EL on the pharmacodynamics and pharmacokinetics of carboplatin chemotherapy, *Cancer Chemother. Pharmacol.*, 2004, vol. 54, no. 5, pp. 407–414.

11. Loi S., Rischin D., Michael M., et al. A randomized cross-over trial to determine the effect of Cremophor EL on the pharmacodynamics and pharmacokinetics of carboplatin chemotherapy // Cancer Chemother. Pharmacol. – 2004. – Vol. 54, No. 5. – P. 407–414.

ORIGINAL ARTICLES

SOLUBILIZATION OF HYDROPHOBIC BACTERIOCHLORIN–BASED PHOTOSENSITIZER IN MICELLES OF SURFACTANTS

Plotnikova E.A.[1], Stramova V.O.[1], Morozova N.B.[1], Plyutinskaya A.D.[1], Ostroverkhov P.V.[2], Grin M.A.[2], Mironov A.F.[2], Yakubovskaya R I.[1], Kaprin A.D.[1]
[1]P.A. Herzen Moscow Oncology Research Center – branch of FSBI NMRRC of the Ministry of Health of Russia, Moscow, Russia
[2]Federal State Budget Educational Institution of Higher Education "MIREA – Moscow Technological University", Moscow, Russia

Abstract

The aim of the paper was to obtain a stable micellar emulsion of potent photosensitizer (PS) – *O*-propyloxime-*N*-propoxybacteriopurpurinimide methyl ester absorbing light in long-wave region of the spectrum (λ_{max} = 800±2 нм). Solubilizates of the dye based on different surfactants (Kolliphor ELP, Poloxamer 407, Emuxol 268) were obtained. Taking into account the physical and chemical parameters, the most potent micellar emulsion for injection was selected and characterized. The emulsion based on Kolliphor ELP remains stable for 4 months, with no changes in the fluorescence spectrum and absorption, as well as the particle diameter.

Keywords: photosensitizer, photodynamic therapy, bacteriochlorin, solubilizer, emulsion.

For citations: Plotnikova E.A., Stramova V.O., Morozova N.B., Plyutinskaya A.D., Ostroverkhov P.V., Grin M.A., Mironov A.F., Yakubovskaya R.I., Kaprin A.D. Solubilization of hydrophobic bacteriochlorin–based photosensitizers in micelles of surfactants, *Biomedical Photonics,* 2019, vol. 8, no. 1, pp. 18–23. (in Russian) doi: 10.24931/2413–9432–2019–8–1-18–23.

Contacts: Plotnikova E.A., e-mail: plotnikovaekaterina62@gmail.com

СОЛЮБИЛИЗАЦИЯ ГИДРОФОБНОГО ФОТОСЕНСИБИЛИЗАТОРА БАКТЕРИОХЛОРИНОВОГО РЯДА В МИЦЕЛЛАХ ПОВЕРХНОСТНО-АКТИВНЫХ ВЕЩЕСТВ

Е.А. Плотникова[1], В.О. Страмова[1], Н.Б. Морозова[1], А.Д. Плютинская[1], П.В. Островерхов[2], М.А. Грин[2], А.Ф Миронов[2], Р.И. Якубовская[1], А.Д. Каприн[1]
[1]МНИОИ им. П.А. Герцена – филиал ФГБУ «НМИЦР» Минздрава РФ, Москва, Россия,
[2]МИРЭА – Российский технологический университет, Москва, Россия

Резюме

Целью настоящей работы являлось получение стабильной мицеллярной эмульсии перспективного фотосенсибилизатора (ФС) – метилового эфира *О*-пропилоксим-*N*-пропоксибактериопурпуринимида, поглощающего в длинноволновой области спектра (λ_{max} = 800±2 нм). В процессе работы были получены солюбилизаты красителя на основе поверхностно-активных веществ (ПАВ): Kolliphor ELP, Poloxamer 407, Эмуксол 268. По физико-химическим параметрам отобрана и охарактеризована наиболее перспективная мицеллярная эмульсия ФС для парентерального введения. Выбранная эмульсия на основе Kolliphor ELP остается стабильной в течение 4 мес, в течение которых остаются неизменными спектр флуоресценции и поглощения и диаметр мицелл.

Ключевые слова: фотосенсибилизатор, фотодинамическая терапия, бактериохлорин, солюбилизатор, эмульсия.

Для цитирования: Плотникова Е.А., Страмова В.О., Морозова Н.Б., Плютинская А.Д., Островерхов П.В., Грин М.А., Миронов А.Ф., Якубовская Р.И., Каприн А.Д. Солюбилизация гидрофобного фотосенсибилизатора бактериохлоринового ряда в мицеллах поверхностно-активных веществ // Biomedical Photonics. – 2019. – Т. 8, № 1. – С. 18–23. doi: 10.24931/2413–9432–2019–8–1-18–23.

Контакты: Плотникова Е.А., e-mail: plotnikovaekaterina62@gmail.com

Introduction

Photodynamic therapy (PDT) is a dynamically developing method of treating pathologies of various nature, including malignant neoplasms. With its high efficiency of treatment, PDT has been widely used in clinical practice [1-3]. The advantages of PDT are its minimal invasiveness, selectivity of exposure, possibility of repeated use if necessary, a favorable cosmetic effect, as well as the ability to use the technique both as an independent treatment method and in combination with other antitumor therapy methods [4–6].

To date, the main drugs used in PDT are photosensitizers (PS) based on porphyrins, chlorins, and phthalocyanines [7, 8], which are intensively absorbed in the region of 630–685 nm, where the permeability of biological tissues is low. This PS group is characterized by high activity against tumors of small volume. It should be noted that phthalocyanine-type PSs circulate continuously in the body, which leads to prolonged skin toxicity [9]. In connection with the above reasons, the researchers are conducting a directed search for new highly effective dyes, including among compounds of the bacteriochlorin series, which absorb in the region of 700–900 nm [10–13]. PSs of this type are predominantly hydrophobic compounds; therefore, in order to make their intravenous administration possible, the dosage form of the dye has to be a stable emulsion [14].

The most common surfactants used to produce injectable forms of hydrophobic substances are the following: polyethylene glycol, cremophore, pluronics and their aqueous solutions. Co-solvents of this series are pharmaceutical excipients that increase the solubility and stability of drugs, increase the bioavailability and, therefore, the effectiveness of the treatment with the use of photodynamic therapy [14-17].

The aim of this work was to obtain a stable micellar emulsion of methyl ester O-propyloxime-N-propoxybacteriopurpurinimide.

Materials and methods

Photosensitizer

The photosensitizer substance is O-propyloxime-N propoxybacteriopurpurinimide methyl ester absorbing in the region of 800±2 nm [18].

Producing colloidal solutions of surfactants

To obtain colloidal surfactant solutions with a concentration of 4% (mass/volume), weighed portions of solubilizers Kolliphor ELP (BASF, Germany), Poloxamer 407 (Sigma-Aldrich, USA), Emuksol 268 (FSUE "SSC" NIOPIK", Russia) were dissolved in injection-grade water (LLC "Groteks", Solopharm, Russia) and stirred for 10 minutes until complete dissolution. Stirring was done with a magnetic stirrer (ThermoScientific, UK) at a temperature of 25, 40, 50, 60, 70, and 80°C. Next, the colloidal solution was subjected to sonication for 10 or 20 minutes. The efficiency of the formation of colloidal solutions was evaluated by the nature of micelles formation by dynamic light scattering which determined the diameter of the particles in the solution. The analysis was performed on a Delsa™Nano C particle size, ξ potential, and flat surface analyzer (BeckmanCoulter, USA). The light source was a diode laser operating at a fixed wavelength of 658 nm. Each measurement was carried out at least 3 times, then the average value of the diameter of the micelles was calculated.

Preparation of solubilizers based on surfactants

To obtain a PS emulsion based on various surfactants (Kolliphor ELP, Poloxamer 407, Emuxol 268), a dye sample was dissolved in methylene chloride (dichloromethane, CP, OOO "Khimmed", Russia) and added in small portions to a 4% surfactant solution heated on magnetic stirrer to 42°C, which is the boiling point of methylene chloride, with constant stirring and barbotage with argon. The process was continued until the solvent completely evaporated, then the emulsion was cooled to room temperature and sterilized through a Millipore membrane filter (Corning, Germany) with a pore size of 0.22 μm.

The assessment of the stability of solubilizers based on surfactants

The stability assessment included an analysis of the absorption and fluorescence spectra over time and the particle size distribution of surfactant-based photosensitizer emulsions.

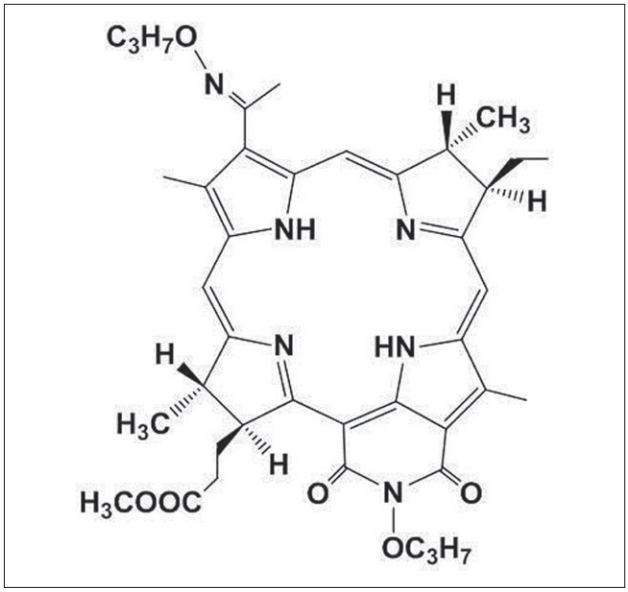

Рис. 1. Химическая формула фотосенсибилизатора
Fig. 1. Chemical formula of the photosensitizer

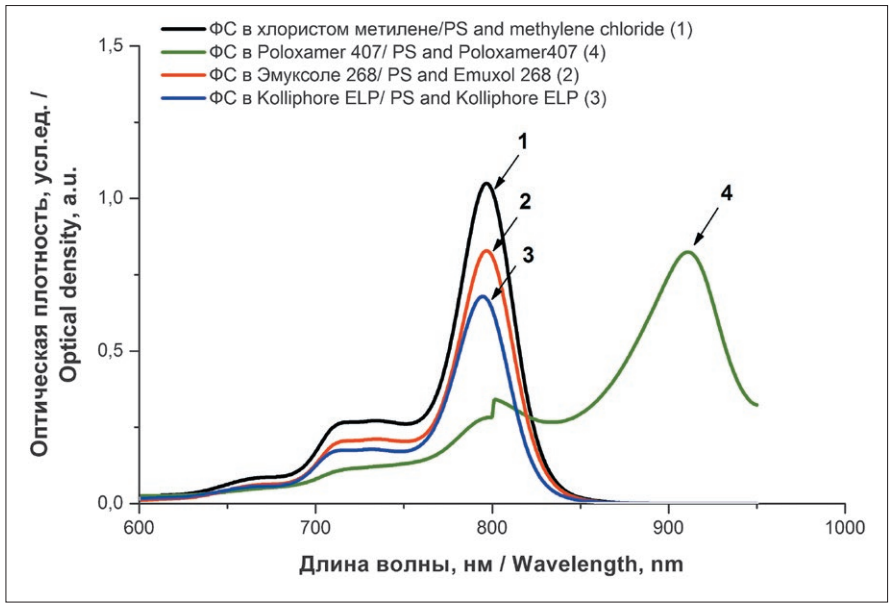

Рис. 2. Абсорбционные спектры ФС в хлористом метилене (1), в составе эмульсии на основе Kolliphor ELP (2), Poloxamer 407 (3) и Эмуксол 268 (4)
Fig. 2. Absorption spectra of the PS in dichloromethane (1), in the emulsion based on Kolliphor ELP (2), Poloxamer 407 (3) and Emuxol 268 (4)

PS solutions were prepared *ex tempore* by serial dilution of the starting emulsions with known concentrations. Absorption and fluorescence spectra were recorded on a Genesys 2 spectrophotometer (ThermoSpectronic, USA) and on a laser analyzer for fluorescence diagnosis of LESA tumors (OOO "BIOSPEC", Russia), respectively. The measurements were carried out *ex tempore*, as well as after 2, 4, 24 hours, 7 days, 1 and 4 months of storage in a dark place. Fluorescence was excited by a He-Ne laser at a generation wavelength of 632.8 nm with an optical resolution of 2 nm in the wavelength range from 400 to 1000 nm. During mathematical processing, the spectrum of the background fluorescence of the solvent was subtracted from the recorded spectra and integrated within the range from 300 to 900 nm. The concentration of the active substance in the solution was 20 μg/ml. In the course of the studies, the position of the maxima on the absorption and fluorescence spectra, the optical density, the fluorescence intensity, and also the nature of the change in the profile of the PS spectra were evaluated.

To determine the particle size in solution, the dynamic laser light scattering (DLS) method was used. The analysis was performed on a Delsa™Nano C particle size, ξ potential, and flat surface analyzer. Before the experiment, the emulsions were sterilized through a 0.22 μm Millipore membrane filter. The solutions for the research were prepared *ex tempore* by successive dilutions of the starting emulsions to a final concentration of the active substance of 40 μg/ml. Each measurement was carried out at least 3 times, after which the average diameter of empty micelles and micelles with the introducted photosensitizer was calculated.

Photosensitizer photo stability assessment

The solutions were prepared *ex tempore* by successive dilutions of the initial emulsion in the Igla MEM culture medium (NPE "PanEco", Russia) containing 10% fetal calf serum to a final concentration of the active substance of 25 μg/ml. 150 μl of PS solution was introduced to the wells of a flat-bottomed 96-well microplate (Corning, USA). A 500 W halogen lamp with a KS-19 broadband filter (λ ≥ 720 nm) and a 5 cm thick water filter were used as an optical radiation source. The power density was 18 ± 1.0 mW/cm^2, and the light dose was 5, 10, 20, 50, and 100 J/cm^2. The radiation power was monitored with an IMPO meter (RPA "Polyus", Moscow). The fluorescence intensity was evaluated before and after irradiation. During mathematical processing, the spectrum of the background fluorescence of the solvent was subtracted from the recorded spectra and integrated within the range from 300 to 900 nm.

Results and discussion

Producing colloidal solutions of surfactants

To solubilize PS, the following surfactants were used as cosolvents: Kolliphor ELP, Emuxol 268 and Poloxamer 407. Kolliphor ELP is a non-ionic solubilizer obtained by mixing castor oil with ethylene oxide in a ratio of 1:35; Emuxol 268 is a block copolymer of ethylene oxide with

Таблица
Физико-химические свойства солюбилизатов на основе различных ПАВ
Table
Physicochemical properties of solubilizates based on various surfactants

Название ПАВ Name of surfactant	$\omega_{ПАВ}$, % $\omega_{surfactants}$, %	λ_{max}, нм λ_{max}, nm	ε, $M^{-1}cm^{-1}$ ε, $M^{-1}cm^{-1}$	Диаметр частиц, нм Diameter of particles, nm		Стабильность Stability
				Без субстанции Without substance	С субстанцией With substance	
Kolliphor ELP	4	800±2	29285	10,7±0,3	10,5±0,40	4 мес 4 months
Emuxol 268	4	910±2	–	12,0±1,1	362±15 535 ±201	не стабилен not stable
Poloxamer 407	4	800±2	23492	28,5±2,0	27,5±2,5	2 ч 2 hours

propylene oxide and propylene glycol; Poloxamer 407 is a triple block copolymer of ethylene oxide and propylene oxide [19]. During the preparation of colloidal solutions, it was found that Kolliphor ELP effectively forms micelles at room temperature without the use of ultrasound. The size of the resulting particles in this case is 10.7 ± 0.3 nm.

The smallest particle size in a colloidal solution based on Emuxol 268 was observed after heating to 40°C and sonicated for 10 min (12.0±1.1 nm). Samples based on Poloxamer 407, prepared at 40 and 50°C and sonicated for 10 min, had a particle diameter of not more than 30.0 nm. Thus, a heating temperature of 40°C and the ultrasonication time of 10 minutes were chosen as the most optimal emulsion preparation parameters.

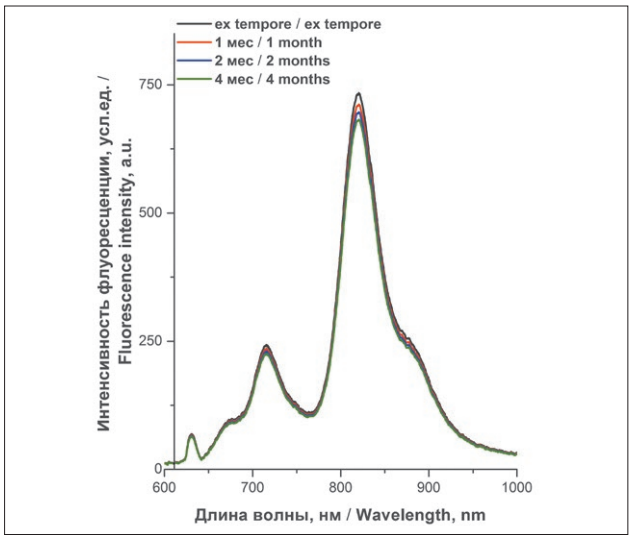

Рис. 3. Спектры флуоресценции ФС в составе эмульсии на основе 4% Kolliphor ELP во времени
Fig. 3. Fluorescence spectra of the PS in the 4% Kolliphor ELP-based emulsion in time

Assessment of physicochemical properties of surfactant-based solubilizates

An analysis of the obtained data showed that the intensity of the main absorption band of solubilizates based on Kolliphor ELP (OD = 0.810) and Poloxamer 407 (OD = 0.635) was the highest (Fig. 2). Perhaps this is due to the fact that these surfactants have the longest hydrophobic regions, while Poloxamer 407 has a larger hydrophobic core volume [20, 21]. It was shown that the choice of a particular solubilizer does not affect the form of the electronic absorption spectrum of the substance (Fig. 3). The maximum fluorescence of PS under these conditions is recorded at 822 ± 2 nm.

The solubilization of the substance in Emuxol 268 led to its instant aggregation, with the expansion of the main absorption band and the formation of a new band with a maximum in the region of 910±2 nm, which corresponds to the formation of an aggregated form of the dye (Fig. 2). The data on the determination of particle diameter confirm the aggregation of the dye, with the diameter of the solubilizate micelles exceeding 5000 nm (see table).

Solubilizers based on Kolliphor ELP and Poloxamer 407 were monodisperse with an average particle diameter of 10.5±0.40 and 27.5±2.5 nm, respectively.

The photosensitizer in the composition of the Poloxamer 407-based emulsion is stable for 2 hours, after which the shape of the electronic spectrum changes with the appearance of a high-intensity long-wave peak in the region of 895±2 nm, as well as the disappearance of the main absorption band in the region of 800±2 nm, which indicates aggregation of the substance in the solution resulting in a 100% decay of fluorescence. Perhaps this effect is due to the fact that a large hydrophilic part of the Poloxamer 407 polyethylene oxide blocks is capable of hydration, the result of which is the penetration of

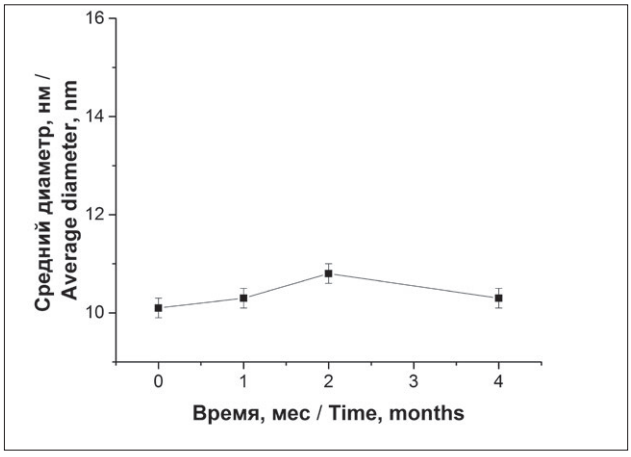

Рис. 4. Изменение диаметра частиц ФС в составе эмульсии на основе 4% Kolliphor ELP во времени
Fig. 4. Change in the diameter of the PS particles in the on 4% Kolliphor ELP-based emulsion in time

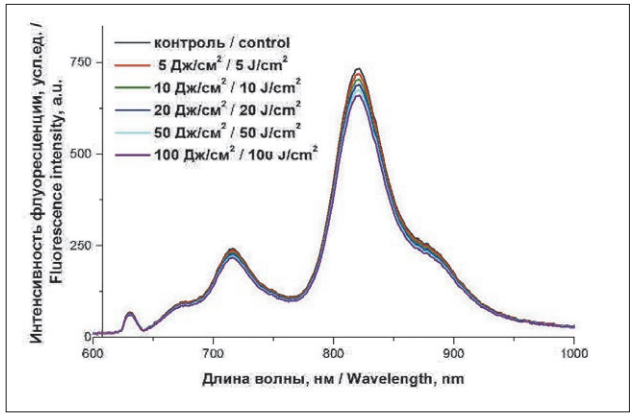

Рис. 5. Спектры флуоресценции ФС в составе эмульсии на основе 4% Kolliphor ELP до воздействия света и после облучения дозой света в 5, 10, 20, 50 и 100 Дж/см²
Fig. 5. Fluorescence spectra of the PS in the 4% Kolliphor ELP-based emulsion: before and after irradiation at a dose of 5, 10, 20, 50 and 100 J/cm²

water into the micelle nuclei and their further aggregation.

Based on the obtained data, it was found that the Kolliphor ELP-based solubilizate remains stable for 4 months, and throughout the entire observation period there are no changes in the fluorescence and absorption spectra and particle diameter (table, Fig. 3-4).

Assessment of the photostability of a photosensitizer in an emulsion based on Kolliphor ELP

It is shown that when the studied PS is irradiated in the composition of an emulsion based on Kolliphor ELP up to 100 J/cm² the dye is not prone to fading: no changes in the spectrum profile and fluorescence intensity were observed (Fig. 5).

Conclusion

Based on the data on solubility and stability, a micellar emulsion of PS based on Kolliphor ELP was selected, characterized by stability both during storage (4 months) and irradiation (up to 100 J/cm²). The micellar emulsion of methyl ester of O-propyloxy N-propoxybacteriopurpurinimide based on Kolliphor ELP is a promising substance and is of great interest for further studies in the field of photodynamic therapy of malignant neoplasms, since the use of this dye will make it possible to treat patients with large volume and deep-laying tumor formations.

REFERENCES

1. Titova V.A. The role and place of photodynamic therapy in multimodal treatment programs for malignant tumors, *Biomedical Photonics*, 2012, vol. 1, no. 1, pp. 3–5. (in Russian)
2. Dabrowski J.M., Arnaut L.G. Photodynamic Therapy (PDT) of Cancer: From a Local to a Systemic Treatment, *Photochem. Photobiol. Sci.*, 2015, vol. 14(10), pp. 1765–1780.
3. Agostinis P., Berg K., Cengel K.A., Foster T.H., Girotti A.W., Gollnick S.O., Hahn S.M., Hamblin M.R., Juzeniene A., Kessel D., Korbelik M., Moan J., Mroz P., Nowis D., Piette J., Wilson B.C., Golab J. Photodynamic Therapy of Cancer: An Update, *CA Cancer J Clin*, 2011, vol. 61(4), pp. 250–281.
4. Kimura M., Miyajima K., Kojika M., Kono T., Kato H. Photodynamic Therapy (PDT) with Chemotherapy for Advanced Lung Cancer with Airway Stenosis, *Int J Mol Sci*, 2015, vol. 16(10), pp. 25466–25475.
5. Obaid G., Huang H.-C., Hasan T. Targeted Photodynamic Therapy – An Assimilation of Successes, Challenges and Future Directions. In: *Photodynamic Medicine: From Bench to Clinic*. London: RSC, 2016. pp. 137–160.
6. Chilakamarthi U., Giribabu L. Photodynamic Therapy: Past, Present and Future, *Chem Rec*, 2017, vol. 17(8), pp. 775–802.

ЛИТЕРАТУРА

1. Титова В.А. Роль и место фотодинамической терапии в мультимодальных программах лечения злокачественных опухолей // Biomedical Photonics. – 2012. – Т. 1, № 1. – С. 3–5.
2. Dabrowski J.M., Arnaut L.G. Photodynamic Therapy (PDT) of Cancer: From a Local to a Systemic Treatment // Photochem. Photobiol. Sci. – 2015. – Vol. 14(10). – P. 1765–1780.
3. Agostinis P., Berg K., Cengel K.A., et al. Photodynamic Therapy of Cancer: An Update // CA Cancer J Clin. – 2011. – Vol. 61(4). – P. 250–281.
4. Kimura M., Miyajima K., Kojika M., et al. Photodynamic Therapy (PDT) with Chemotherapy for Advanced Lung Cancer with Airway Stenosis // Int J Mol Sci. – 2015. – Vol. 16(10). – P. 25466–25475
5. Obaid G., Huang H.-C., Hasan T. Targeted Photodynamic Therapy – An Assimilation of Successes, Challenges and Future Directions. In: Photodynamic Medicine: From Bench to Clinic. – London: RSC, 2016. – P. 137–160.
6. Chilakamarthi U., Giribabu L. Photodynamic Therapy: Past, Present and Future // The Chemical Record. – 2017. – Vol. 17(8). – P. 775–802.

7. Filonenko E.V., Serova L.G. Photodynamic therapy in clinical practice, *Biomedical Photonics*, 2016, vol. 5, no. 2, pp. 26–37. (in Russian)
8. Ethirajan M., Chen Y., Joshi P., Pandey R.K. The role of porphyrin chemistry in tumor imaging and photodynamic therapy, *Chem Soc Rev*, 2011, vol. 40(1), pp. 340–362.
9. Machinskaya E.A., Ivanova-Radkevich V.I. Review of the mechanisms of selective accumulation of photosensitizers of various chemical structures in tumor tissue, *Biomedical photonics*, 2013, vol. 2, no. 4, pp. 28–33. (in Russian)
10. Lukyanets E.A. Search for new photosensitizers for photodynamic therapy, *Biomedical photonics*, 2013, vol. 2, no. 3, pp. 3–16. (in Russian)
11. Staron J., Boron B., Karcz D., Szczygieł M., Fiedor L. Progress in Chemical Modifications of Chlorophylls and Bacteriochlorophylls or the Applications in Photodynamic Therapy, *Curr. Med. Chem.*, 2015, vol. 22(26), pp. 3054–3074.
12. Suvorov N.V., Grin M.A., Popkov A.M., Gagarina A.S., Mironov A.F., Majouga A.G. Novel Photosensitizer Based on Bacteriopurpurinimide and Magnetite Nanoparticles, *Makrogeterotsikly*, 2016, vol. 9(2), pp. 175–179.
13. Huang Y., Luo D., Hamblin M.R. Stable synthetic bacteriochlorins: potent light activated anti-cancer drugs, *Curr. Org. chem.*, 2015, vol. 19(10), pp. 948–957.
14. Kawakami K., Oda N., Miyoshi K., Funaki T., Ida Y. Solubilization behavior of a poorly soluble drug under combined use of surfactants and cosolvents, *Eur J Pharm Sci*, 2006, vol. 28(1–2), pp. 7–14.
15. Sosnov A.V., Ivanov R.V., Balakin K.V., Shobolov D.L., Fedotov Yu.A., Kalmykov Yu.M. Development of drug delivery systems using micro- and nanoparticles, Kachestvennaya klinicheskaya praktika, 2008, no. 2, pp. 4–12. (in Russian)
16. Gulyakin I.D., Oborotova N.A., Pechennikov V.M. Solubilization of hydrophobic anticancer drugs, *Khimiko-farmatsevticheckii zhurnal*, 2014, vol. 48, no. 3, pp. 46–50. (in Russian)
17. Zhang Z., Cui C., Wei F., Lv H. Improved solubility and oral bioavailability of Apigeninvia Soluplus®/Pluronic F127 binary mixed micelles system, *Drug Dev Ind Pharm*, 2017, vol. 43(8), pp. 1276–1282.
18. Pantyushenko I.V., Grin M.A., Yakubovskaya R.I., Plotnikova E.A., Morozova N.B, Tsygankov A.A., Mironov A.F. New highly effective bacteriochlorophyll a series IR-photosensitizer for photodynamic cancer therapy, *Vestnik MITKhT*, 2014, vol. 9, no. 3, pp. 3–10. (in Russian)
19. Lastovoi A.P., Avramenko G.V. Study of the association of tetramethyltribenzotetraazachlorin in binary mixtures of polar solvents and in colloidal solutions of nonionic surfactants, *Makrogeterotsikly*, 2013, Vol. 6(1), pp. 98–105. (in Russian)
20. Varela-Moreira A., Shi A., Fens M., Lammers T., Hennink W.E., Schiffelers R.M. Clinical application of polymeric micelles for the treatment of cancer, *Mater. Chem. Front.*, 2017, vol. 1(8), pp. 1485–1501.
21. Kabanov A.V., Batrakova E.V., Alakhov V.Y. Pluronic block copolymers as novel polymer therapeutics for drug and gene delivery, *J Control Release*, 2002, vol. 82(2–3), pp. 189–212.

7. Филоненко Е.В., Серова Л.Г. Фотодинамическая терапия в клинической практике // Biomedical Photonics. – 2016. – Т. 5, № 2. – С. 26–37.
8. Ethirajan M., Chen Y., Joshi P., Pandey R.K. The role of porphyrin chemistry in tumor imaging and photodynamic therapy // Chem Soc Rev. – 2011. – Vol. 40(1). – P. 340–362.
9. Мачинская Е.А., Иванова-Радкевич В.И. Обзор механизмов селективного накопления фотосенсибилизаторов различной химической структуры в опухолевой ткани // Biomedical photonics. – 2013. – Т. 2, № 4. – С. 28–33.
10. Лукьянец Е.А. Поиск новых фотосенсибилизаторов для фотодинамической терапии // Biomedical photonics – 2013. – Т. 2, № 3. – С. 3–16.
11. Staron J., Boron B., Karcz D., et al. Progress in Chemical Modifications of Chlorophylls and Bacteriochlorophylls or the Applications in Photodynamic Therapy // Curr. Med. Chem. – 2015. – Vol. 22(26). – P. 3054–3074.
12. Suvorov N.V., Grin M.A., Popkov A.M., et al. Novel Photosensitizer Based on Bacteriopurpurinimide and Magnetite Nanoparticles // Makrogeterotsikly. – 2016. – Vol. 9(2). – P. 175–179.
13. Huang Y., Luo D., Hamblin M.R. Stable synthetic bacteriochlorins: potent light activated anti-cancer drugs // Curr. Org. chem. – 2015. – Vol. 19(10). – P. 948–957.
14. Kawakami K., Oda N., Miyoshi K., et al. Solubilization behavior of a poorly soluble drug under combined use of surfactants and cosolvents // Eur J Pharm Sci. – 2006. – Vol. 28(1–2). – P. 7–14.
15. Соснов А.В., Иванов Р.В., Балакин К.В. и др. Разработка систем доставки лекарственных средств с применением микро- и наночастиц // Качественная клиническая практика. – 2008. – № 2. – С. 4–12.
16. Гулякин И.Д., Оборотова Н.А., Печенников В.М. Солюбилизация гидрофобных противоопухолевых препаратов // Химико-фармацевтический журнал. – 2014. – Т. 48, № 3. – С. 46–50.
17. Zhang Z., Cui C., Wei F., Lv H. Improved solubility and oral bioavailability of Apigeninvia Soluplus®/Pluronic F127 binary mixed micelles system // Drug Dev Ind Pharm. – 2017. – Vol. 43(8). – P. 1276–1282.
18. Пантюшенко И.В., Грин М.А., Якубовская Р.И. и др. Новый высоко-эффективный ИК-фотосенсибилизатор в ряду бактериохлорофилла а для фотодинамической терапии рака // Вестник МИТХТ. – 2014. – Т. 9, № 3. – С. 3–10.
19. Ластовой А.П., Авраменко Г.В. Исследование ассоциации тетраметилтрибензотетраазахлорина в бинарных смесях полярных растворителей и в коллоидных растворах НПАВ // Макрогетероциклы. – 2013. – Т. 6(1). – С. 98–105.
20. Varela-Moreira A., Shi A., Fens M., et al. Clinical application of polymeric micelles for the treatment of cancer // Mater. Chem. Front. – 2017. – Vol. 1(8). – P. 1485–1501.
21. Kabanov A.V., Batrakova E.V., Alakhov V.Y. Pluronic block copolymers as novel polymer therapeutics for drug and gene delivery // J Control Release. – 2002. – Vol. 82(2–3). – P. 189–212.

ORIGINAL ARTICLES

PHOTODYNAMIC THERAPY IN PATIENTS WITH SKIN METASTASES OF DESSIMINATED MELANOMA

Tzerkovsky D.A., Petrovskaya N.A., Mazurenko A.N.
N.N. Alexandrov National Cancer Centre of Belarus, Lesnoy, Republic of Belarus

Abstract

The aim of the study was to evaluate the immediate results of photodynamic therapy (PDT) in patients with intradermal metastases of skin melanoma. The study included 50 patients who received treatment at the department of hyperthermia and photodynamic therapy. The study included 23 (46%) men and 27 (54%) women with an average age of 60.7±10.4 years. PDT of tumors was carried out 3–4 hours after intravenous administration of a chlorine-based photosensitizer (Photolon) in doses of 1.5–3 mg/kg using a semiconductor laser «UPL-PDT» (Lemt, Belarus, λ=660±5 nm). The exposure doses varied from 100 to 400 J/cm^2; power density – from 0.2 to 0.9 W/cm^2; power – from 0.25 to 1 W and time of PDT of one focus was dependent on the size and location of the tumor and was 5 to 20 minutes. Evaluation of antitumor efficacy of PDT was carried out according to WHO criteria. The terms of follow-up of patients were between 3 and 23 months. At follow-up observation, 1–3 months after the treatment, complete regression of intradermal metastases of skin melanoma was achieved in 9 (18%) patients, partial – in 28 (56%), process stabilization in 8 (16%) and progression in 5 (10%)) patients. The objective effect was achieved in 74% of patients, the therapeutic – in 90%. PDT can be used in the treatment of intradermal metastases of disseminated skin melanoma with palliative purposes and allows reducing the tumor volume, which significantly improves the quality of life of patients.

Keywords: skin melanoma, intradermal metastases, photodynamic therapy.

For citations: Tzerkovsky D.A., Petrovskaya N.A., Mazurenko A.N. Photodynamic therapy in patients with skin metastases of disseminated melanoma, *Biomedical Photonics*, 2019, vol. 8, no. 1, pp. 14–28 (in Russian) 10.24931/2413–9432–2019–8–1-24–28.

Contacts: Tzerkovsky D.A., e-mail: tzerkovsky@mail.ru

ФОТОДИНАМИЧЕСКАЯ ТЕРАПИЯ ПАЦИЕНТОВ С ВНУТРИКОЖНЫМИ МЕТАСТАЗАМИ ДИССЕМИНИРОВАННОЙ МЕЛАНОМЫ КОЖИ

Д.А. Церковский, Н.А. Петровская, А.Н. Мазуренко
Республиканский научно-практический центр онкологии и медицинской радиологии им. Н.Н. Александрова, Лесной, Республика Беларусь

Резюме

Целью работы была оценка непосредственных результатов применения фотодинамической терапии (ФДТ) у пациентов с внутрикожными метастазами меланомы кожи. В исследование было включено 50 пациентов с внутрикожными метастазами диссеминированной меланомы кожи, получавших лечение на базе отделения гипертермии и фотодинамической терапии. Среди них было 23 (46%) мужчины и 27 (54%) женщин; средний возраст пациентов составил 60,7±10,4 лет. Облучение опухолей проводили через 3–4 ч после внутривенного введения фотосенсибилизатора хлоринового ряда (фотолон) в дозах 1,5–3 мг/кг с использованием полупроводникового лазера «УПЛ-ФДТ» (НТЦ «ЛЭМТ» БелОМО, Республика Беларусь, λ=660±5 нм). Суммарная доза света варьировалась от 100 до 400 Дж/см^2; плотность мощности – от 0,2 до 0,9 Вт/см^2; мощность – от 0,25 до 1 Вт; длительность облучения одного очага зависела от размеров и локализации опухоли и составляла от 5 до 20 мин. Оценку противоопухолевой эффективности ФДТ осуществляли по критериям ВОЗ. Сроки наблюдения за пациентами составили от 3 до 23 мес. При контрольном наблюдении через 1–3 мес после проведенного лечения полная регрессия внутрикожных метастазов меланомы кожи достигнута у 9 (18%), частичная – у 28 (56%), стабилизация процесса – у 8 (16%) и прогрессирование – у 5 (10%) пациентов. Объективный эффект достигнут у 74% пациентов, лечебный – у 90%. Метод ФДТ может быть применен в лечении внутрикожных метастазов диссеминированной меланомы кожи в паллиативных целях и позволяет уменьшать объем опухоли, что существенно повышает качество жизни пациентов.

Ключевые слова: меланома кожи, внутрикожные метастазы, фотодинамическая терапия.

Для цитирования: Церковский Д.А., Петровская Н.А., Мазуренко А.Н. Фотодинамическая терапия пациентов с внутрикожными метастазами диссеминированной меланомы кожи // Biomedical photonics. – 2019 – Т. 8, № 1 – С. 24–28. doi: 10.24931/2413–9432–2019–8–1-24–28.

Контакты: Церковский Д.А., e-mail: tzerkovsky@mail.ru

Introduction

Skin melanoma is one of the aggressive forms of malignant tumors with high growth and regional metastasis potential, with the ability to disseminate over the skin and produce multiple hematogenous metastases. The number of patients with this pathology has increased significantly in the recent years: the average annual growth rate of the incidence of melanoma in the world is about 5%, which can be considered one of the highest among all malignant neoplasms. Despite the fact that the proportion of melanoma in the structure of all tumor skin diseases is on average 4%, this disease is the main cause of death for patients with skin cancer. The average life expectancy of patients with melanoma varies from 6 to 9 months with a 5-year survival rate of less than 18% [1].

Today, one of the most challenging problems of clinical oncology is the treatment of disseminated melanoma, which is associated with the low sensitivity of this tumor to the traditionally used chemo-, hormone-, and immunotherapy. Despite certain advances in drug therapy for the metastatic form of skin melanoma and the variety of antitumor drugs, only a small fraction of them are found to achieve with relative success in the treatment of this disease.

All of the above shows that the problem of the combined treatment of disseminated skin melanoma is still far from being resolved and remains very relevant for clinical oncology. Insufficient efficiency of the existing therapies for disseminated skin melanoma is the main prerequisite for the search and testing of new methods in this area.

One of the methods which have proven their effectiveness and safety in clinical settings, is photodynamic therapy (PDT).

PDT is a method of local activation of the photosensitizer (PS) selectively accumulated in the tumor tissue with visible red color, which in the presence of tissue oxygen leads to the development of photochemical reactions of types I and II, which lead to the destruction of tumor cells [2].

PDT is the result of the combined interaction of three components: PS, light and oxygen. The implementation of the antitumor effect is based on selective laser photodestruction of pre-sensitized tumor tissue. One of the main targets for photodynamic effects is blood vessel endotheliocytes and a system of macrophage cells, irradiation of which leads to the development of inflammatory mediators and cytokines (lymphokines, thromboxanes, prostoglandins) playing a significant role in the vascular component of tumor stroma destruction [3]. The PDT mechanism includes a direct cytotoxic effect on the tumor, leading to the necrosis and apoptosis of the tumor cell, damage to the microvascular bed of the tumor due to developing vascular stasis, thrombosis and hemorrhage. The result of these processes is tumor hypoxia and its subsequent death [4].

There have been a number of publications on the results of experimental and clinical studies that confirm the sensitivity of skin melanoma to PDT with the use of photosensitizing agents of various classes [1, 5–7].

The purpose of this work was to study the effectiveness of PDT with chlorine-type PS in patients with intradermal metastases of skin melanoma.

Materials and methods

Patients

The study included 50 patients with intradermal metastases of disseminated skin melanoma. The sample was 23 (46%) men and 27 (54%) women aged 27 to 82, the average age of patients being 60.7 ±10.4 years. In 32 (64%) patients, the primary focus was localized on the lower extremities, in 14 (28%), on the upper limbs, and in 4 (8%), on the trunk. In all patients, the diagnosis was morphologically verified and at the time of the clinical examination corresponded to stage IV cancer (T1-4N0-2M1 (a, b, c)) (according to AJCC classification, Cutaneous melanoma: ESMO Clinical Practice Guidelines for diagnosis, treatment and follow-up, 2002). All patients included in the study previously underwent combination treatment consisting of surgical excision of the primary tumor, radiation therapy, polychemotherapy and hormone therapy. At the beginning of treatment, all patients showed progression of the disease (numerous metastatic lesions on the skin). PDT method was used against the background of mono- or polychemotherapy. The exposure parameters were selected individually for each patient, depending on the general status, location of the lesion, the number and size of tumor foci. All patients included in the study were informed about the method of PDT, its possible adverse reactions and complications, the timing of follow-up and recommendations after treatment. Every patient signed an informed consent.

Photosensitizer

The PS was Photolon (RUE Belmedpreparaty, Republic of Belarus, registration certificate П N015948/01

of November 30, 2012), which is a complex of trisodium salt of chlorin e_6 with polyvinylpyrrolidone (RUE Belmedpreparaty, Republic of Belarus). Photolon was dissolved in 200 ml of physiological saline and was administered intravenously, by drop infusion, for 30 minutes at doses of 1.5–3 mg/kg.

A PDT session

One PDT session per patient was performed, in a darkened room 3-4 hours after intravenous administration of photolon ith the use of UPL-PDT semiconductor laser apparatus (STC LEMT BelOMO, Republic of Belarus, λ = 660 nm). Immediately before tumor irradiation, laser devices were calibrated with the help of power meters. Eye-protection glasses were used to protect the eyes of patients and medical personnel. Immediately before the session, patients were premedicated with intramuscular administration of Ketorolac 4.0. Tumors were irradiated remotely, perpendicularly to the surface of the pathological focus, with a fiber equipped with a microlens (Polironik, Russia) using one, two or three fields. The light dose of radiation ranged from 100 to 400 J/cm^2. The power density ranged from 0.2 to 0.9 W/cm^2, the laser radiation power was from 0.25 to 1 W. The size of the irradiation fields varied from 0.5 to 2.0 cm, and the number of fields ranged from 3 to 17. The total number of irradiation sessions was 125. The duration of irradiation of one lesion depended on the size and location of the tumor and ranged from 5 to 20 minutes. In order to prevent local marginal recurrence, normal unchanged tissues were exposed to radiation along the periphery of the tumor focus at a distance of 5–7 mm from its edges.

Efficiency evaluation criteria

For all patients, the antitumor efficacy of PDT for intradermal metastases of melanoma was assessed according to WHO criteria, based on clinical trial data in 1-3 months after treatment.

The criteria were as follows:

- complete regression (CR): 100% resorption of tumor foci 1 month after PDT, confirmed 3 months after treatment;
- partial regression (PR): a decrease in the total size of the tumor lesion by 50% or more with subsequent stabilization established after 1 month and confirmed 3 months after the PDT session;
- stabilization of the process: no increase in the tumor nodes size, no new nodes or other signs of disease progression within 3 months;
- progression of the process: an increase in the total size of the tumor node by 25% or more, or the development of new tumor foci.

Objective (the sum of CR and PR) and therapeutic (the sum of PR, CR and stabilization) effects were also evaluated.

Results and discussion

The tolerance of the method was estimated based on the general condition of the patients before the PDT session, after the administration of the PS, after light exposure, and daily until the patient was discharged from the hospital, for 3 to 5 days. There were no adverse reactions during photolon infusion and PDT sessions.

During the PDT session, most patients experienced phenomena characteristic of the photodynamic reaction as a whole, such as itching, burning sensation, and soreness in the irradiated area. In the case of severe pain, non-narcotic analgesics were used and/or the laser radiation power was reduced while maintaining the light dose due to a proportional increase in the exposure time. In some cases, patients experienced symptoms of skin phototoxicity, which were due to non-observance of the light regime.

After a PDT session, hemorrhagic necrosis developed in tumor foci, followed by the formation of a scab within 4–12 days. In all cases, it was a dense crust of a dark brown color fused to the underlying tissues, which was independently rejected 3–6 weeks after treatment (Fig. 1).

At the site of the tumor focus, a connective tissue scar was formed, which was a smooth pinkish surface, sometimes with a small depression in the center.

To prevent skin phototoxicity, patients were prescribed antioxidants and light-protective ointments, which contributed to the early epithelization of the wound and increased connective tissue growth.

No adverse reactions and phenomena associated with the introduction of PS were observed.

When evaluating skin phototoxicity, it should be noted that in all patients who observed the photo regime for 2–3 days after a PDT session, i. e., avoided direct sunlight, there were no adverse reactions in the form of skin burns of various degrees and the development of hyperpigmentation. In the rare cases of intentional or unintentional non-compliance with the recommendations, mild hyperemia of the exposed skin areas of the skin was observed, which lasted for several hours.

The follow-up observation of the patients ranged from 3 to 23 months. During clinical follow-up, 1-3 months after the treatment, CR of intradermal metastases of cutaneous melanoma was achieved in 9 (18%), PR in 28 (56%), stabilization of the process in 8 (16%), and progression was observed in 5 (10%) patients. Objective therapeutic effect was achieved in 74% of patients, and therapeutic effect in 90%.

The results of PDT use in the treatment of patients with intradermal metastases of disseminated melanoma are consistent with the available literature. Thus, in the study of Professor M. A. Kaplan et al., 1–2 months after focal PDT, CR was achieved in 7 (11.5%) patients with skin

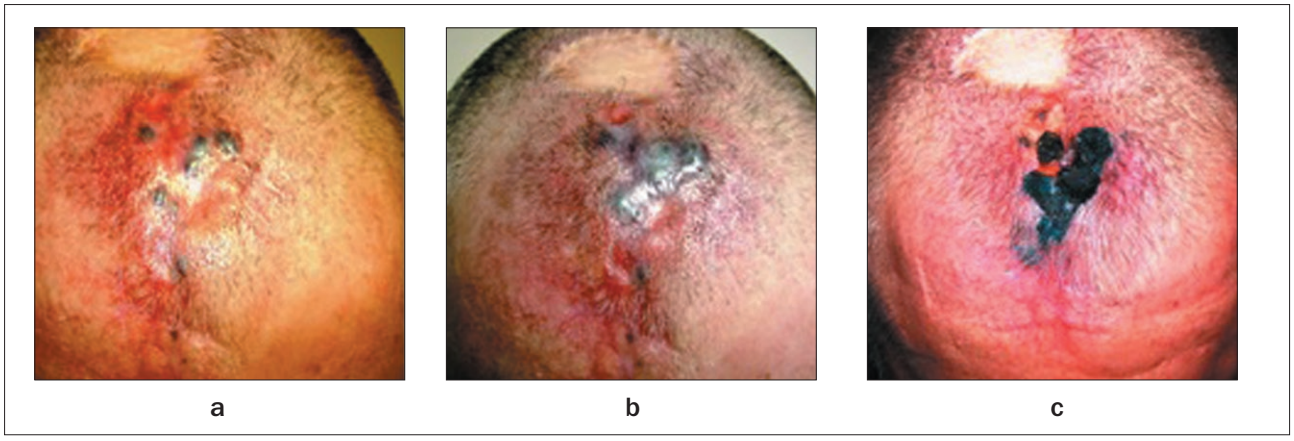

Рис. 1. Меланома кожи теменной области (T3N0M0). Состояние после хирургического лечения (2014 г.). Прогрессирование: внутрикожные метастазы лобно-теменной области:
а – состояние до ФДТ;
б – состояние непосредственно после сеанса ФДТ с фотолоном;
с – состояние через 1 мес после ФДТ

Fig. 1. Melanoma of the skin of the parietal region (T3N0M0). Condition after surgical treatment (2014). Progression: intradermal metastasis of the fronto-parietal region:
a – before PDT;
b – immediately after the PDT session with photolon;
c – 1 month after PDT

lesions, PR in 33 (54.1%) patients with skin and soft tissue lesions. The frequency of objective responses was 65.6%. Stabilization lasting more than 6–8 weeks was recorded in 13 (21.3%) foci. The therapeutic effect was achieved in 86.9% of the cases. At the same time, it should be noted that our colleagues used significantly higher light doses (600–900 J/cm^2) for irradiating tumor foci compared with our study [1].

Conclusion

Thus, the advantage of PDT is the selectivity of tumor tissue targeting, the absence of severe local and systemic adverse reactions, and the possibility of repeating sessions. However, it should be noted that the treatment of patients with this pathology can be carried out on an outpatient basis, which provides economic advantages. The PDT method in the treatment of intradermal metastases of disseminated skin melanoma can be used for palliative purposes, its use can reduce the tumor volume and significantly improve the quality of life of patients.

REFERENCES

1. Kaplan M.A., Kudryavtseva G.T., Kapinus V.N., Zakurdyaeva I.G., Borgul O.V. Photodynamic therapy of disseminated skin melanoma using Fotolon photosensitizer, *Sib. onkol. zhurn.*, 2011, no. 1. pp. 56–60.
2. Stranadko E.F. Historical essay on the development of photodynamic therapy, *Lazernaya medicina*, 2002, vol. 6, is. 1, pp. 4–8.
3. Mroz P., Yaroslavsky A., Kharkwal G.B. Cell death pathways in photodynamic therapy of tumors, *Cancers*, 2011, vol. 3, pp. 2516–2539.
4. Weiss A., den Bergh H.V., Griffioen A.W. Angiogenesis inhibition for the improvement of photodynamic therapy: The revival of a promising idea, *Biochim. Biophys. Acta*, 2012, vol. 1826, pp. 53–70.
5. Sharma K.V., Bowers N., Davids L.M. Photodynamic therapy-induced killing is enhanced in depigmented metastatic melanoma cells, *Cell Biol. Int.*, 2011, vol. 35, pp. 939–949.
6. Sparsa A., Bellaton S., Naves T., Jauberteau M.O., Bonnetblanc J.M. Photodynamic treatment induces cell death by apoptosis or autophagy depending on the melanin content in two B16 melanoma cell lines, *Oncol. Rep.*, 2013, vol. 29, pp. 1196 –1200.

ЛИТЕРАТУРА

1. Каплан М.А., Кудрявцева Г.Т., Капинус В.Н. и др. Фотодинамическая терапия диссеминированной меланомы кожи с фотосенсибилизатором «Фотолон» // Сиб. онкол. журн. – 2011. – № 1. – С. 56–60.
2. Странадко Е.Ф. Исторический очерк развития фотодинамической терапии // Лазерная медицина. – 2002. – Т.6, вып. 1. – С. 4–8.
3. Mroz P., Yaroslavsky A., Kharkwal G.B. Cell death pathways in photodynamic therapy of tumors // Cancers. – 2011. – Vol. 3. – P. 2516–2539.
4. Weiss A., den Bergh H.V., Griffioen A.W. Angiogenesis inhibition for the improvement of photodynamic therapy: The revival of a promising idea // Biochim. Biophys. Acta. – 2012. – Vol. 1826. – P. 53–70.
5. Sharma K.V., Bowers N., Davids L.M. Photodynamic therapy-induced killing is enhanced in depigmented metastatic melanoma cells // Cell Biol. Int. – 2011. – Vol. 35. – P. 939–949.
6. Sparsa A., Bellaton S., Naves T., et al. Photodynamic treatment induces cell death by apoptosis or autophagy depending on the

7. Chang C.J., Yu J.S., Wei F.C. In vitro and In vivo photosensitizing applications of photofrin in malignant melanoma cells, *Chang Gung Med. J.*, 2008, vol. 31, pp. 260–267.

melanin content in two B16 melanoma cell lines // Oncol. Rep. – 2013. – Vol. 29. – P. 1196–1200.
7. Chang C.J., Yu J.S., Wei F.C. In vitro and In vivo photosensitizing applications of photofrin in malignant melanoma cells // Chang Gung Med. J. – 2008. – Vol. 31. – P. 260–267.

IMPROVING THE EFFICIENCY OF BLADDER CANCER DIAGNOSTIC CYSTOSCOPY WITH 5-ALA HEXYL ESTER

Kaprin A.D. [1,2], **Trushin A.A.**[3], **Golovachenko M.P.**[1], **Ivanova-Radkevich V.I.**[2], **Chissov V.I.**[3], **Filonenko E.V.**[1]
[1]P.A. Herzen Moscow Oncology Research Center – branch of FSBI NMRRC of the Ministry of Health of Russia, Moscow, Russia
[2]Peoples' Friendship University of Russia (RUDN University), Moscow, Russia
[3]Sechenov First Moscow State Medical University, Moscow, Russia

Abstract

This article presents the results of a clinical study that examined the diagnostic efficacy of fluorescent diagnostics (FD) of non-muscular-invasive bladder cancer using a photosensitizer of FD of malignant neoplasms – 5-aminolevulinic acid hexyl ester (5-ALA HE) compared with standard cystoscopy. The study involved 110 patients. The study began with intravesical administration of 50 ml of 0.2% solution of 5-ALA HE, the exposure time was 1 hour, after which the drug was removed from the organ. During the next hour, the mucous membranes were examined in two cystoscopy modes, followed by a standard transurethral resection of all urothelium sites with suspicion for tumor lesion based on white light and visible red fluorescence, and a control blind biopsy from the visually unchanged and non-fluorescent mucous tissue in each patient. The results of the study indicate the high effectiveness of the developed FD methodology with 5-ALA HE in detecting non-muscular-invasive bladder cancer during intravesical administration of the drug, due to selective accumulation of hexasens-induced PPIX in the tumor tissue compared with healthy mucosa. Compared with the results of standard cystoscopy, fluorescence diagnostics significantly increased diagnostic sensitivity by 24.4% (from 75.1% to 99.5%), diagnostic accuracy – by 15.8% (from 82.4% to 98.2%) and a negative predictive value – by 33.2% (from 65.8% to 99%) ($p \leq 0.05$). Additionally, a total of 37 (33.6%) patients was found to have 63 foci of fluorescence with a diameter of 2.5 to 3.0 mm. 59 of these were morphologically confirmed to contain cancer cells.

Key words: 5-aminolevulinic acid hexyl ester, bladder cancer, fluorescent diagnostics.

For citations: Kaprin A.D., Trushin A.A., Golovachenko M.P., Ivanova-Radkevich V.I., Chissov V.I., Filonenko E.V. Improving the efficiency of bladder cancer diagnostic cystoscopy with 5-ALA hexyl ester, *Biomedical Photonics*, 2019, vol. 8, no. 1 , pp. 29–37. (in Russian) doi: 10.24931/2413–9432–2019–8–1-29–37.

Contacts: Trushin A.A., e-mail: a.trooshin@gmail.com

ПОВЫШЕНИЕ ЭФФЕКТИВНОСТИ ДИАГНОСТИКИ РАКА МОЧЕВОГО ПУЗЫРЯ ПРИ ИСПОЛЬЗОВАНИИ ЦИСТОСКОПИИ С ГЕКСИЛОВЫМ ЭФИРОМ 5-АЛК

А.Д. Каприн[1,2], **А.А. Трушин**[3], **М.П. Головащенко**[1], **В.И. Иванова-Радкевич**[2], **В.И. Чиссов**[3], **Е.В. Филоненко**[1]
[1]МНИОИ им. П.А. Герцена – филиал ФГБУ «НМИЦР» Минздрава РФ, Москва, Россия
[2]Российский Университет дружбы народов, Москва, Россия
[3]ФГАОУ ВО Первый МГМУ им. И.М. Сеченова Минздрава России (Сеченовский Университет), Москва, Россия

Резюме

В работе отражены результаты клинического исследования, в котором изучена диагностическая эффективность флуоресцентной диагностики (ФД) немышечно-инвазивного рака мочевого пузыря с использованием препарата для ФД злокачественных новообразований – гексилового эфира 5-аминолевулиновой кислоты (ГЭ 5-АЛК) в сравнении со стандартной цистоскопией. В исследование участвовали 110 пациентов. Исследование начинали с внутрипузырного введения 50 мл 0,2%-го раствора ГЭ 5-АЛК, время экспозиции составило 1 ч, после чего препарат удаляли из органа. В течение последующего часа проводили осмотр слизистой в двух режимах цистоскопии. Затем проводили трансуретальную рецзекцию всех подозрительных участков уротелия на опухолевое поражение в белом свете и из зон визуальной красной флуоресценции, а также у каждого пациента осуществляли контрольную «слепую» биопсию из визуально неизмененной и нефлуоресцирующей слизистой. Результаты исследования свидетельствуют о

высокой эффективности разработанной методики. Флуоресцентная диагностика по сравнению с результатами стандартной цистоскопии достоверно повысила чувствительность диагностики на 24,4% (с 75,1% до 99,5%), точность диагностики – на 15,8% (с 82,4% до 98,2%) и отрицательную прогностическую ценность – на 33,2% (с 65,8% до 99%) ($p \leq 0,05$). Дополнительно, в общей сложности у 37 (33,6%) больных, обнаружены 63 очага флуоресценции диаметром от 2,5 до 3,0 мм, на неизмененных в белом свете участках слизистой оболочки, в 59 из которых морфологически подтвержден рак мочевого пузыря.

Ключевые слова: гексиловый эфир 5-аминолевулиновой кислоты, рак мочевого пузыря, флуоресцентная диагностика.

Для цитирования: Каприн А.Д., Трушин А.А., Головащенко М.П., Иванова-Радкевич В.И., Чиссов В.И., Филоненко Е.В. Повышение эффективности диагностики рака мочевого пузыря при использовании цистоскопии с гексиловым эфиром 5-АЛК // Biomedical Photonics. – 2019. – Т. 8, № 1. – С. 29–37. Doi: 10.24931/2413–9432–2019–8–1-29–37.

Контакты: Трушин А.А., e-mail: a.trooshin@gmail.com

Introduction

The number of newly diagnosed cases of malignant neoplasms in the world is growing steadily, and bladder cancer (BC) is no exception. In the general structure of cancer incidence, this pathology has the 9th place [1]. In Russia, in 2017, bladder cancer accounted for 2.7% and had 70% in the total prevalence of all genitourinary system neoplasms. Bladder cancer is the second most prevalent urological disease and the third in the group in terms of lethality. Every year, over 13,000 patients in our country are registered with the diagnosis of bladder cancer diagnosed for the first time, and more than 6,000 patients with the disease die each year. Over the past ten years, an increase in incidence of 24.35% has been recorded, with an average annual increase of 2.15% [2].

An extremely important task is early detection of bladder tumors, the morphological structure of which in more than 90% of cases is represented by urothelial cancer. When bladder cancer is first diagnosed, 70–85% of cases are those of a non-muscle-invasive tumor (Ta, Tis, T1), which is diagnosed in the Russian Federation in no more than 30% of cases, which is significantly inferior to world best practices, where this figure reaches 80% [3, 4].

The problem of identifying early forms of bladder cancer is an urgent topic in modern oncourology, obviously related not only to untimely diagnosis of malignant tumors, but also to incorrect staging, where the error rate reaches 73% [5]. Bladder tumors with invasion no deeper than the mucosal/submucosal layer often remain unnoticed due to the impossibility of visualization of all the foci during standard cystoscopy in white light due to its resolution [6]. In some cases, this routine diagnostic method does not allow to determine the true boundaries of the lesion, to obtain sufficient information about the number of multifocal lesions, to assess the depth of the invasion, to visualize the foci of *carcinoma in situ* (CIS), and it also does not provide a sufficiently complete quantitative and prognostic characteristic of Ta and T1 tumors [7].

An inadequate assessment of tumor lesions in urothelium after transurethral resection (TUR) can lead to errors in the choice of treatment tactics, and also leads to a high risk of residual Cis, Ta, T1 foci, while in 81% of patients relapses are localized in the surgical area [8]. Moreover, standard cystoscopy does not make it possible to remove the tumor tissue completely, and its residual fragments often remain in the surgical margin of the resection, as it is diagnosed in 40–70% of secondary TUR [9]. These are not true recurrences, and they are more associated with many undetected tumor buds, fuzzy visualization of malignant changes in the resection margin, and false negative results of the biopsy taken randomly [10].

Thus, the limitations in the use of standard cystoscopy and its low information value in the diagnosis of intraepithelial tumor formations have led to an increased interest in studying the effectiveness of various diagnostic approaches capable of recognizing microscopic tumors, often outwardly not different from surrounding healthy tissues, and this was the beginning of the search for new modern techniques capable of improving the light marking of malignant neoplasms, among which the most promising is fluorescence diagnosis (FD). This method is based on the possibility of recognizing, with the use of special equipment, the pathological tissues by the characteristic fluorescence of exogenous or endogenous fluorochromes induced by light radiation, which makes it possible to clarify the boundaries of a tumor and detect foci that are not visible to the naked eye in white light [11].

The effectiveness of the method depends on the level of accumulation and localization of the dye in individual structures of the tumor focus and the surrounding tissue, which can be achieved by stimulating the body to produce endogenous photoactive compounds, porphyrins, in particular, endogenous photoactive protoporphyrin IX (PPIX) [12]. The induction of this biological substance is visualized by the high fluorescence contrast between the tumor and the surrounding tissue, which is important for identifying and clarifying the boundaries of the spread of the tumor, as the method simultane-

ously increases the radicalness of the surgical effect and reduces the damage to the tissues surrounding the tumor. Such a compound is 5-aminolevulinic acid (5-ALA), one of the intermediate products of synthesis of heme, the precursor of porphyrins, which is quickly utilized in healthy tissues, turning into heme under the action of ferrochelatase. Tumor tissue is found to be deficient in this enzyme, and with excessive administration of 5-ALA, a temporary but significant increase in the level of porphyrins occurs [13].

Continued research to improve the physicochemical properties of porphyrins and the diagnostic ability of PD has led to the development of a drug based on 5-ALA of the second generation, 5-ALA hexyl ester (HE 5-ALA), which is metabolized to 5-ALA in the body. Being more lipophilic compounds than 5-ALA, esters are better at penetrating biological membranes, so they accumulate in cells faster and to a greater extent, and become included in biosynthesis as PPIX precursors [14].

One of the promising directions for the use of HE 5-ALA as an agent for PD in oncourology is the diagnosis of early stage bladder cancer in the process called fluorescence cystoscopy with the use of blue light and various photosensitizers for marking tumors by intravesical administration [15, 16].

The purpose of the study was to increase the efficiency of the diagnosis of non-muscle-invasive bladder cancer with intravesical administration of 5-ALA hexyl ester.

Materials and methods

The study included 110 patients, more than half of whom had complaints were associated with a pre-cancer pathology of the genitourinary system, mainly those of disuria, discomfort in the bladder, as well as macro- and microhematuria. The study group was represented mainly by males, in a ratio of 3.7:1, aged over 60.

At the first stage, all patients underwent an outpatient screening examination in order to identify primary patients with non-muscle-invasive bladder cancer . Significant factors affecting the selection of patients were cystoscopy, echographic and, in some cases, X-ray studies which were used to evaluate the number and size of tumor foci and their localization.

Standard cystoscopy in white light mode and fluorescence mode was performed with the use of the instruments and equipment manufactured by Karl Storz (Germany), including a hard cystoscope equipped with a special filter with transmission characteristics corresponding to the maximum excitation in the blue range of the PPIX fluorescence spectrum (380-440 nm) which makes it possible to visualize pathological changes in urothelium against the background of surrounding healthy tissues. A hard resectoscope equipped with fluorescence optics, with an outer diameter of F26 was used for endo-surgical intervention on the bladder mucosa.

For fluorescence diagnostics, HE 5-ALA was used, which is an odorless, hygroscopic fine-crystalline white powder, readily soluble in water and water-salt solutions.

The study began with the intravesical administration of 50 ml of a 0.2% solution of HE 5-ALA, for the exposure of 1 hour, after which the solution was removed from the bladder. Over the next hour, a series of sequential and successive stages were carried out, which included standard and fluorescence cystoscopy and TUR of the tumor in PD conditions. During cystoscopy in the white light mode, attention was paid to the volume of the organ, changes in the state and color of the mucosa at the site where the search for pathological lesions was performed. The characteristics evaluated in the visualization of the tumor foci were their localization, macroscopic structure (the nature of the villi structure), size, growth pattern, quantity, condition of the surrounding mucous membrane, relation to the mouths of the ureters, the severity of the vascular pattern of the tumor itself and the submucosal layer.

The transition to fluorescence mode made it possible to identify the following types of sites: Type I: sites suspicious of cancer in white light and not fluorescent in blue light; Type II: sites suspicious of cancer in white light and fluorescent in blue light; Type III: additional foci that fluoresce in blue light with sizes from 2.5 to 3.0 mm in diameter and are not visible in ordinary light; Type IV: non-fluorescent normal white parts of the unchanged mucosa. After the completion of the mucosal examination in the two modes of cystoscopy, a standard TUR was performed in respect of all urothelium sites suspicious for tumor lesion in white light and the sites of visual red fluorescence, and in each patient a control "blind" biopsy was performed from a visually unchanged and non-fluorescent mucosa. Electroresection of the mucosa of the bladder was carried out within the mucosa or with the removal of the base of the pathological focus with muscle wall in order to determine the depth of the invasion in case the tumor nature of the changes is confirmed. After the completion of all stages of the study, a second blue-light inspection was performed to control the radical extent of TUR. Any fluorescent sites that were detected were resected. All the collected histological material was subjected to a routine study, the result of which was final in the diagnosis of intravesical pathology and made it possible to determine the nature of morphostructural changes in the bladder mucosa. The average number of foci studied in one patient was 3.2.

Focal formations of the bladder mucosa identified during cystoscopy in the two diagnostic modes were marked in accordance with the classification developed by P. A. Herzen Moscow Oncology Research Center: V (+): the tumor is determined visually when viewed in white light, V (-): when viewed in white light, the tumor is not determined; F (+): a focus of fluorescence, F (-): fluores-

cence is not determined; T (+): elements of a malignant neoplasm were detected, T (-): elements of a malignant neoplasm were not found. Depending on the results of standard and fluorescence cystoscopy and morphological data, a calculation was performed of true positive (TP), true negative (TN), false positive (FP), and false negative (FN) results.

Results

The total number of foci studied in the two modes of cystoscopy in all patients was 352: 179 (50.8%) with visually detectable pathology suspicious of the tumor process; 173 (49.2%) unchanged in the white light. Fluorescence was recorded in 241 (68.5%) of the foci; in the remaining 111 (31.5%), no fluorescence was observed. The bright fluorescence of HE 5-ALA-induced PPIX was visualized in 178 (99.4%) foci (V(+)F(+)) which in white light were found to have a cellular or rough mucosa with hypervascularization elevated relative to the surrounding tissues, and also those with single or multiple papillomatous growths. The majority of the villous formations had microscopic dimensions, less than 0.5 cm (79.6%), while the rest were up to 3.0 cm (12.5%) and over 5.0 cm (7.9%). Additionally, in 37 (33.6%) patients, 63 (36.4%) foci of fluorescence with a diameter of 2.5 mm to 3.0 mm were detected, unchanged in white light (V(-)F(+)), with the maximum number of such lesions found in one patient being 3. From the point of view of increasing the efficiency of bladder tumors diagnosis, the PD method is aimed at identifying these very areas that cannot be detected in white light but are highly likely to be tumors, and, therefore, are of considerable practical interest. Fluorescence was not determined in one focus with the clinical picture of hyperemia, which was highly suspicious of tumor changes (0.9%) (V(+)F(-)), and in all 110 (99.1%) areas of control biopsies (V(-)F(-)) (Table 1).

A histological examination of all urothelium biopsy specimens (n = 241) resected in the foci with bright fluorescence verifiedurothelial cancer (T+) in 236 (97.9%) of them, and non-specific inflammatory process in the remaining 5 (2.1%). Moreover, of 236 F(+)T(+) foci: there were 177 foci of V(+) and 59 foci of V(-); and among 5 foci F(+) T(-): there was 1 focus of V(+) and 4 foci of V(-).

In the study of 178 urothelium tissue samples represented in white light by foci of intense hyperemia highly suspicious of cancer and emitting bright fluorescence (V(+)F(+)) in blue light mode, tumor changes were detected in 177 (99.4%) of them (T(+)). In one (0.6%) biopsy sample collected in a cancer-suspected vascularization site, which in the blue light mode had a brightly fluorescent epithelium (V(+)F(+)), no tumor changes were found during histological examination, and a metaplastic process had place (T(-)).

A histological examination of 63 foci of additionally detected red fluorescence which in the white light mode looked like urothelium without pathological changes (V(-)F(+)) revealed transitional cancer (T(+)) in 59 (93.6%) of the foci. In all these cases, tumor growth was determined in multifocal buds not visible in the white light mode. In the remaining 4 (6.4%) foci of additional fluorescence (V(-)F(+)), which seemed unchanged in standard cystoscopy, inflammatory changes of a nonspecific nature were diagnosed: granular and glandular cystitis (T(-)).

In one focus (0.9%) of hypervascularization suspicious of a tumor process, but without fluorescence phenomena (V(+)F(-)), a nonspecific inflammatory process of glandular cystitis type was histologically diagnosed (T(-)) (Table 2). All data of histological examination of biopsy specimens performed according to the results of cystoscopic examination in the two imaging modes were statistically significant ($p \leq 0.05$). (Table 2.). It should be noted that in foci with visually unchanged mucosa, fluorescence was more intense with tumor lesions than in epithelium with a non-specific inflammatory process.

The morphological structure of tumors in all urothelium biopsy specimens was represented by transitional cell carcinoma of varying degrees of differentiation. Stages Ta-T1 and Tis were diagnosed in 156 (87.6%) and 21 (11.8%) foci of V(+)F(+), respectively, including low grade (G1): 51.1%, intermediate grade (G2): 38.6%; and high grade (G3): 10.3%. In 9 (15.3%) additionally identified foci with malignant changes in the surface epithelium (V(-)F(+)), Ta-T1 stages were established, and Tis was found in 50 (84.7%), with the degree of tumor differentiation being mainly G1 and G2. Almost the same percentage of CIS cases was found in tumors with exophytic growth and those almost undetectable in the white light mode. In the first case, the surface epithelium in the CIS localization zone was accompanied by the phenomena

Таблица 1
Результаты стандартной и флуоресцентной цистоскопии с ГЭ 5-АЛК при внутрипузырном введении

Table 1
Results of standard and fluorescent cystoscopy with 5-ALA HE with intravesical administration

Результаты стандартной цистоскопии и ФД Results of standard and fluorescent cystoscopy			
V(+)F(+)	V(–)F(+)	V(+)F(–)	V(–)F(–)
178 (73,8%)	63 (26,2%)	1 (0,9%)	110 (99,1%)
F(+) n=241		F(–) n=111	

«V(+)» – в белом свете определяется опухоль, «V(–)» – опухоль в белом свете не определяется, «F(+)» – участки флуоресцирующей ткани, «F(–)» – участки не флуоресцирующей ткани.

V(+) – tumor is detected in white light, V(–) – tumor is not detected in white light, F(+) – areas of fluorescent tissue, F(–) – areas of non-fluorescent tissue.

Таблица 2
Сопоставление результатов стандартной и флуоресцентной цистоскопии с данными гистологического исследования
Table 2
Comparison of standard and fluorescent cystoscopy results with histological examination data

Гистологическое исследование Histological examination	V(+)F(+)	V(+)F(–)	V(–)F(–)	V(–)F(+)
T(+) n=236	177 (75,0%)	–	–	59 (25,0%)
T(–) n=116	1 (0,9%)	1 (0,9%)	110 (94,8%)	4 (3,4%)
n= 352	n=178	n=1	n=110	n=63

«V(+)» – в белом свете определяется опухоль, «V(–)» – опухоль в белом свете не определяется; «F(+)» – участки флуоресцирующей ткани, «F(–)» – участки не флуоресцирующей ткани. «T(+)» данные морфологического исследования подтверждают наличие РМП; «T(–)» данные морфологического исследования не подтверждают наличие РМП.

V(+) – tumor is detected in white light, V(–) – tumor is not detected in white light, F(+) – areas of fluorescent tissue, F(–) – areas of non-fluorescent tissue, T(+) –the presence of bladder cancer is confirmed by morphology, T(–) – the presence of bladder cancer is not confirmed by morphology .

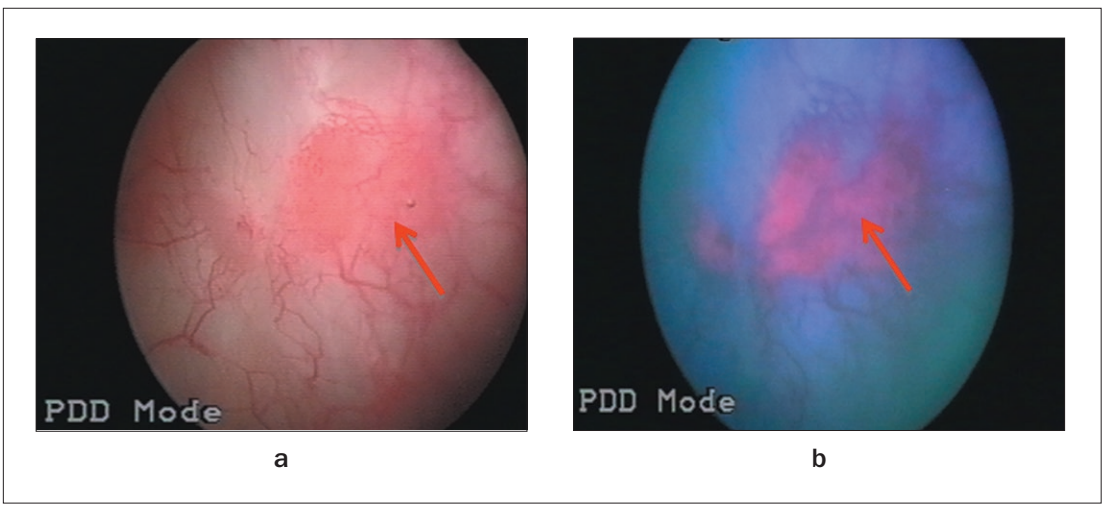

Рис. 1. Участок уротелия с картиной гиперемии подозрительного на рак характера *(a)*, флуоресцирующий ярким свечением *(b)*
Fig. 1. An area of urothelium with hyperemia with cancer-like characteristics *(a)*, with bright fluorescence *(b)*

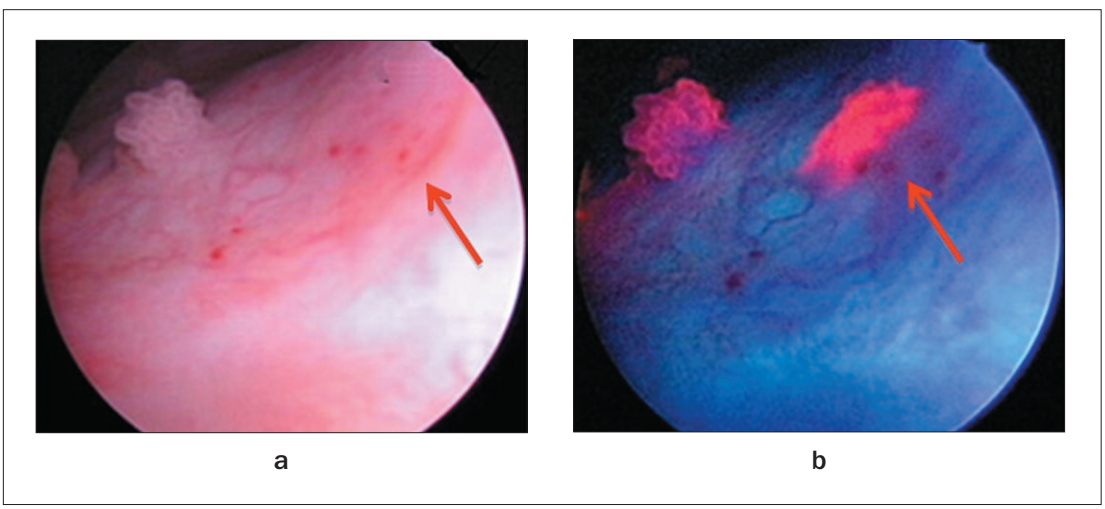

Рис. 2. Участок слизистой оболочки неизмененный в режиме белого света *(a)*, флуоресцирующий ярким свечением *(b)*
Fig. 2. An area of the mucous membrane almost unchanged in the white light mode *(a)*, with bright fluorescence *(b)*

Таблица 3
Оценка результатов цистоскопии в белом свете
Table 3
Evaluation of the results of cystoscopy in white light

Цистоскопия в белом свете Cystoscopy in white light	Всего Total	Морфологическое исследование Morphological examination		Оценка результатов Evaluation of results
		T(+)	T(–)	
V(+)	179	177 (97,6%)	2 (2,4%)	ИП 177; ЛП 2 TP 177; FP 2
V(–)	173	59 (34,2%)	114 (65,8%)	ЛО 59; ИО 114 FN 59; TN 114

«V(+)» – в белом свете определяется опухоль, «V(–)» – опухоль в белом свете не определяется. «T(+)» – морфологически подтверждена ткань опухоли, «T(–)» – морфологически подтверждена ткань мочевого пузыря.

ИП – истинноположительный. ИО – истинноотрицательный. ЛП – ложноположительный. ЛО – ложноотрицательный.

V(+) – tumor is detected in white light, V(–) – tumor is not detected in white light, T(+) –the presence of bladder cancer is confirmed by morphology, T(–) – the presence of bladder cancer is not confirmed by morphology .

TP – true positive. TN – true negative. FP – false positive. FN – false negative.

Таблица 4
Оценка результатов флуоресцентной цистоскопии
Table 4
Evaluation of the fluorescent cystoscopy results

Флуоресцентная цистоскопии Fluorescent cystoscopy	Всего Total	Морфологическое исследование Morphological examination		Оценка результатов Evaluation of results
		T(+)	T(–)	
F(+)	241	236 (97,9%)	5 (2,1%)	ИП 236; ЛП 5 TP 236; FP 5
F(–)	111	–	111 (100%)	ЛО 0; ИО 111 FN 0; TN 111

«F(+)» – участки флуоресцирующей ткани, «F(–)» – участки не флуоресцирующей ткани, «T(+)» – морфологически подтверждена ткань опухоли, «T(–)» – морфологически подтверждена ткань мочевого пузыря.

ИП – истинноположительный. ИО – истинноотрицательный. ЛП – ложноположительный. ЛО – ложноотрицательный.

F(+) – areas of fluorescent tissue, F(–) – areas of non-fluorescent tissue, T(+) –the presence of bladder cancer is confirmed by morphology, T(–) – the presence of bladder cancer is not confirmed by morphology.

TP – true positive. TN – true negative. FP – false positive. FN – false negative.

of hyperemia or inflammation, had a pronounced cellular or rough appearance (Fig. 1), in the second, the sites had virtually unchanged mucosa site (Fig. 2). Fluorescence with HE 5-ALA made it possible to detect intraepithelial malignant changes more than twice as often as with standard cystoscopy, since microscopic CIS can be skipped during cystoscopy or considered as an area of inflammation if a biopsy is not performed. In more than half of the cases (54.6%), these foci of tumor growth were isolated, in 32.6%, they were localized along the edge of papillary growths, and in a smaller percentage of cases, in their structure (12.8%).

With standard cystoscopy, 177 (97.6%) foci with visually determined tumor pathology were recognized as true positive. 2 foci (2.4%) were treated as false positive due to the absence of a malignant process in the test material, but the endoscopic pattern was highly suspicious of urothelial cancer. A false-negative result was found in 59 (34.1%) foci of urothelium unchanged in the white light, but the histological examination revealed non-muscle-invasive bladder cancer detected only by HE-ALK-induced PPIX fluorescence. True negative cases were reported in 4 (2.3%) tissue samples without visually detectable pathology, but with fluorescence phenomena caused by nonspecific inflammation. 110 (63.5%) control biopsies (V(-)F(-)) were also classified as true negative results, with tumor cells found in none of them (Table 3).

236 (97.9%) foci of bright red luminescence of HE 5-ALA-induced PPIX represented by transition-cell bladder cancer were classified as true positive (TP) results of fluorescence cystoscopy: 177 (75.0%) clinically determined and 59 (25%) additionally identified. In 5 (2.1%)

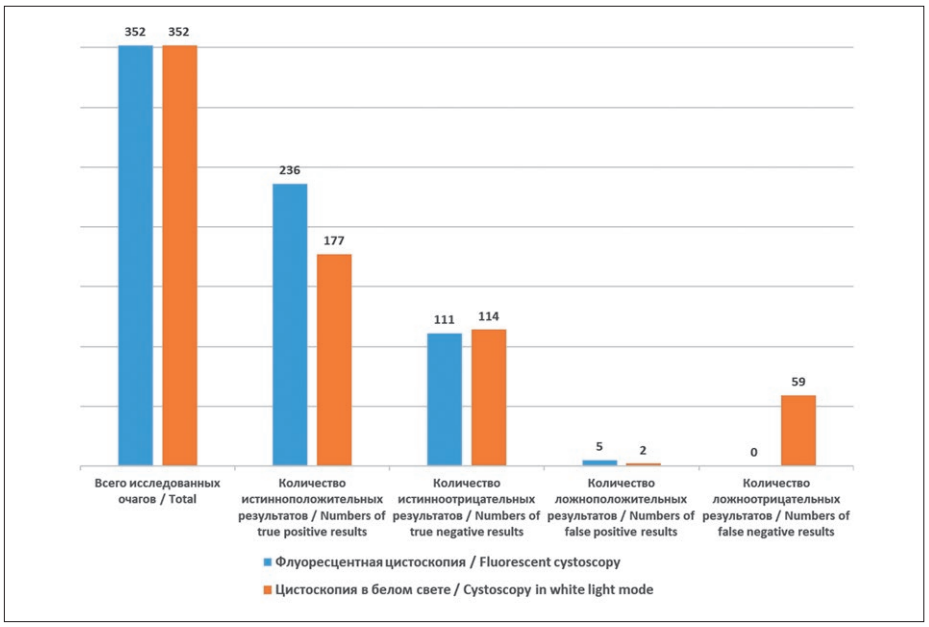

a

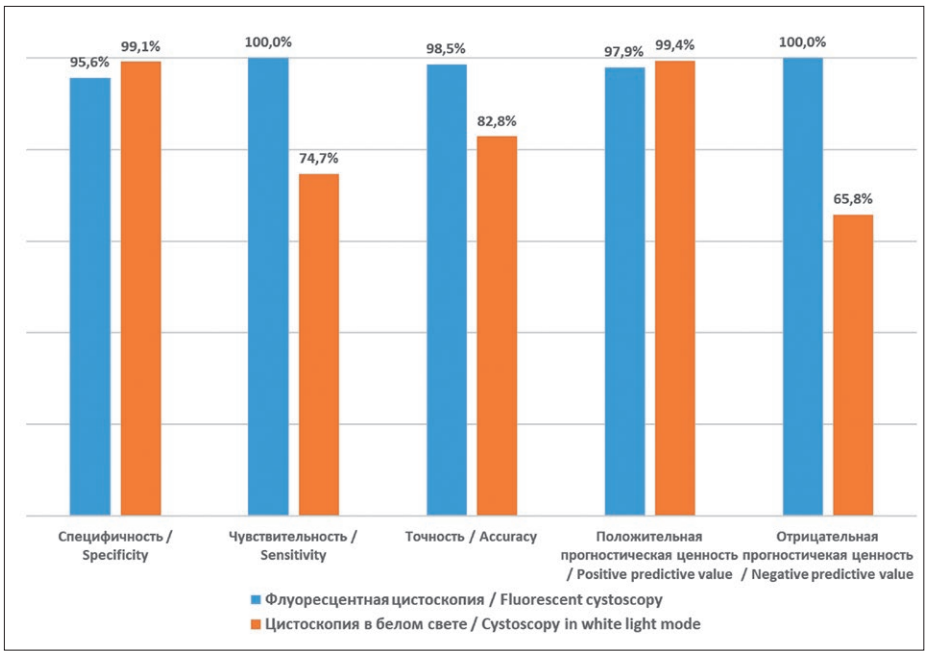

b

Рис. 3. Показатели диагностической эффективности флуоресцентной и стандартной цистоскопии *(a, b)*
Fig. 3. Indicators of diagnostic efficiency of fluorescent and standard cystoscopy *(a, b)*

fluorescence sites, the tumor process was not confirmed, which indicates a false-positive result: in 4 samples of resected urothelium, inflammatory changes of glandular and granular cystitis type were diagnosed, and metaplasia in 1 case. A truly negative result was established in 110 control studies (n = 110), in each of which there was no fluorescence and the tumor process was not detected. In one case (0.9%), a truly negative result was found at a site suspicious for cancer but without fluorescence phenomena, in which a nonspecific inflammatory process of glandular cystitis type was revealed. None of the studies found false negative results (Table 4).

The sensitivity of standard cystoscopy was 74.7%, its specificity: 99.1%. The positive predictive value was

99.4%, the negative predictive value was 65.8%. The accuracy value was 82.8%.

The sensitivity of fluorescence cystoscopy was 100%, and its specificity 95.6%. The positive predictive value corresponded to 97.9%, the negative predictive value was 100%, and accuracy rate was 98.5%. The results of the assessment of diagnostic parameters of cystoscopy in white light and in the fluorescence mode are shown in Fig. 3.

As can be seen from the data presented in Fig. 3b, PD significantly increased the sensitivity of diagnosis by 25.3% (from 74.7% to 100%), the accuracy of diagnosis by 15.7% (from 82.8% to 98.5%) and its negative predictive value by 34.2% (from 65.8% to 100%) ($p \leq 0.05$).

The sensitivity index seems to be a very important parameter at the stage of preoperative diagnosis, since it characterizes the possibility of identifying tumor foci that were not detected by standard cystoscopy and makes it possible to perform a more complete surgical removal of the tumor.

A greater number of false-positive results was obtained in PD (5 foci in 4 patients) than with standard cystoscopy (1 focus in 1 patient). These cases of false glow of urothelium were observed in the foci of inflammation, which led to a slight decrease in the specificity and positive prognostic value of PD (95.6% and 97.9%, respectively) in relation to the values of white light cystoscopy (99.1% and 99.4%, respectively) ($p \leq 0.05$).

A clinically significant difference in the diagnostic efficacy of fluorescence and standard cystoscopy was assumed to be a difference of more than 10%. Based on this value, we can conclude that the effectiveness of the PD method in terms of sensitivity, accuracy and negative prognostic value is significantly higher than the effectiveness of cystoscopy in white light. At the same time, the difference in specificity and positive prognostic value was significantly less than 10% (3.5% and 1.5%, respectively) and, therefore, cannot be considered clinically significant.

Conclusion

Thus, the results of the study indicate the high efficiency of the developed PD technique with the intravesical administration of HE 5-ALA in the detection of non-muscle-invasive bladder cancer due to the selective accumulation of HE 5-ALA induced PPIX in tumor tissue compared to healthy mucosa. The high contrast between the tumor and the surrounding tissues due to fluorescence revealed 59 additional tumor sites, which is 2.3 times higher than with standard cystoscopy. A significant increase in the diagnostic sensitivity from 74.7% (with standard cystoscopy) to 100% was achieved by detecting hidden foci of multifocal growth and determination of the true boundaries of the malignant process between the altered and unchanged epithelium, making them more clear and visible than with standard cystoscopy. The approach with the use of fluorescence during primary TUR determines the radical volume of treatment, which significantly reduces the likelihood of residual processes in the bladder mucosa, respectively reducing the risk of identification of a malignant process at a later stage, the development of relapses and disease progression.

REFERENCES

1. Antoni S., Ferlay J., Soerjomataram I., Znaor A., Jemal A., Bray F. Bladder Cancer Incidence and Mortality: A global Overview and Trends, *Eur.urol.*,2017, vol. 71(1), pp. 96–108.
2. *Zlokachestvennye novoobrazovaniya v Rossii v 2016 godu (zabolevaemost' i smertnost')* [Malignant neoplasms in Russia in 2016 (morbidity and mortality)], by Kaprin A.D., Starinskii V.V., Petrova G.V. as eds. Moscow, MNIOI im. P.A. Gertsena – filial FGU «NMIRC» Minzdrava Rossii Publ., 2018. 250 p.
3. Lelyavin K.B., Dvornichenko V.V. Muscle non-invasive bladder cancer: clinical and morphological features, results of treatment, survival analysis, *Byulleten VSNC SO RAMN*, 2013, vol. 93, no, 5, pp. 53–59.
4. Morgan T.M., Keegan K.A., Clark P.E. Bladder cancer, *Curr Opin Oncol*, 2011, vol. 23, pp. 275–282.
5. Schenkman E., Lamm D.L. Superficial bladder cancer therapy, *Scientific World Journal*, 2004, vol 28, no. 4, suppl. 1, pp. 387–99.
6. Volkova M.I., Matveev V.B., Medvedev S.V., Nosov D.A., Figurin K.M., Khmelevskiy E.V., Chernyaev V.A. *Klinicheskie rekomendacii po diagnostike i lecheniyu bolnykh rakom mochevogo puzyrya* [Clinical guidelines for the diagnosis and treatment of patients with bladder cancer]. Moscow, 2014. 32 p. URL: http://www.oncology.ru/association/clinical-guidelines/2014/25.pdf
7. Martov A.G., Ergakov D.V., Andronov A.S. Recurrence of muscular non-invasive bladder cancer: possible endoscopic solutions, *Onkourologiya*, 2010, no. 1, pp. 6–13.

ЛИТЕРАТУРА

1. Antoni S., Ferlay J., Soerjomataram I., et al. Bladder Cancer Incidence and Mortality: A global Overview and Trends // Eur. urol. – 2017. – Vol. 71(1). – P. 96–108.
2. Злокачественные новообразования в России в 2016 году (заболеваемость и смертность) / под ред. А.Д. Каприна, В.В. Старинского, Г.В. Петровой. – М.: МНИОИ им. П.А. Герцена – филиал ФГУ «НМИРЦ» Минздрава России, 2018. – 250 с.
3. Лелявин К.Б., Дворниченко В.В. Мышечно-неинвазивный рак мочевого пузыря: клинические и морфологические особенности, результаты лечения, анализ выживаемости // Бюллетень ВСНЦ СО РАМН. – 2013. – Т. 93, № 5. – С. 53–59.
4. Morgan T.M., Keegan K.A., Clark P.E. Bladder cancer // Curr Opin Oncol. – 2011. – Vol. 23. – P. 275–282.
5. Schenkman E., Lamm D.L. Superficial bladder cancer therapy // Scientific World Journal. – 2004. – Vol 28, No. 4, Suppl. 1. – P. 387–99.
6. Волкова М.И., Матвеев В.Б., Медведев С.В. и др. Клинические рекомендации по диагностике и лечению больных раком мочевого пузыря. – Москва, 2014. – 32 р. URL http://www.oncology.ru/association/clinical-guidelines/2014/25.pdf
7. Мартов А.Г., Ергаков Д.В., Андронов А.С. Рецидивирование мышечно-неинвазивного рака мочевого пузыря: возможные эндоскопические пути решения проблемы // Онкоурол. – 2010. – № 1. – С. 6–13.

8. Van Rhijn B.W.G., Burger M., Lotan Y. Reccurrence and Progression of disease in Non-Muscle Invasive Bladder Cancer: From Epidemiology to Treatment Strategy, *Eur. Urol.*, 2009, vol. 56, no. 3, pp. 430–442.
9. Adiyat K.T., Katkoori D., Soloway C.T., De los Santos R., Manoharan M., Soloway M.S. Complete transurethral resection of bladder tumor: are the guidelines being followed?, *Urology*, 2010, vol. 75, pp. 365–367.
10. Mariappan P., Zachou A., Grigor K.M. Detrusor muscle in the first, apparently complete transurethral resection of bladder tumour specimen is a surrogate marker and is dependent on operator experience, *Eur. Urol.*, 2010, vol. 57(5), pp. 843–849.
11. *Fluorestsentnaya diagnostika i fotodinamicheskaya terapiya v onkologii. Monografiya* [Fluorescent diagnostics and photodynamic therapy in oncology. Monograph], by Chissov V.I., Filonenko E.V. as eds. Moscow, Triumf Publ., 2012. 269 p.
12. Stepp H.G., Baumgartner R., Beyer W., Knuechel R., Koerner T.O., Kriegmair M., Rick K., Steinbach P., Hofstetter A.G. Fluorescence imaging and spectroscopy of ALA –induced protoporphyrin IX preferentially accumulated in tumor tissue, *Proc. SPIE*, 1995, vol. 2627, pp. 13–24.
13. Fotinos N., Campo M.A., Popowycz F., Gurny R., Lange N. 5-Aminolevulinic acid derivatives in photomedicine: Characteristics, application and perspectives, *Photochem Photobiol*, 2006, vol. 82, no. 4, pp. 994–1015
14. Yakubovskaya R.I., Kazachkina N.I., Plyutinskaya A.D. The new Russian agent Hexasens-lio for fluorescence diagnosis and photodynamic therapy for malignancies, *Rossiyskiy onkologicheskiy zhurnal*, no. 2, 2009.
15. Slesarevskaya M.N., Sokolov A.V. Experience of using fluorescent cystoscopy in the diagnosis of superficial bladder cancer, *Urologicheskie vedomosti*, 2014, vol. IV, no. 1, pp. 3–7.
16. Ivanova-Radkevich V.I., Filonenko E.V., Slovokhodov E.K., Smirnova I.P., Kuznetsova O.M., Lobaeva T.A., Gushchina Y.S., Khadasheva Z.S. Organization of clinical trials of photosensitizer based on 5-aminolevulinic acid hexyl ester, *Indian Journal of Science and Technology*, 2016, vol. 9(18). doi: 10.17485/ijst/2016/v9i18/93759

8. Van Rhijn B.W.G., Burger M., Lotan Y. Reccurrence and Progression of disease in Non-Muscle Invasive Bladder Cancer: From Epidemiology to Treatment Strategy // Eur. Urol. – 2009. – Vol. 56, No. 3. – P. 430–442.
9. Adiyat K.T., Katkoori D., Soloway C.T., et al. Complete transurethral resection of bladder tumor: are the guidelines being followed? // Urology. – 2010. – Vol. 75. – P. 365–367.
10. Mariappan P., Zachou A., Grigor K.M. Detrusor muscle in the first, apparently complete transurethral resection of bladder tumour specimen is a surrogate marker and is dependent on operator experience // Eur. Urol. – 2010. – Vol. 57(5). – P. 843–849.
11. Флуоресцентная диагностика и фотодинамическая терапия в онкологии. Монография / под ред. В.И. Чиссова, Е.В. Филоненко. – Москва: Триумф, 2012. – 269 с.
12. Stepp H.G., Baumgartner R., Beyer W., et al. Fluorescence imaging and spectroscopy of ALA –induced protoporphyrin IX preferentially accumulated in tumor tissue // Proc. SPIE. – 1995. – Vol. 2627. – P. 13–24.
13. Fotinos N., Campo M.A., Popowycz F., et al. 5-Aminolevulinic acid derivatives in photomedicine: Characteristics, application and perspectives // Photochem Photobiol. – 2006. – Vol. 82, No. 4. – P. 994–1015
14. Якубовская Р.И., Казачкина Н.И., Плютинская А.Д. Новый отечественный препарат гексасенс-лио для флуоресцентной диагностики и фотодинамической терапии злокачественных новообразований // Российский онкологический журнал. – № 2. – 2009.
15. Слесаревская М.Н., Соколов А.В. Опыт применения флуоресцентной цистоскопии в диагностике поверхностного рака мочевого пузыря // Урологические ведомости. – 2014. – Т. IV. – № 1. – С. 3–7.
16. Ivanova-Radkevich V.I., Filonenko E.V., Slovokhodov E.K., et al. Organization of clinical trials of photosensitizer based on 5-aminolevulinic acid hexyl ester // Indian Journal of Science and Technology. – 2016. – Vol. 9(18). doi: 10.17485/ijst/2016/v9i18/93759

ORIGINAL ARTICLES

LASER FLUORESCENT SPECTROSCOPY AND OPTICAL TISSUE OXIMETRY IN DIAGNOSTICS OF SKIN FIBROSIS

Chursinova Yu.V.[1], Kulikov D.A.[1], Rogatkin D.A.[1], Raznitsyna I.A.[1,2], Mosalskaya D.V.[1], Bobrov M.A.[1], Petritskaya E.N.[1], Molochkov A.V.[1]
[1]Moscow Regional Research and Clinical Institute ("MONIKI"), Moscow, Russia
[2]National Research Nuclear University MEPhI (Moscow Engineering Physics Institute), Moscow, Russia

Abstract

There are currently no effective measures to combat fibrosis in modern medical practice. One of the reasons for that is the late diagnosis associated with the lack of available clinical biomarkers and effective methods of non-invasive detection of the process. Fibrosis of the skin is characterized by fibrosis of the dermis, underlying tissues and is represented by a wide range of nosologies. Scleroderma and scars are of the greatest interest for the study. Skin changes in the development of bleomycin-induced fibrosis was studied in the experimental model using laser fluorescence spectroscopy and optical tissue oximetry. A significant increase in the rates of endogenous fluorescence of porphyrins, caused by inflammation and hypoxia, was detected at 7 and 21 days. An increased intensity of endogenous collagen fluorescence and a decreased specific oxygen uptake due to excess accumulation of the extracellular matrix were recorded on the 21st day after bleomycin treatment. Synchronous measurements of the collagen fluorescence and the specific oxygen uptake allowed to correlate the obtained data and the phases of the fibrogenic response described morphologically. The results allow to judge the severity of inflammation and hypoxia in the process of the fibrosis development. The objective and quantitative nature of the recorded parameters makes it possible to develop criteria for diagnosing the phases of fibrosis development.

Keywords: fibrosis, laser fluorescence spectroscopy, optical tissue oximetry, diagnostics in vivo

For citations: Chursinova Yu.V., Kulikov D.A., Rogatkin D.A., Raznitsyna I.A., Mosalskaya D.V., Bobrov M.A., Petritskaya E. N.., Molochkov A.V. Laser fluorescence spectroscopy and optical tissue oximetry in the diagnosis of skin fibrosis, *Biomedical Photonics*, 2019, vol. 8, no. 1 pp. 38–45 (in Russ.). doi: 10.24931/2413–9432–2019–8–1-38–45.

Contacts: Chursinova Yu.V., e-mail: yu.chursinova@monikiweb.ru

ЛАЗЕРНАЯ ФЛУОРЕСЦЕНТНАЯ СПЕКТРОСКОПИЯ И ОПТИЧЕСКАЯ ТКАНЕВАЯ ОКСИМЕТРИЯ В ДИАГНОСТИКЕ ФИБРОЗА КОЖИ

Ю.В. Чурсинова[1], Д.А. Куликов[1], Д.А. Рогаткин[1], И.А. Разницына[1,2], Д.В. Мосальская[1], М.А. Бобров[1], Е.Н. Петрицкая[1], А.В. Молочков[1]
[1]Государственное бюджетное учреждение здравоохранения Московской области «Московский областной научно-исследовательский клинический институт им. М.Ф. Владимирского» (ГБУЗ МО МОНИКИ им. М.Ф. Владимирского), Москва, Россия
[2]Национальный исследовательский ядерный университет МИФИ, Москва, Россия

Резюме

В современной медицинской практике нет эффективных мер борьбы с фиброзом. Одна из причин – поздняя диагностика, связанная с отсутствием доступных клинических биомаркеров и эффективных методов неинвазивного обнаружения этого процесса. Фиброзирующие заболевания кожи характеризуются фиброзом дермы, подлежащих тканей и представлены широким спектром нозологий. Наибольший интерес для изучения представляют склеродермия и рубцы кожи. На экспериментальной модели методами лазерной флуоресцентной спектроскопии и оптической тканевой оксиметрии изучены изменения кожи в рамках развития блеомицин-индуцированного фиброза. Выявлен достоверный рост показателей эндогенной флуоресценции порфиринов на 7 и на 21 сут, вызванный воспалением и гипоксией. Зафиксированы повышение интенсивности эндогенной флуоресценции коллагена и снижение показателей удельного потребления кислорода на 21 сут исследования, связанные с избыточным накоплением межклеточного матрикса. Синхронные измерения флуоресценции коллагена и удельного потребления кислорода позволили провести корреляцию с фазами фиброгенного ответа, описанного морфологически. Полученные результаты позволяют судить о выраженности воспаления и гипоксии в процессе развития фиброза. Объективный и количественный характер регистрируемых параметров дает возможность разработки критериев для диагностики фаз развития фиброза.

Ключевые слова: фиброз, лазерная флуоресцентная спектроскопия, оптическая тканевая оксиметрия, диагностика *in vivo*.

Для цитирования: Чурсинова Ю.В., Куликов Д.А., Рогаткин Д.А., Разницына И.А., Мосальская Д.В., Бобров М.А., Петрицкая Е. Н., Молочков А.В. Лазерная флуоресцентная спектроскопия и оптическая тканевая оксиметрия в диагностике фиброза кожи // Biomedical Photonics. – 2019. – Т. 8, № 1. – С. 38–45. doi: 10.24931/2413–9432–2019–8–1-38–45.

Контакты: Чурсинова Ю.В., e-mail: yu.chursinova@monikiweb.ru

Introduction

Systemic and organ fibrosis are some of the serious medical problems affecting a significant proportion of the world's population [1]. Fibrosis is a leading process in the development of autoimmune conditions, such as rheumatoid arthritis, Crohn's disease, ulcerative colitis, systemic lupus erythematosus, as well as in diseases of the liver, kidneys, pulmonary alveolitis and heart failure [2].

In the Russian medical academic tradition, an excessive accumulation of connective tissue in the skin is commonly referred to as sclerosis, which is the final stage of tissue fibrosis, with the loss of functions of the organ [3]. The term «fibrosis» in modern periodicals is more and more often used to refer to accumulation and disorganization of connective tissue [4].

Skin fibrosis is most often manifested as scleroderma, hypertrophic and keloid scars [5]. Fibrous changes in this case can have a different degree of severity: from cosmetic defects in the case of cicatricial deformity to life-threatening conditions in the case of systemic scleroderma [6–8]. The pathogenesis of skin fibrosis in different diseases has similar features and is characterized by proliferation of fibroblasts, myofibroblasts, excessive synthesis and accumulation of connective tissue [9]. Fibroblast activation is always a key link in skin fibrosis [10]. It is known that their uncontrolled proliferation can be caused by chronic inflammation, infection, autoimmune and allergic reactions, as well as damage to the skin due to radiation or chemical exposure. Persistent activation of fibroblasts in this case promotes excessive synthesis of intercellular substance which mainly consists of collagen, elastin, non-collagen glycoprotein and proteoglycan [11]. Excessive fiber synthesis and deposition of the intercellular matrix result in skin fibrosis.

There is a point of view discussed in the scientific literature that describes fibrosis not as the outcome of tissue damage, but as a dynamically progressing and reversible process associated with inflammation and hypoxia [12, 13], so that timely intervention enhances the therapeutic options [14]. Thus, the justified choice of the treatment method for the developing hypertrophic and keloid scars is based on the understanding of the prevailing process involved (inflammation/hypoxia/fibrosis). Studies in this area show that the response of fibrosed tissues to a particular type of treatment depends on the adequacy of the current treatment factor to the nature of the pathological process that determines the functional state of the tissue [15]. During the examination, a clinician may not objectively determine the activity and contribution of individual processes (inflammation/hypoxia/fibrosis). Histological examination makes it possible to get more of objective information, however, the process of collecting biological material (biopsy) can cause subsequent excessive growth of the scar [16]. Today, there are no generally accepted algorithms for choosing a method for scar treatment, and the tactics of managing a particular patient are based on the personal experience of the doctor and the traditions of individual clinical schools and organizations [17].

The analysis of modern research has shown that non-invasive methods for diagnosing skin fibrosis, such as ultrasound, elastography, confocal microscopy, optical coherence tomography, still have not become wide-spread in everyday medical practice. First of all, this is due to the lack of criteria that reliably characterize fibrosis [18]. Therefore, we can definitely say that the task of developing a method for rapid, non-invasive, quantitative assessment of fibrosis remains relevant for medicine. We believe that optical technologies can have diagnostic potential, which may provide the basis for a fundamentally new approach to an integrated assessment of this process. For example, it is known that excess collagen can be detected by laser fluorescence spectroscopy, since this substance fluoresces under the influence of light in the UV range [19], and fluorophores responsible for inflammation and hypoxia can also be detected in the red and green spectra [20]. Optical tissue oximetry methods make it possible to determine the specific oxygen consumption of tissues, which characterizes the activity of proliferative processes. Therefore, it can be presumed that the results of laser fluorescence spectroscopy and optical tissue oximetry taken together could help determine the leading pathological process, which will allow a personalized approach to the selection of therapy.

The purpose of our work was to study the diagnostic capabilities of optical methods of laser fluorescence spectroscopy and optical tissue oximetry in assessing fibrosis in animal skin.

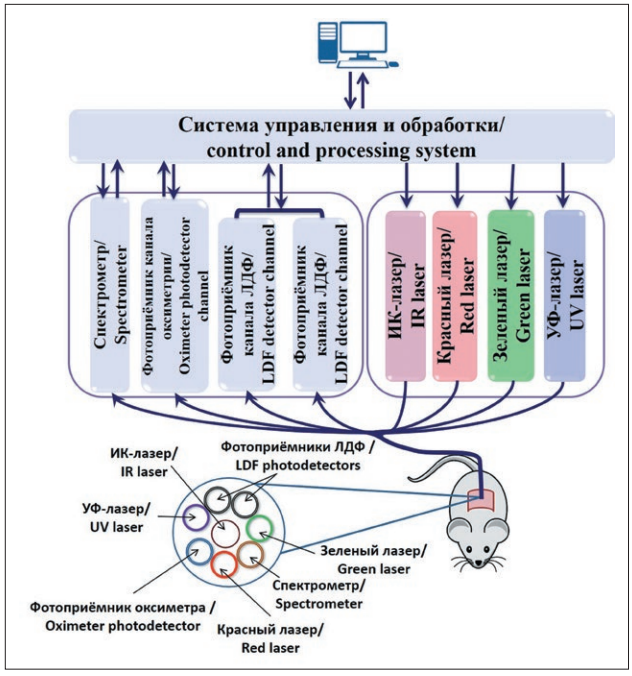

Рис. 1. Схема экспериментальной установки и расположение осветительных и приёмных волокон в оптоволоконном жгуте
Fig. 1. Experimental setup and location of illuminating and receiving optical fibers in the probe

Materials and methods

The study was conducted on outbred white mice, males, aged 6 weeks, weighing 25-30 g, number of animals (N): 47. The animals were kept in standard vivarium conditions at a temperature of 21–23°C, humidity of 50–65%, and 14-hour long daylight. They received a balanced granular food which contained no fluorophores and had unlimited access to drinking water.

The experiment was carried out in compliance with the principles of the Declaration of Helsinki on the Humane Treatment of Animals, the principles of humanity set forth in the European Community Directive (86/609/EC), the European Convention for the Protection of Vertebrate Animals Used for Experimental and other Scientific Purposes (ETS 123) Strasbourg, 1986.

Fibrosis was created with the use of the relevant model of skin fibrosis in animals, which is used to study scleroderma and cicatricial changes in the skin [21, 22]. The animals were divided into 2 groups. The first group (N = 30) was administered subcutaneous injections of bleomycin (BLM) at a dosage of 0.1 ml (concentration 0.5 mg/ml). The second (control) group (N = 17) was administered subcutaneous injections of 0.1 ml of 0.9% NaCl (PBS). All animals were injected daily for 21 days into the previously depilated skin of the interscapular region of the back. The first four injections were administered at the vertices of a 1 cm^2 square previously marked with a marker, and the fifth was made in the center of the square.

On days 0, 7, 14, and 21, the intensity of endogenous fluorescence, tissue saturation of oxyhemoglobin, and volumetric blood filling of the skin *in vivo* were measured. Indications were taken from the skin surface directly above the experimental site (Fig. 1). All measurements were performed with a multifunctional laser diagnostic complex «LAKK-M» (OOO RPE «LAZMA», Russia) [23].

Fig. 1 shows a schematic diagram of «LAKK-M» complex. The complex operates in «fluorescence» and «microcirculation» modes. In the «microcirculation» mode, the complex continuously measures the hemoglobin oxygen saturation and the volume of the hemoglobin fraction at the site subject to probing. These indicators are calculated according to the methodology of absorption spectroscopy, which is based on the difference in the recorded signals when probing biological tissue in the red and green spectral wavelength ranges. Hemoglobin oxygen saturation is determined on the basis of different optical properties of the oxygenated and deoxygenated hemoglobin fractions contained in the diagnostic blood volume. Based on these indicators averaged over the measurement time (15 s), the specific oxygen consumption by cells (U) was calculated, which characterizes the oxygen consumption per unit volume of blood circulating in the blood tissue according to the formula [24]:

$$U = \frac{(S_pO_2 - S_tO_2)}{V_b},$$

where S_tO_2 is the average tissue saturation of oxyhemoglobin, V_b is the average volumetric blood supply. At the same time, the saturation of oxyhemoglobin (S_pO_2) in arterial blood was assumed to be 98%.

The «fluorescence» operating mode is used to implement the method of laser fluorescence spectroscopy. Radiation from the selected source is delivered to the surface of the test volume with the use of a fiber optic probe through a lighting fiber. Secondary radiation is delivered to the spectrometer through the receiving fiber.

To excite fluorescence in various parts of the spectrum, low-power lasers with wavelengths λ_e = 365 and 535 nm were used. The output power at the distal end of the fiber optic probe is about 2-3 mW for each light source. The wavelengths at which the fluorescence of the studied fluorophores reaches the values that are most effective for recording are hereinafter denoted by λ_f. For collagen, λ_f = 445–455 nm, for porphyrin, λ_f = 600–620 nm [19]. It should be noted that the contributions of collagen and elastin to the total spectrum are difficult to separate, therefore, it was further considered that fluorescence in the wavelength range λ_f = 445–455 nm reflects the presence of both fluorophores. In this study, we estimated the dynamics of the intensity at given wavelengths (hereinafter referred to as «fluorescence intensity») with equal laser powers that were tracked.

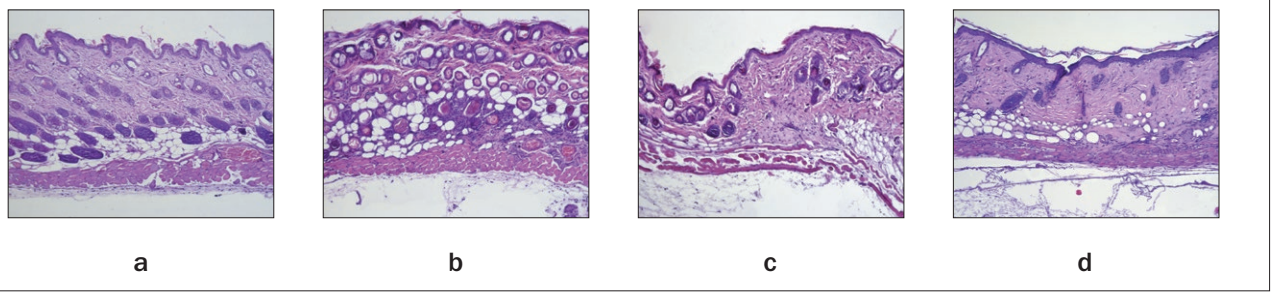

Рис. 2. Кожа мышей в группе BLM. Гистологические препараты, окраска гематоксилином и эозином (увеличение ×100):
a – 0 сут, структура эпидермиса и дермы не изменена;
b – 7 сут, воспалительная инфильтрация долек жировой ткани лимфоцитами и гистиоцитами;
c – 14 сут, частичное замещение жировой ткани межклеточным матриксом, уменьшение воспалительной инфильтрации;
d – 21 сут, обширные очаги накопления межклеточного матрикса, обедненные клеточными элементами (гипоцеллюлярный фиброз), сглаженность коллагеновых волокон

Fig. 2. The skin of mice in the BLM group. Histological preparations, hematoxylin and eosin staining (magnification ×100):
a – Day 0: the structure of epidermis and dermis is not changed;
b – Day 7: inflammation in the lobule of adipose tissue due to infiltration of lymphocytes and histiocytes;
c – Day 14: partial replacement of the adipose tissue by extracellular matrix, reduction of inflammatory infiltration;
d – Day 21: extensive foci of the extracellular matrix deposition, depleted of cellular elements (hypocellular fibrosis), smoothness of collagen fibers

Samples for histological studies were taken on days 0, 7, 14 and 21. From the study area, skin fragments of 1.0 × 1.0 cm were isolated, after which the histological preparations were stained with hematoxylin-eosin. The study of the morphological picture involved the evaluation of the state of the epidermis, the inflammatory changes in the dermis, subcutaneous fat and the structure of collagen fibers.

Statistical analysis was performed with the use of Microsoft Excel (Microsoft Corp., USA). The hypotheses about the presence of differences between groups were checked by comparing the arithmetic mean values and constructing 95% confidence intervals for the arithmetic mean values.

Results and discussion

During the experiment, skin fibrosis confirmed histologically was reproduced in the BLM group of animals (Fig. 2).

Fig. 4a shows the dynamics of the group-averaged fluorescence intensity of collagen and elastin. We believe that a decrease in the intensity of endogenous collagen fluorescence on day 7 compared to day 0 in the BLM group is most likely due to tissue edema due to inflammatory exudation, which was histologically most pronounced at that time. An increase in the intensity of endogenous fluorescence of collagen and elastin on day 21 in the BLM group is caused by their accumulation in

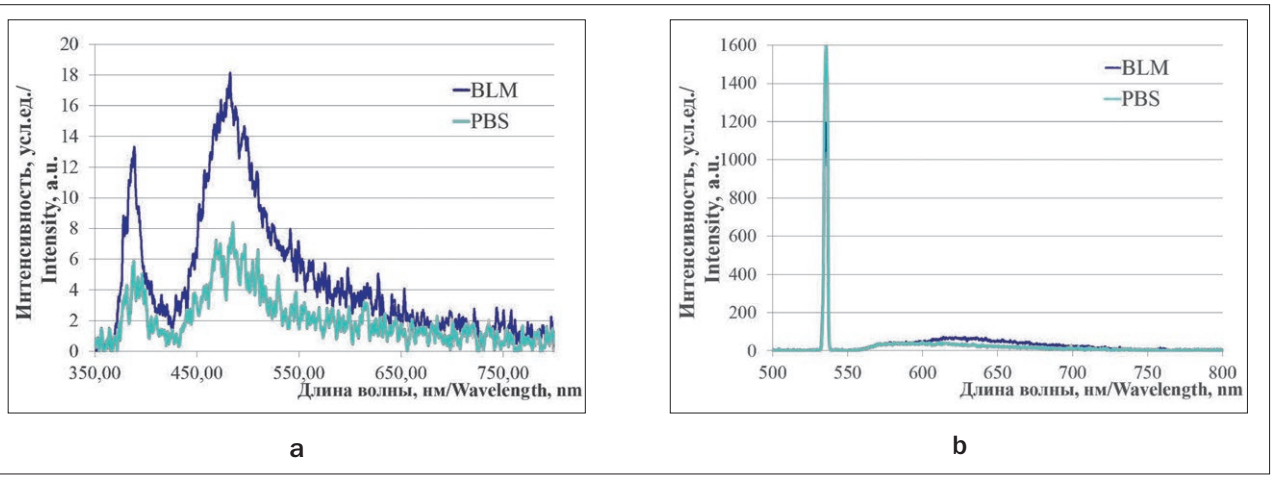

Рис. 3. Примеры спектров флуоресценции в области инъекций на 21 сут:
a – в УФ-диапазоне (λ_e = 365 нм);
b – в зеленом диапазоне (λ_e = 535 нм)

Fig. 3. Example of the fluorescence spectra at the injection site at day 21:
a – in the UV wavelength range (λ_e = 365 nm);
b – in the green wavelength range (λ_e = 535 nm)

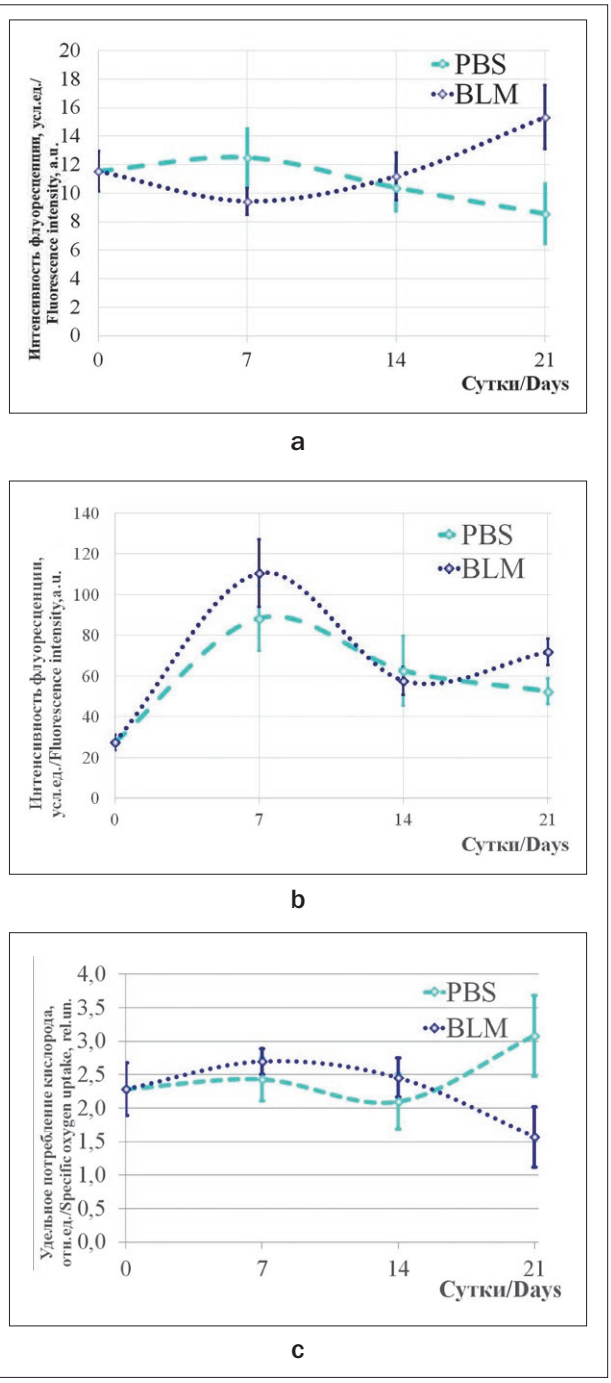

Рис. 4. Динамика показателей оптической диагностики в группах BLM (инъекция блеомицина) и PBS (инъекция физраствора):
a – интенсивности флуоресценции коллагена и эластина (λ_e = 365 нм, λ_f = 445–455 нм);
b – интенсивности флуоресценции порфирина (λ_e = 535 нм, λ_f = 610 нм);
c – удельного потребления кислорода тканями

Fig.4. Dynamics of optical diagnostic indicators in the BLM (bleomycin injection) and PBS (saline injection) groups:
a – fluorescence intensity of collagen and elastin (λ_e = 365 nm, λ_f = 455 nm);
b – fluorescence intensity of porphyrin (λ_e = 535 nm, λ_f = 610 nm);
c – specific oxygen uptake by tissues

the region of the formed fibrosis, which also corresponds to the morphological picture of skin fibrosis. As collagen is the main extracellular substance of connective tissue in case of skin fibrosis [25], the contribution of elastin fluorescence in this case is insignificant.

Porphyrins have been found to rapidly respond to metabolic changes in tissues. In particular, their synthesis is actively increased in cells in a state of chronic hypoxia and inflammation [26]. The dynamics of porphyrin fluorescence averaged over intensity groups (Fig. 4b) shows a significant increase in parameters by 7 days compared to day 0 of the experiment in both groups of animals, which probably reflects the inflammatory processes caused by daily subcutaneous injections. In addition, significant differences in the BLM and PBS groups were obtained on day 21 of the experiment. We believe that an increase in the intensity of endogenous fluorescence of porphyrins in skin with fibrosis during this period is caused by hypoxia, which occurred primarily due to impaired perfusion in tissues [27].

The results of measuring specific oxygen consumption show a significant decrease in its indices by day 21 in the BLM group (Fig. 4c), presumably due to the formation of hypocellular fibrosis with low metabolic activity.

It is reliably known that inflamed and proliferating tissue has a high oxygen demand. This is most pronounced in the structure of immature metabolically active scar tissues. However, when the fibrosis has established, this demand decreases, including due to the reduction in the number of cellular elements [28]. In our experiment, we confirmed this histologically, and this dependence was shown by the results of the calculation of the specific oxygen consumption by the cells and the endogenous fluorescence of collagen on days 14 and 21 in the BLM group (Fig. 5).

The modern concept allows us to divide the fibrogenic response into four overlapping phases: phase 1: the initiation of the response caused by primary damage, phase 2: activation of effector cells, phase 3: production of the extracellular matrix, phase 4: dynamic deposition/insufficient resorption of the extracellular matrix [4]. The results of measuring collagen fluorescence and specific oxygen consumption in combination with the morphological picture of the skin allow us to correlate them with the phases of the fibrogenic response. Thus, in phases 1 and 2 (0–7 days), an increase in oxygen consumption by effector cells is observed due to primary tissue damage and subsequent inflammation and hypoxia of consumption. In phase 3 (7-14 days), collagen fluorescence increases, as evidenced by the accumulation of the intercellular matrix, and oxygen consumption decreases, which is confirmed by the weakening of the inflammation process. Phase 4 (14–21 days) is characterized by excessive accumulation of the intercellular matrix deficient in cellular elements and a sharp drop in oxygen

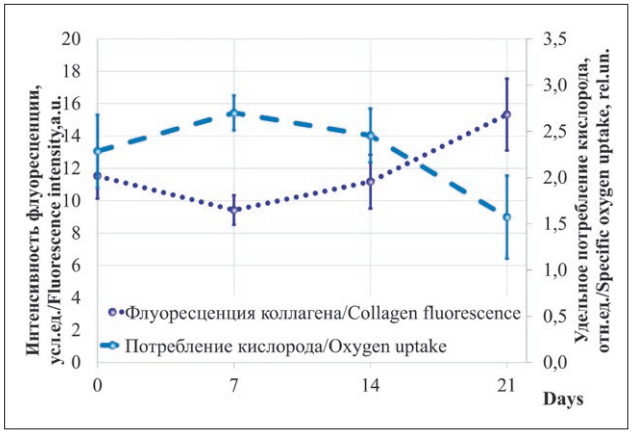

Рис. 5. Динамика интенсивности флуоресценции коллагена и эластина (λ_e = 365 нм, λ_f = 445–455 нм) и удельного потребления кислорода тканями.
Fig. 5. Dynamics of collagen and elastin fluorescence intensity (λ_e = 365 nm, λ_f = 445–455 nm) and specific oxygen uptake by tissues

consumption. However, it is worth noting that the time boundaries at this stage are conventional due to the characteristics of the experiment.

A number of researchers believe that fibrosis is irreversible if the tissue becomes paucicellular and, as a result, poor in biologically active molecules necessary for the degradation of the extracellular substance of connective tissue [29, 30]. This corresponds to the period when an increase in the specific consumption of oxygen is replaced by its decline due to a decrease in the number of cells consuming it. At the same time, an increase in the fluorescence of collagen, as the main biomarker of fibrosis, is recorded. We believe that the simultaneous measurement of collagen fluorescence and specific oxygen consumption will allow us to record not only the synchronous nature of the processes of inflammation and hypoxia involved in fibrogenesis, but also provide new opportunities for the diagnosis of fibrosis phases.

Conclusion

The results of the study demonstrated the possibility of objective non-invasive dynamic monitoring of inflammation and hypoxia in the development of skin fibrosis with the use of laser fluorescence spectroscopy and optical tissue oximetry. The development of the proposed approaches can be implemented by establishing quantitative criteria for a clear periodization of fibrosis formation. The objectivity of the study can also be enhanced through the use of additional methods that simultaneously evaluate and compare the manifestations of the processes under study at the molecular, cellular and tissue levels. This, in turn, will expand the capabilities of practitioners in diagnosing fibrosis, personalizing treatment tactics, and predicting the outcome of the disease.

The study was carried out with the financial support of the Russian Federal Property Fund in the framework of research project No. 18-02-02-00564/18.

REFERENCES

1. Wynn T.A., Ramalingam T.R. Mechanisms of fibrosis: therapeutic translation for fibrotic disease, *Nature medicine*, 2012, vol. 18, no. 7, pp. 1028–1040.
2. Wynn T.A. Integrating mechanisms of pulmonary fibrosis, *Journal of Experimental Medicine*, 2011, vol. 208, no. 7, pp. 1339–1350.
3. Strukov A.I., Serov V.V. *Patologicheskaya anatomiya. 6-e izd.* [Pathological anatomy. 6th ed.]. Moscow, GEOTAR-Media Publ., 2015. pp. 254–255.
4. Rockey D.C., Bell P.D., Hill J.A. Fibrosis–a common pathway to organ injury and failure, *New England Journal of Medicine*, 2015, vol. 372, no. 12, pp. 1138–1149.
5. Andrews J.P., Marttala J., Macarak E., Rosenbloom J., Uitto J. Keloids: The paradigm of skin fibrosis–Pathomechanisms and treatment, *Matrix Biology*, 2016, vol. 51, pp. 37–46.
6. Bijlard E., Kouwenberg C.A., Timman R., Hovius S.E., Busschbach J.J., Mureau M.A. Burden of keloid disease: A cross-sectional health-related quality of life assessment, *Acta dermato-venereologica*, 2017, vol. 97, no. 2, pp. 225–229.
7. Bock O., Schmid-Ott G., Malewski P., Mrowietz U. Quality of life of patients with keloid and hypertrophic scarring, *Archives of dermatological research*, 2006, vol. 297, no. 10, pp. 433.
8. Muangchan C., Harding S., Khimdas S., Bonner A., Canadian Scleroderma Research group, Baron M., Pope J. Association of C-reactive protein with high disease activity in systemic sclerosis: Results from the Canadian Scleroderma Research Group, *Arthritis Care Res (Hoboken)*, 2012, vol. 64, no. 9, pp. 1405–1414.

ЛИТЕРАТУРА

1. Wynn T.A., Ramalingam T.R. Mechanisms of fibrosis: therapeutic translation for fibrotic disease //Nature medicine. – 2012. – Vol. 18. – №. 7. – P. 1028–1040.
2. Wynn T.A. Integrating mechanisms of pulmonary fibrosis // Journal of Experimental Medicine. – 2011. – Vol. 208. – No. 7. – P. 1339–1350.
3. Струков А.И., Серов В.В. Патологическая анатомия. 6-е изд. – М.: ГЭОТАР-Медиа, 2015. – С. 254–255.
4. Rockey D.C., Bell P.D., Hill J.A. Fibrosis–a common pathway to organ injury and failure //New England Journal of Medicine. – 2015. – Vol. 372. – No. 12. – P. 1138–1149.
5. Andrews J.P., Marttala J., Macarak E., et al. Keloids: The paradigm of skin fibrosis–Pathomechanisms and treatment //Matrix Biology. – 2016. – Vol. 51. – P. 37–46.
6. Bijlard E., Kouwenberg C.A., Timman R., et al. Burden of keloid disease: A cross-sectional health-related quality of life assessment //Acta dermato-venereologica. – 2017. – Vol. 97, No. 2. – P. 225–229.
7. Bock O., Schmid-Ott G., Malewski P., Mrowietz U. Quality of life of patients with keloid and hypertrophic scarring //Archives of dermatological research. – 2006. – Vol. 297, No. 10. – P. 433.
8. Muangchan C., Harding S., Khimdas S., et al. Association of C-reactive protein with high disease activity in systemic sclerosis: Results from the Canadian Scleroderma Research Group // Arthritis Care Res (Hoboken). – 2012. – Vol. 64, No. 9. – P. 1405–1414.
9. Habiel D.M., Hogaboam C. Heterogeneity in fibroblast proliferation and survival in idiopathic pulmonary fibrosis // Frontiers in pharmacology. – 2014. – Vol. 5, No. 2. – P. 1–6.

9. Habiel D.M., Hogaboam C. Heterogeneity in fibroblast proliferation and survival in idiopathic pulmonary fibrosis, *Frontiers in pharmacology*, 2014, vol. 5, no. 2, pp. 1–6.
10. Wang W., Qu M., Xu L., Wu X., Gao Z., Gu T., Zhang W., Ding X., Liu W., Chen Y.L. Sorafenib exerts an anti-keloid activity by antagonizing TGF-β/Smad and MAPK/ERK signaling pathways, *J Mol Med (Berl)*, 2016, vol. 94, no. 10, pp. 1181–1194.
11. Driskell R.R., Lichtenberger B.M., Hoste E., Kretzschmar K., Simons B.D., Charalambous M., Ferron S.R., Herault Y., Pavlovic G., Ferguson-Smith A.C., Watt F.M. Distinct fibroblast lineages determine dermal architecture in skin development and repair, *Nature*, 2013, vol. 504, pp. 277–281.
12. Manresa M.C., Godson C., Taylor C.T. Hypoxia-sensitive pathways in inflammation-driven fibrosis, *American Journal of Physiology-Regulatory, Integrative and Comparative Physiology*, 2014, vol. 307, no. 12, pp. R1369-R1380.
13. Iredale J.P. Models of liver fibrosis: exploring the dynamic nature of inflammation and repair in a solid organ, *The Journal of clinical investigation*, 2007, vol. 117, no. 3, pp. 539–548.
14. Lokmic Z., Musyoka J., Hewitson T.D., Darby I.A. Hypoxia and hypoxia signaling in tissue repair and fibrosis, *Int Rev Cell Mol Biol*, 2012, vol. 296, pp. 139–185.
15. Guller A.E., Shekhter A.B. Clinical type and histological structure of skin scars as prognostic factors of treatment outcome, *Annaly plasticheskoy, rekonstruktivnoy i ehsteticheskoy hirurgii*, 2007, no. 4, pp. 19–31. (in Russ.)
16. Monstrey S., Hoeksema H., Verbelen J., Pirayesh A., Blondeel P. Assessment of burn depth and burn wound healing potential, *Burns*, 2008, vol. 34, no. 6, pp. 761–769.
17. Mustoe T.A., Cooter R.D., Gold M.H., Hobbs F.D., Ramelet A.A., Shakespeare P.G., Stella M., Téot L., Wood F.M., Ziegler U.E. International Advisory Panel on Scar Management. International clinical recommendations on scar management, *Plast Reconstr Surg*, 2002, vol. 110, no. 2, pp. 560–571.
18. Kang T., Abignano G., Lettieri G., Wakefield R.J., Emery P., Del Galdo F. Skin imaging in systemic sclerosis, *Eur J Rheumatol*, 2014, vol. 1, no. 3, pp. 111–116.
19. Smirnova O.D., Rogatkin D.A., Litvinova K.S. Collagen as in vivo quantitative fluorescent biomarkers of abnormal tissue changes, *Journal of Innovative Optical Health Sciences*, 2012, vol. 5, no. 2, p. 1250010.
20. Franco W., Gutierrez-Herrera E., Kollias N., Doukas A. Review of applications of fluorescence excitation spectroscopy to dermatology, *Br J Dermatol*, 2016, vol. 174, no. 3, pp. 499–504.
21. Avouac J. Mouse model of experimental dermal fibrosis: the bleomycin-induced dermal fibrosis, *Methods Mol Biol*, 2014, vol. 1142, pp. 91–98.
22. Li Y., Zhang J., Zhang W., Liu Y., Li Y., Wang K., Zhang Y., Yang C., Li X., Shi J., Su L., Hu D. MicroRNA-192 regulates hypertrophic scar fibrosis by targeting SIP1, *J Mol Histol*, 2017, vol. 48, no. 5–6, pp. 357–366.
23. Rogatkin D.A., Lapaeva L.G., Petrinskaya E.N., Sidorov V.V., Shumskiy V.I. Multifunctional laser noninvasive spectroscopic system for medical diagnostics and metrological provisions for that, *Proceedings of SPIE – The International Society for Optical Engineering*, 2009. DOI: 10.1117/12.831602
24. Rogatkin D., Shumskiy V., Tereshenko S., Polyakov P. Laser-based non-invasive spectrophotometry – An overview of possible medical applications, *Photon Lasers Med*, 2013, vol. 2, no. 3, pp. 225–240.
25. Ho Y.Y., Lagares D., Tager A.M., Kapoor M. Fibrosis–a lethal component of systemic sclerosis, *Nat Rev Rheumatol*, 2014, vol. 10,
26. \no. 7, pp. 390–402.
27. Petritskaya E.N., Kulikov D.A., Rogatkin D.A., Guseva I.A., Kulikova P.A. Use of fluorescence spectroscopy for diagnosis of hypoxia and inflammatory processes in tissue, *Journal of Optical Technology*, 2015, vol. 82, no. 12, pp. 810–814.
28. Van Hal T.W., van Bon L., Radstake T.A system out of breath: how hypoxia possibly contributes to the pathogenesis of systemic sclerosis, *International Journal of Rheumatology*, 2011, vol. 2011, p. 824972

10. Wang W., Qu M., Xu L., et al. Sorafenib exerts an anti-keloid activity by antagonizing TGF-β/Smad and MAPK/ERK signaling pathways // J Mol Med (Berl). – 2016. – Vol. 94, No. 10. – P. 1181–1194.
11. Driskell R.R., Lichtenberger B.M., Hoste E., et al. Distinct fibroblast lineages determine dermal architecture in skin development and repair // Nature. – 2013. – Vol. 504. – P. 277–281.
12. Manresa M.C., Godson C., Taylor C.T. Hypoxia-sensitive pathways in inflammation-driven fibrosis // American Journal of Physiology-Regulatory, Integrative and Comparative Physiology. – 2014. – Vol. 307, No. 12. – P. R1369-R1380.
13. Iredale J.P. Models of liver fibrosis: exploring the dynamic nature of inflammation and repair in a solid organ //The Journal of clinical investigation. – 2007. – Vol. 117, No. 3. – P. 539–548.
14. Lokmic Z., Musyoka J., Hewitson T.D., Darby I.A. Hypoxia and hypoxia signaling in tissue repair and fibrosis // Int Rev Cell Mol Biol. – 2012. – Vol. 296. – P. 139–185.
15. Гуллер А.Е., Шехтер А.Б. Клинический тип и гистологическая структура кожных рубцов как прогностические факторы исхода лечения // Анналы пластической, реконструктивной и эстетической хирургии. – 2007. – №. 4. – С. 19–31.
16. Monstrey S., Hoeksema H., Verbelen J., et al. Assessment of burn depth and burn wound healing potential // Burns. – 2008. – Vol. 34, No. 6. – P. 761–769.
17. Mustoe T.A., Cooter R.D., Gold M.H., et al. International Advisory Panel on Scar Management. International clinical recommendations on scar management // Plast Reconstr Surg. – 2002. – Vol. 110, No. 2. – P. 560–571.
18. Kang T., Abignano G., Lettieri G., et al. Skin imaging in systemic sclerosis // Eur J Rheumatol. – 2014. – Vol. 1, No. 3. – P. 111–116.
19. Smirnova O.D., Rogatkin D.A., Litvinova K.S. Collagen as in vivo quantitative fluorescent biomarkers of abnormal tissue changes // Journal of Innovative Optical Health Sciences. – 2012. – Vol. 5, No. 2. – P. 1250010.
20. Franco W., Gutierrez-Herrera E., Kollias N., Doukas A. Review of applications of fluorescence excitation spectroscopy to dermatology // Br J Dermatol. – 2016. – Vol. 174, No. 3. – P. 499–504.
21. Avouac J. Mouse model of experimental dermal fibrosis: the bleomycin-induced dermal fibrosis // Methods Mol Biol. – 2014. – Vol. 1142. – P. 91–8.
22. Li Y., Zhang J., Zhang W., et al. MicroRNA-192 regulates hypertrophic scar fibrosis by targeting SIP1 // J Mol Histol. – 2017. – Vol. 48, No. 5–6. – P. 357–366.
23. Rogatkin D.A., Lapaeva L.G., Petrinskaya E.N., et al. Multifunctional laser noninvasive spectroscopic system for medical diagnostics and metrological provisions for that // Proceedings of SPIE – The International Society for Optical Engineering. – 2009. DOI: 10.1117/12.831602
24. Rogatkin D., Shumskiy V., Tereshenko S., Polyakov P. Laser-based non-invasive spectrophotometry – An overview of possible medical applications // Photon Lasers Med. – 2013. – Vol. 2, No. 3. – P. 225–240.
25. Ho Y.Y., Lagares D., Tager A.M., Kapoor M. Fibrosis–a lethal component of systemic sclerosis // Nat Rev Rheumatol. – 2014. – Vol. 10, No. 7. – P. 390–402.
26. Petritskaya E.N., Kulikov D.A., Rogatkin D.A., et al. Use of fluorescence spectroscopy for diagnosis of hypoxia and inflammatory processes in tissue // Journal of Optical Technology. – 2015. – Vol. 82, No. 12. – P. 810–814.
27. Van Hal T.W., van Bon L., Radstake T.A system out of breath: how hypoxia possibly contributes to the pathogenesis of systemic sclerosis // International Journal of Rheumatology. – 2011. – Vol. 2011. – P. 824972
28. Darby I.A., Hewitson T.D. Hypoxia in tissue repair and fibrosis // Cell and tissue research. – 2016. – Vol. 365, No. 3. – P. 553–562.

29. Darby I.A., Hewitson T.D. Hypoxia in tissue repair and fibrosis, *Cell and tissue research*, 2016, vol. 365, no. 3, pp. 553–562.
30. Issa R., Zhou X., Constandinou C.M., Fallowfield J., Millward-Sadler H., Gaca M.D., Sands E., Suliman I., Trim N., Knorr A., Arthur M.J., Benyon R.C., Iredale J.P. Spontaneous recovery from micronodular cirrhosis: evidence for incomplete resolution associated with matrix cross-linking, *Gastroenterology*, 2004, vol. 126, no. 7, pp. 1795–1808.
31. Iredale J.P. Models of liver fibrosis: exploring the dynamic nature of inflammation and repair in a solid organ, *Journal of clinical investigation*, 2007, vol. 117, no. 3, pp. 539–548.

29. Issa R., Zhou X., Constandinou C.M., et al. Spontaneous recovery from micronodular cirrhosis: evidence for incomplete resolution associated with matrix cross-linking // Gastroenterology. – 2004. – Vol. 126, No. 7. – P. 1795–1808.
30. Iredale J.P. Models of liver fibrosis: exploring the dynamic nature of inflammation and repair in a solid organ // Journal of clinical investigation. – 2007. – Vol. 117, No. 3. – P. 539–548.

ORIGINAL ARTICLES

OPTICAL SPECTROANALYZER WITH EXTENDED DYNAMIC RANGE FOR PHARMACOKINETIC INVESTIGATIONS OF PHOTOSENSITIZERS IN BIOTISSUE

Meerovich G.A.[1,2], **Akhlyustina E.V.**[2], **Savelieva T.A.**[1,2], **Linkov K.G.**[1], **Loschenov V.B.**[1,2]
[1]Prokhorov General Physics Institute of the Russian Academy of Sciences, Moscow, Russia
[2]National Research Nuclear University MEPhI (Moscow Engineering Physics Institute), Moscow, Russia

Abstract

Currently, the most promising method for the study of pharmacokinetics of drugs with fluorescent properties is the spectral-fluorescent method. In this article, we propose an algorithm for expanding the dynamic range of the spectrum analyzer by automatically monitoring the maximum spectral density in the recorded fluorescence spectrum and automatically controlled changes in the accumulation time depending on this value, followed by compensation of the output signal with regard to this change, as well as hardware circuit solutions that allow this algorithm.
Testing of LESA-01-"Biospec" spectrum analyzer, upgraded using the proposed approach, was carried out on photosensitizer dispersions based on tetra-3-phenylthiophthalocyanine hydroxyaluminium of various concentrations (from 0.01 mg/l to 50 mg/l), approximately corresponding to the concentrations realized in the process of studying pharmacokinetics in calibration samples and tissues of experimental animals.
The proposed solutions that implement the algorithm for recording fluorescence spectra with automatic change of accumulation time depending on the signal level, ensured a significant expansion of the dynamic range of the spectrum analyzer (up to 3.5 orders of magnitude) and improved accuracy in pharmacokinetic studies

Keywords: fluorescence diagnostics, pharmacokinetics, spectrum, intensity, exposure.

For citations: Meerovich G.A., Akhlyustina E.V., Savelieva T.A., Linkov K.G., Loschenov V.B. Optical spectroanalyzer with extended dynamic range for pharmacokinetic investigations of photosensitizers in biotissue, *Biomedical Photonics*, 2019, vol. 8, no. 1, pp. 46–51. (in Russian) doi: 10.24931/2413–9432–2019–8–1-46–51.

Contacts: Meerovich G.A., e-mail: meerovich@mail.ru

ОПТИЧЕСКИЙ СПЕКТРОАНАЛИЗАТОР С РАСШИРЕННЫМ ДИНАМИЧЕСКИМ ДИАПАЗОНОМ ДЛЯ ФАРМАКОКИНЕТИЧЕСКИХ ИССЛЕДОВАНИЙ ФЛУОРЕСЦИРУЮЩИХ ПРЕПАРАТОВ В БИОТКАНЯХ

Г.А. Меерович[1,2], **Е.В. Ахлюстина**[2], **Т.А. Савельева**[1,2], **К.Г. Линьков**[1], **В. Б. Лощенов**[1,2]
[1]Институт общей физики им. А.М. Прохорова Российской академии наук, Москва, Россия
[2]Национальный исследовательский ядерный университет МИФИ, Москва, Россия

Резюме

В настоящее время наиболее перспективным методом для исследования фармакокинетики препаратов, обладающих выраженными флуоресцентными свойствами, является спектрально-флуоресцентный метод. В этой статье мы предлагаем алгоритм расширения динамического диапазона спектроанализатора путем автоматического мониторинга максимального значения спектральной плотности в регистрируемом спектре флуоресценции и автоматического контролируемого изменения времени накопления в зависимости от этого значения с последующей компенсацией выходного сигнала с учетом этого изменения, а также схемные решения, позволяющие реализовать этот алгоритм.
Тестирование спектроанализатора ЛЭСА-01-«Биоспек», модернизированного с использованием предложенного подхода, проводилось на дисперсиях фотосенсибилизатора на основе тетра-3-фенилтиофталоцианина гидроксиалюминия различной концентрации (от 0,01 мг/л до 50 мг/л), примерно соответствующих концентрациям, реализующихся в процессе исследования фармакокинетики в калибровочных образцах и тканях экспериментальных животных. Предложенные решения, реализующие алгоритм регистрации спектров флуоресценции с автоматическим изменением времени накопления в зависимости от уровня сигнала, обеспечили существенное расширение динамического диапазона спектроанализатора (до 3.5 порядков) и повышение точности при фармакокинетических исследованиях.

Ключевые слова: флуоресцентная диагностика, фармакокинетика, спектр, интенсивность, экспозиция.

Для цитирования: Меерович Г.А., Ахлюстина Е.В., Савельева Т.А., Линьков К.Г., Лощенов В. Б. Оптический спектроанализатор с расширенным динамическим диапазоном для фармакокинетических исследований флуоресцирующих препаратов в биотканях // Biomedical Photonics.– 2019. – Т. 8, № 1. – С. 46–51. doi: 10.24931/2413–9432–2019–8–1-46–51.

Контакты: Меерович Г.А., e-mail: meerovich@mail.ru

Introduction

The study of the pharmacokinetics and biodistribution of a medicinal substance is based on an assessment of its concentration in organs, tissues and biological body fluids at specific points in time after administration [1]. One of the most important requirements for such studies is a wide dynamic range of the measurement method, which must be at least three orders of magnitude.

Currently, the most promising technique for studying the pharmacokinetics of drugs with pronounced fluorescent properties is the spectral-fluorescent method [1-4]. It is widely used to assess the level and selectivity of the accumulation of photosensitizers (PS) intended for photodynamic therapy and fluorescent diagnostics in biological tissues.

The spectroscopic equipment used for such studies usually includes a laser, a polychromator, a fiber-optic probe containing illuminating fibers which deliver excitation radiation to the biological tissue, and receiving optical fibers for delivering fluorescence radiation from the biological tissue to the polychromator input, and a matrix photodetector at the polychromator output, in particular, a charge-coupled device (CCD) or CMOS-ruler («Complementary Metal-Oxide-Semiconductor structure»). The signal recording system from each of the cells of the ruler, proportional to its charge, includes an analog-to-digital converter (ADC), a block of buffer memory and a personal computer (PC) [2, 5]. In a spectral-fluorescent study, the radiation from the laser output is introduced into the light conductor of the optical fiber probe. Coming out of the distal end of the illuminating fiber, this radiation irradiates the biological tissue containing the fluorescent drug, and initiates the fluorescence of its molecules. The intensity of the characteristic fluorescence band of the pharmaceutical agent in the first approximation is proportional to its content in the biotissue. The receiving optical fibers of the fiber-optic probe deliver the fluorescence radiation from the biological tissue to the input of the polychromator, where the spectral decomposition of this radiation takes place, after which the radiation falls on the ruler. The signal from the output of the ruler enters the ADC and the buffer memory unit. The computer uses digital data coming from the output of the buffer memory, corresponding to the intensity of the signal from each cell of the photodetector, and cell numbers of the photodetector, for which a certain wavelength is set according to the calibration results, to form a spectral curve (intensity vs. wavelength) that is displayed on the screen of the computer.

The dynamic range of the spectrum analyzer is mainly determined by the characteristics of the ruler. With high levels of incident light on a cell of the ruler, this cell and the adjacent cells of the ruler may undergo charge saturation; at low levels, the signal associated with the incident light may be hardly distinguishable against the background of hardware noise of the device (first of all, the noise of the ruler). Because of this, the dynamic range of known devices does not normally exceed two orders of magnitude.

This article discusses the possibility of expanding the dynamic range of a spectrum analyzer for pharmacokinetic studies of fluorescent drugs.

Materials and methods

Samples of liposomal dispersions of tetra-3-phenylthiophthalocyanine hydroxyaluminium in distilled water with concentrations of 0.01 mg/ml; 0.05 mg/ml; 0.1 mg/ml; 0.5 mg/ml; 2 mg/ml; 10 mg/ml; 25 mg/ml; 50 mg/ml in Eppendorf tubes were used as test objects. The control sample was an Eppendorf tube with water.

Fluorescence studies were performed with the use of a laser electron spectral analyzer LESA-01-Biospec (OOO «BIOSPEC», Russia).

Results and discussion

The study of the dependence of the output signal of the spectrum analyzer on the time of accumulation

The results of studies of the spectra of liposomal dispersions of tetra-3-phenylthiophthalocyanine hydroxyaluminium in various concentrations show that for small values of the accumulation time, LESA-01-Biospec spectrum analyzer provides undistorted recording of the signals of the fluorescence of dispersions with a high concentration. However, the fluorescence signals of dispersions with a low concentration are almost indistinguishable against the background of curcuit noise (Fig. 1a).

With high values of accumulation time, the spectrum analyzer performs accurate recordings of fluorescence signals at low PS concentrations. However, when registering fluorescence of PS with a high concentration,

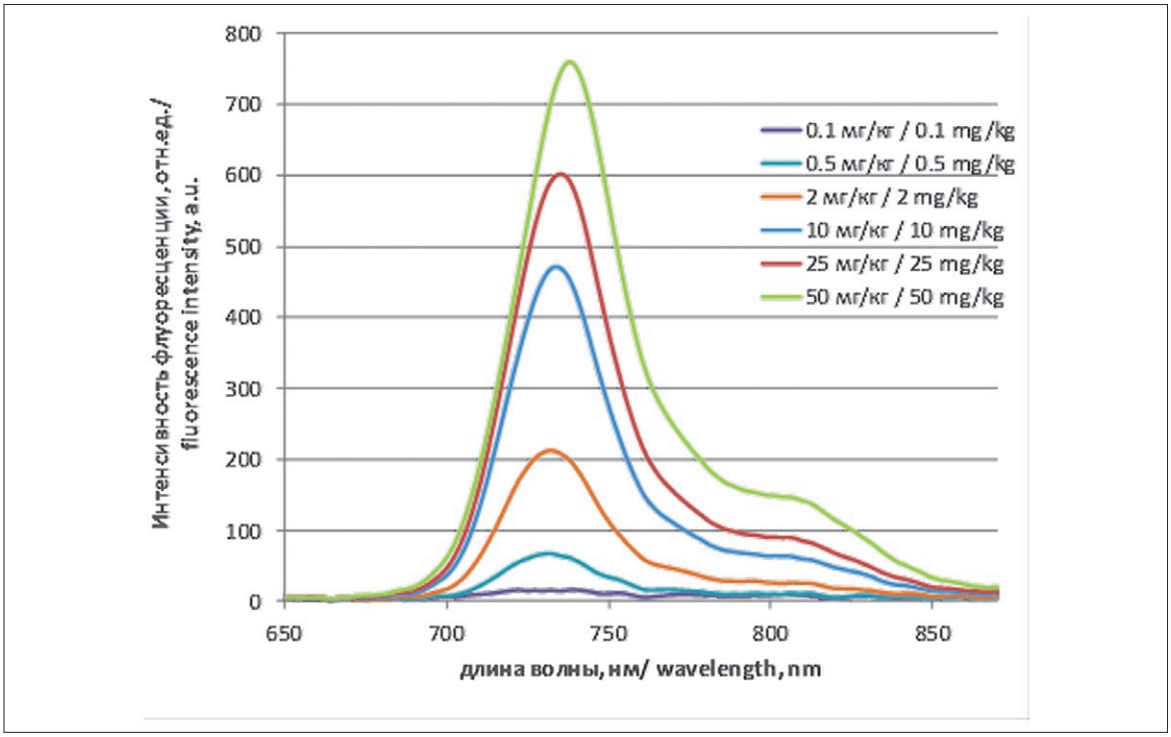

a

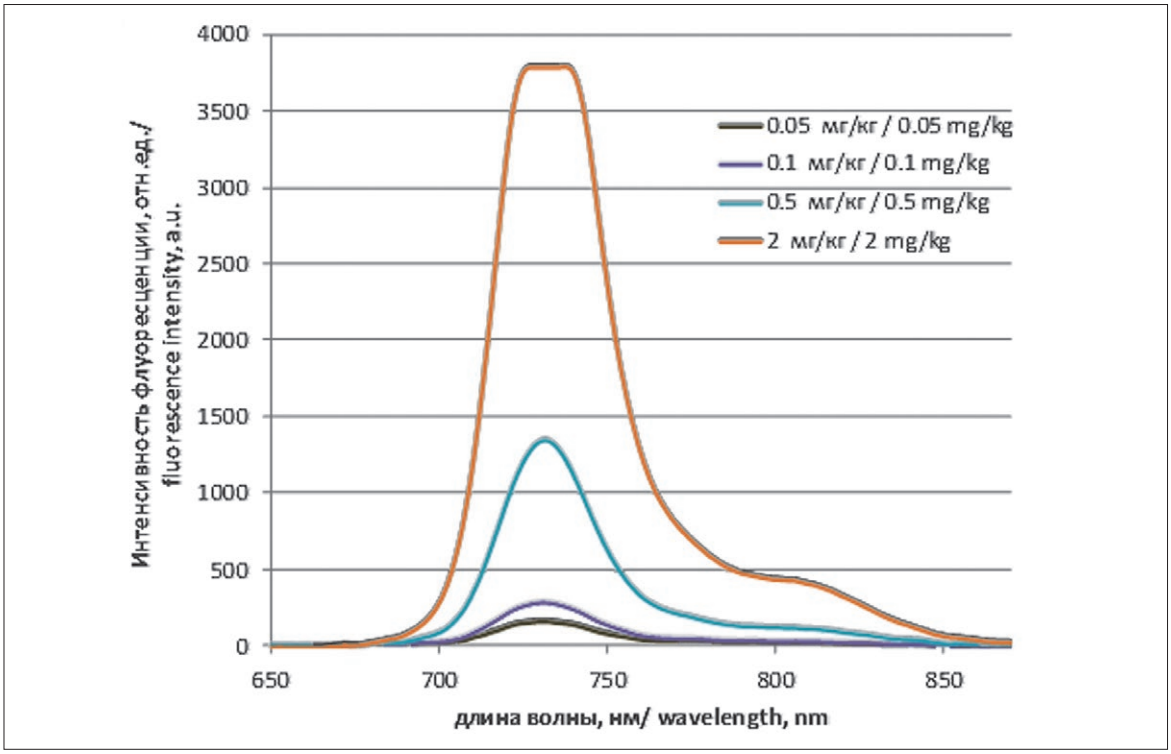

b

Рис. 1. Спектры флуоресценции дисперсий ФС разной концентрации при времени накопления:
a – при 12 мс;
b – при 300 мс.
Fig. 1. Fluorescence spectra of PS dispersions of various concentrations with an exposure time:
a – 12 ms;
b – 300 ms

when the intensity of the fluorescence signal is high, the cells of the ruler corresponding to the region of the spectral maximum of fluorescence may undergo charge saturation (Fig. 1b). Therefore, the work of the spectrum analyzer becomes incorrect due to hardware distortion of the spectrum shape.

The expansion of the dynamic range of the intensity of detected fluorescence signals

In order to extend the dynamic range of the fluorescence signal intensity, the following approach has been proposed. The maximum and minimum values of the spectral density are automatically monitored throughout the period of spectral signal registration. If this value falls outside the limits of the specified range, the algorithm of automatic adjustment of the photodetector exposure, processing and recording of the polychromator ruler signals is launched.

Fig. 2 shows an improved block diagram of the recording system of the spectrum analyzer [5] with the following designations: 1 – laser for excitation of fluorescence; 2 – a fiber-optic probe containing light-guiding fibers for delivering excitation radiation to biological tissue and receiving optical fibers for delivering fluorescence radiation from a biological tissue to the input of the polychromator; 3 – biological tissue; 4 – polychromator; 5 – CCD or CMOS ruler at the output of the polychromator; 6 - ADC; 7 - buffer memory unit; 8– comparator; 9 - upper reference signal setter; 10 - comparator; 11 - lower upper reference signal setter; 12 — accumulation time control unit; 13 — accumulation correction unit; 14 - personal computer (PC).

If the signal of all cells of the ruler 5 is less than the voltage of the reference signal supplied to the reference input of the comparator 8 from setting device 9, or more voltage of the reference signal to the reference input of comparator 10 of setting device 11, the set of signals corresponding to the fluorescence spectrum comes unchanged from block 7 of the buffer memory to the input of PC 14, which constructs and displays the spectrum.

If the signal from any of the cells of ruler 5 is greater than the voltage of the reference signal input to the comparator 8 from setting device 9, the command from comparator 8 is sent to the accumulation time control unit 12, which sends a command to ruler 5 to reduce the accumulation time. With a reduced accumulation time, the signal from the output of ruler 5, reduced in proportion to the accumulation time, is fed to the input of the buffer memory unit 6, and from the buffer memory unit, to the signal inputs of the comparators. If, at a reduced accumulation time, the signal from any of the cells of the ruler is less than the voltage of the reference signal input to comparator 8 from setting device 9, the set of signals corresponding to the fluorescence spectrum is fed from the buffer memory unit to accumulation correction unit 13, where it changes (increases) in inverse proportion to accumulation time, and then is sent in the digital form to the PC input for the PC to build and display the spectrum. Similarly, if the signal from any of the cells of the ruler is less than the voltage of the reference signal at the input of comparator 10 from setting device 11, a command is sent from comparator 10 to accumulation time control unit 12, which in turn sends a command to the ruler to increase the accumulation time. With increased accumulation time, the signal from the output of the ruler, increased in proportion to the accumulation time, is fed to the input of the buffer memory block, and from the buffer memory block to the signal inputs of comparators 8 and 10. If, with an increased accumulation time, the signal from all the cells of the ruler is higher than the voltage of the reference signal input to comparator 10 from setting device 11, the set of signals corresponding to the fluorescence spectrum is fed from the buffer memory unit to accumulation correction unit 12, where it decreases in inverse proportion to accumulation time, and then is sent in the digital form to the PC input for the PC to build and display the spectrum.

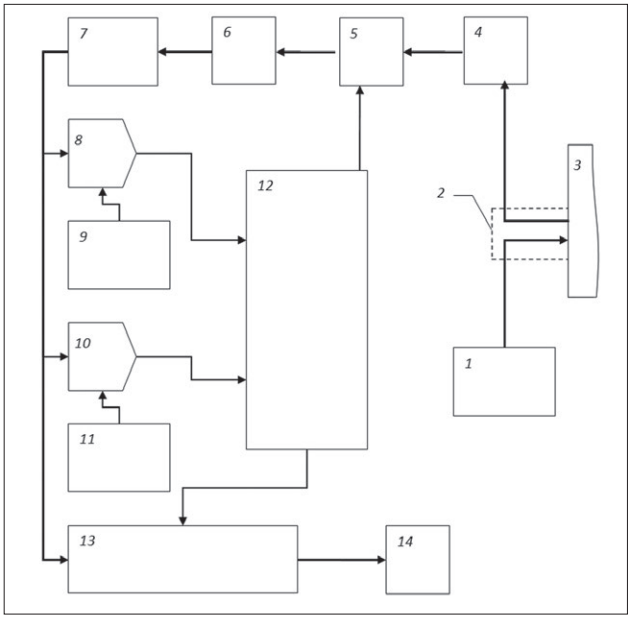

Рис. 2. Блок-схема спектроанализатора для спектрально-флуоресцентных исследований с расширенным динамическим диапазоном интенсивности сигналов флуоресценции
Fig. 2. Block-diagram of the spectra-analyzer for spectral-fluorescent studies with an extended dynamic range of intensity of fluorescence signals

Thus, if the signal value from any cell of the ruler is above the upper limit or below the lower limit of the specified range, the accumulation time of the device decreases (or, accordingly, increases) the set number of times. If the specified exposure adjustment is not sufficient to ensure that the signal is within the per-

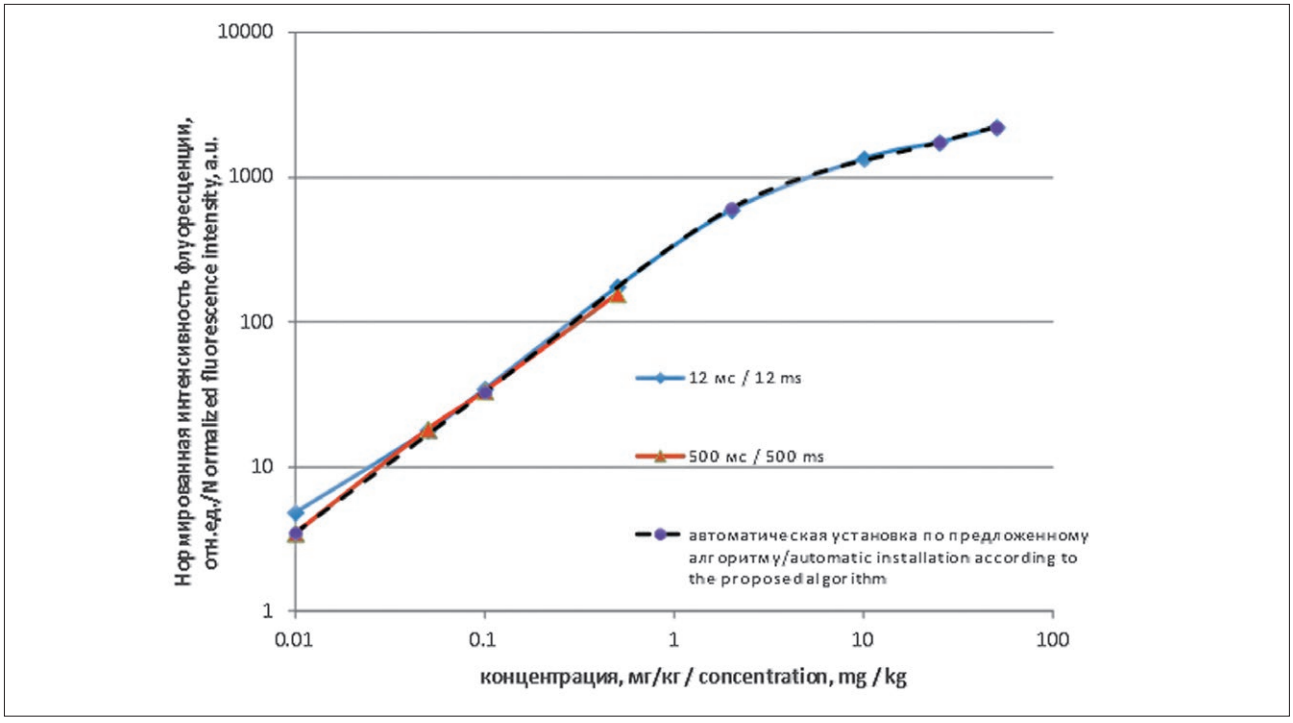

Рис. 3. Зависимость интенсивности флуоресценции ФС от его концентрации при разных временах экспозиции
Fig. 3. Dependence of fluorescence intensity of PS on its concentration at various exposure times

missible range of intensity, exposure adjustment is automatically repeated until the signal falls within this range.

The spectrum analyzer was tested on dispersions of a photosensitizer based on tetra-3-phenylthiophthalocyanine hydroxyalumium of various concentrations (from 0.01 mg/l to 50 mg/l), approximately corresponding to the concentrations used in the process of pharmacokinetics research in calibration samples and tissues of experimental animals.

When registering the fluorescence of PS with a constant small accumulation time, the dependence is distorted in the region of low concentrations, where an additional positive error is added to the signal due to the hardware noise of the spectrum analyzer (Fig. 3, the blue curve). At a constantly high accumulation time (Fig. 3, red curve), an error appears in the fluorescence signal region of dispersions with high concentrations. Moreover, starting with some concentration values, which depend on the accumulation time, signals cannot be recorded due to charge saturation of a part of the ruler.

When the spectrum analyzer is operated according to the proposed registration algorithm (with automatic change of accumulation time depending on the level of the fluorescence signal), the spectral information was recorded at high values of the signal-to-noise ratio and without distortion of the spectrum shape (see the dashed curve).

This made it possible, upon further processing of the signal, to construct the correct (undistorted) dependence of the integral fluorescence intensity of the dispersions of tetra-3-phenylthiophthalocyanine hydroxyaluminium on their concentration in the extended dynamic range of values exceeding 3.5 orders of magnitude (Fig. 3, the dashed curve).

Conclusion

The proposed algorithm for recording fluorescence spectra with an automatic change in the accumulation time depending on the signal level provided a significant expansion of the dynamic range of the spectrum analyzer and an increase in accuracy in pharmacokinetic studies. In addition, in photodynamic therapy, this made it possible to implement a more precise control of PS content in the tumor just before irradiation, during and after irradiation, to optimally choose the time to start irradiation and the whole radiation regime.

The study was done with the financial support of the Russian Foundation for Basic Research (Grant No. 18–08–01112A).

REFERENCES

1. *Rukovodstvo po provedeniyu doklinicheskih issledovaniy lekarstvennyh sredstv. CHast' pervaya* [A guide to preclinical drug research. Part One], ed. A.N. Mironov. Moscow, Grif and K Publ., 2012. 944 p.
2. Loschenov V.B., Linkov K.G., Savelieva T.A., Loschenov M.V., Model S.S., Borodkin A.V. Hardware and tool equipment for fluorescence diagnostics and photodynamic therapy, *Photodynamic therapy and photodyagnosis*, 2013, vol. 2, no. 3, pp. 17–25. (In Russian)
3. Meerovich G.A., Tiganova I.G., Makarova E.A., Meerovich I.G., Romanova Ju.M., Tolordava E.R. , Alekseeva N.V., Stepanova T.V., Koloskova Yu.S., Lukyanets E.A., Krivospitskaya N.V., Sipailo I.P., Baikova T.V., Loschenov V.B., Gonchukov S.A. Photodynamic inactivation of bacteria and biofilms using cationic bacteriochlorins, *J. Phys. Conf. Ser.,* 2016, vol. 691, 012011.
4. Meerovich G.A., Akhlyustina E.V., Tiganova I.G., Panov V.A., Tyukova V.S., Tolordava E.R., Alekseeva N.V., Linkov K.G., Romanova Yu.M., Grin M.A., Mironov A.F.4, Loschenov V.B., Kaprin A.D., Filonenko E.V. Study of photosensitizer for antibacterial photodynamic therapy based on cyclodextrin formulation of 13^3-N-(N-methylnicotinyl)- bacteriopurpurinimide methyl ester, *Biomedical Photonics*, 2017, vol. 6, no. 3, pp. 16–32. (in Russian)
5. Akhlyustina E.V., Bud'ko A.P., Lantsova A.V., Lin'kov K.G., Loschenov V.B., Savelieva T.A. *Ustroystvo dlya spektral'no-fluorestsentnogo issledovaniya soderzhaniya fluorohromov* [Device for spectral fluorescence study of the content of fluorochromes], Patent RF no. 2665628, 2018.

ЛИТЕРАТУРА

1. Руководство по проведению доклинических исследований лекарственных средств. Часть первая // под ред. А.Н. Миронова. – М.: Гриф и К, 2012. – 944 с.
2. Лощенов В.Б., Линьков К.Г., Савельева Т.А., Лощенов М.В., Модель С.С., Бородкин А.В. Аппаратурное и инструментальное обеспечение флюоресцентной диагностики и фотодинамической терапии // Фотодинамическая терапия и фотодиагностика. – 2013. – Т. 2, № 3. – С. 17–25.
3. Meerovich G.A., Tiganova I.G., Makarova E.A., Meerovich I.G., Romanova Ju.M., Tolordava E.R. , Alekseeva N.V., Stepanova T.V., Koloskova Yu.S., Lukyanets E.A., Krivospitskaya N.V., Sipailo I.P., Baikova T.V., Loschenov V.B., Gonchukov S.A. Photodynamic inactivation of bacteria and biofilms using cationic bacteriochlorins // J. Phys.: Conf. Ser. – 2016. – Vol. 691. – 012011.
4. Меерович Г.А., Ахлюстина Е.В., Тиганова И.Г., Панов А.В., Тюкова В.С., Толордава Э.Р., Алексеева Н.В., Линьков К.Г., Романова Ю.М., Грин М.А., Миронов А.Ф., Лощенов В.Б., Каприн А.Д., Филоненко Е.В. Исследование фотосенсибилизатора для антибактериальной фотодинамической терапии на основе циклодекстриновой композиции метилового эфира 13^3-N-(N-метилникотинил)-бактериопурпуримида // Biomedical Photonics. – 2017. – Т. 6, № 3. – С. 16–32.
5. Ахлюстина Е.В., Будько А.П., Ланцова А.В., Линьков К.Г., Лощенов В.Б., Меерович Г.А., Савельева Т.А. Устройство для спектрально-флуоресцентного исследования содержания флуорохромов. – Патент РФ № 2665628, 2018.

THE HISTORY OF RADIATION THERAPY (PART I)

Kaprin A.D.[1], Mardinskiy Yu.S.[2], Smirnov V.P.[3], Ivanov S.A.[2], Kostin A.A.[1], Polikhov S.A.[3], Reshetov I.V.[4], Fatianova A.S.[4], Denisenko M.V.[2], Epatova T.V.[2], Korenev S.V.[5], Tereshchenko A.V.[6], Filonenko E.V.[7], Gafarov M.M.[4], Romanko Yu.S.[2,4]

[1]National Medical Research Radiological Centre of the Ministry of Health of the Russian Federation (NMRRC), Obninsk, Russia
[2]A. Tsyb Medical Radiological Research Centre – branch of the National Medical Research Radiological Centre of the Ministry of Health of the Russian Federation (A. Tsyb MRRC), Obninsk, Russia
[3]Research Institute of Technical Physics and Automation (NIITFA), Moscow, Russia
[4]Sechenov First Moscow State Medical Univesity, Moscow, Russia
[5]Immanuel Kant Baltic Federal University, Kaliningrad, Russia
[6]Kaluga branch of S. Fyodorov Eye Microsurgery Federal State Institution, Kaluga, Russia
[7]P. Herzen Moscow Oncology Research Center – branch of FSBI NMRRC of the Ministry of Health of the Russian Federation (P.A. Herzen Moscow Oncology Research Center), Moscow, Russia

Abstract

In 1903, on the basis of Morozov Institute of the Moscow Imperial University (currently, P. Herzen Moscow Oncology Research Center, a branch of the National Medical Research Radiological Center, Ministry of Health of the Russian Federation), the first specialized unit in Russia was opened – department of radiation therapy of oncological diseases, in which scientific research in the field of medical radiology was officially launched in our country for the first time. The first studies in the field of radiation therapy can be attributed to this period.

The article presents a brief summary of the historical development of radiotherapy in the world and in Russia; provides information on the achievements of global importance, fundamental for this scientific field. The activities of leading Russian organizations in the field of radiation therapy are reviewed; names of scientists, doctors and other specialists who have made a significant contribution to its development are provided. The main literature sources relevant to the field are given.

The data in this article may be of interest and be useful for biomedical scientists, practicing radiologists and radiotherapists, oncologists, medical and graduate students, interns and other specialists.

Key words: history of medicine, development of radiation therapy, radiotherapy, medical radiology, therapeutic radiology, X-ray radiology, X-ray therapy, treatment of malignant neoplasms, radiological methods in oncology, radiation therapy in oncology, radioactivity.

For citations: Kaprin A.D., Mardinskiy Yu.S., Smirnov V.P., Ivanov S.A., Kostin A.A., Polikhov S.A., Reshetov I.V., Fatianova A.S., Denisenko M.V., Epatova T.V., Korenev S.V., Tereshchenko A.V., Filonenko E.V., Gafarov M.M., Romanko Yu.S. The history of radiation therapy (part I), *Biomedical Photonics*, 2019, vol. 8, no. 1, pp. 52–61. (in Russian) doi: 10.24931/2413–9432–2019–8–1-52–62.

Contacts: Gafarov M.M., e-mail: maratgafarov93@mail.ru

К ИСТОРИИ РАЗВИТИЯ ЛУЧЕВОЙ ТЕРАПИИ (ЧАСТЬ I)

А.Д. Каприн[1], Ю.С. Мардынский[2], В.П. Смирнов[3], С.А. Иванов[2], А.А. Костин[1], С.А. Полихов[3], И.В. Решетов[4], А.С. Фатьянова[4], М.В. Денисенко[2], Т.В. Эпатова[2], С.В. Коренев[5], А.В. Терещенко[6], Е.В. Филоненко[7], М.М. Гафаров[4], Ю.С. Романко[2,4]

[1]ФГБУ «НМИЦ радиологии» Минздрава России, Обнинск, Россия
[2]МРНЦ им. А.Ф. Цыба – филиал ФГБУ «НМИЦ радиологии» Минздрава России, Обнинск, Россия
[3]АО «НИИТФА», Москва, Россия
[4]ФГАОУ ВО Первый МГМУ им. И.М. Сеченова Минздрава России, Москва, Россия
[5]ФГАОУ ВО «БФУ им. И. Канта», Калининград, Россия
[6]Калужский филиал ФГАУ НМИЦ «МНТК "Микрохирургия глаза» им. акад. С.Н. Федорова» Минздрава России, Калуга, Россия

[7]МНИОИ им. П.А. Герцена – филиал ФГБУ «НМИЦ радиологии» Минздрава России, Москва, Россия

Резюме

В 1903 г. на базе Института им. Морозовых Императорского Московского университета (ныне Московский научно-исследовательский онкологический институт имени П.А. Герцена – филиал ФГБУ «Национального медицинского исследовательского центра радиологии» Минздрава России) открыли первое в России специализированное подразделение – отдел лучевой терапии онкологических заболеваний, в котором впервые в нашей стране были официально начаты научные исследования в области медицинской радиологии. К этому же периоду можно отнести первые исследования в области лучевой терапии.

В работе освещены основные этапы развития лучевой терапии в нашей стране и в мире; приведена информация о важнейших научных достижениях, имеющих общемировое значение и являющихся основополагающими для данного научного направления. Рассмотрена деятельность ведущих российских организаций в области лучевой терапии; названы имена ученых, врачей и других специалистов, внесших значительный вклад в ее развитие. Приведены основные литературные источники, актуальные в рассматриваемой области.

Данные статьи могут представлять интерес и быть полезными в работе ученых медико-биологического профиля, практикующих врачей-радиологов и радиотерапевтов, онкологов, слушателей факультетов последипломного образования, студентов медицинских факультетов, аспирантов, ординаторов и других специалистов.

Ключевые слова: история медицины, развитие лучевой терапии, радиотерапия, медицинская радиология, терапевтическая радиология, рентгенорадиология, рентгенотерапия, лечение злокачественных новообразований, радиологические методы в онкологии, лучевая терапия в онкологии, радиоактивность.

Для цитирования: Каприн А.Д., Мардынский Ю.С., Смирнов В.П., Иванов С.А., Костин А.А., Полихов С.А., Решетов И.В., Фатьянова А.С., Денисенко М.В., Эпатова Т.В., Коренев С.В., Терещенко А.В., Филоненко Е.В., Гафаров М.М., Романко Ю.С. К истории развития лучевой терапии (часть I) // Biomedical Photonics. – 2019. – Т. 8, № 1. – С. 52 –61. doi: 10.24931/2413–9432–2019–8–1-52–62.

Контакты: Гафаров М.М., e-mail: maratgafarov93@mail.ru

Introduction

2018 marked the 115th anniversary of the beginning of Russia's first research in the field of medical radiology on the basis of the Morozovs Institute of the Imperial Moscow University. Since 2014, this medical institution has been called P. A. Herzen Moscow Oncology Research Center (P. A. Herzen MORC), a Branch of the National Medical Radiology Research Center of the Ministry of Health of the Russian Federation (FSBI NMRC of Radiology of the Ministry of Health of the Russian Federation). In 1903, the first specialized radiological unit in our country, the department of radiation therapy of oncological diseases, was opened at the Morozovs Institute. To date, P. A. Herzen MORC, together with other two leading medical scientific organizations of Russia, A. F. Tsyb MRRC and O. N. Lopatkin Research Institute of Urology and Interventional Radiology, operate as a part of the FSBI NMRC of Radiology of the Ministry of Health of the Russian Federation.

The history of the formation and development of radiation therapy in the world dates back to the end of the 19th century, when the effects of ionizing radiation on the body were first studied. They were initiated by a number of fateful historical events connected with the discovery of artificial and natural radioactivity which caused a real revolution in science, including in the fields of physics, medicine, biology, etc., and predetermined its further development in various spheres of human activity. The history of radiation therapy will always keep the names of the scientists who were at the forefront of the discovery of radioactivity: Wilhelm Conrad Roentgen, Maria and Pierre Curie, Henri Becquerel and their followers [1].

A comprehensive study of the properties of X-rays was started immediately after they were discovered by K. Roentgen on November 8, 1895; it involved the determination of their physical properties, as well as their effects on various biological objects [2-4]. These processes were accelerated by the discovery of natural radioactivity in 1896 [5].

As early as 1896, Russian scientist I. R. Tarkhanov, who was one of the first to substantiate the ability of ionizing radiation to cause functional and structural changes in cells, tissues, organs and throughout the body, foresaw the widespread use of radiological methods in medicine [6].

In the same year, J. Gillman (USA) and V. Despeignes (France) made attempts to treat malignant neoplasms with X-rays [7]. In the same period, several more cases of treatment of cancer patients with X-rays were described.

In 1897, L. Freund (Austria) published data on the use of fractionated radiotherapy for the treatment of extensive pigmented nevus in a child [8]. This message and this date are often referred to as the beginning of radiation therapy, which is currently widely used in foreign and Russian medical practice [9–11].

Radiation therapy received a significant impetus after H. Becquerel described natural radioactivity, followed by radium and polonium discovery by Maria and Pierre Curie [5, 12]. In 1902, radium was successfully used in Vienna for the treatment of pharyngeal cancer, and in 1904 in New York, radium tubes were implanted directly into the tumor [13, 14].

In the Russian Empire, the works of the founder of radiation therapy of malignant tumors, D. F. Reshetillo, were published: the "X-ray Treatment" manual in 1906 [15] and later, in 1910, the monograph "Radium and its use for the treatment of skin diseases, malignant neoplasms and certain diseases of internal organs", which can be considered the first fundamental work published on this topic.

In 1911, Cl. Regaud (France) conducted experiments on the sterilization of a ram with three fractions of ionizing radiation with an interval of 15 days between them. The work by L. Freund and Cl. Regaud's series of experiments formed the basis of fractionated distance radiation therapy [8,16]. In the same period, in 1910, in the USA, O. Pasteau and P. Degrais proposed a brachytherapy method by delivering a radium ampoule through the urethra to the prostate [17, 18].

Cl. Regaud, in collaboration with other scientists at the Radium Institute of Paris, developed various techniques for using radium sources, including as an alternative to surgical resections and for intracavitary therapy of cervical tumors and tumors with other localisations [19].

In the same institute in 1920, H. Coutard successfully used fractional remote radiation therapy to treat a variety of head and neck tumors. The dose rate guidelines were the reactions to radiation of the skin and mucous membranes. H. Coutard proposed collimation in the formation of beams and the use of metal filters for the formation of monochrome radiation [20].

An important contribution to the development of the phenomenon of the time-dose-effect relationship in radiation therapy was made by the work of E. Quimby and M. Strandquist (USA) [21, 22]. Within this framework, F. Ellis (England) proposed using the concept and formula of a nominal standard dose, which compared different treatment regimens based on the total dose, the number of fractions and the total treatment time [23]. The work performed in this direction in respect of individual types of tumors and normal tissues remains relevant to this day, as well as the linear quadratic model used, which takes into account the ratio of unrepairable and repairable radiation damage for various cell types.

The energy of the first X-ray therapy installations did not exceed 100 keV, which limited their practical application. In 1913, W. Coolidge (USA) developed X-ray tubes with energy of about 200 keV. Later, the therapy with their use was called orthovoltage. The improvement took place in the direction of monochromization of the beam. Filters and a method of multi-field irradiation were widely used to produce harder X-ray irradiation and improve the dose distribution. In the early 1920s, devices were developed which could rotate beams around the tumor, which significantly expanded the possibilities and efficiency of radiation therapy in oncology. Significant optimization of radiotherapy was achieved after the development of a "cascade" tube, which was installed at the Memorial Hospital in New York, by W. Coolidge in 1926 [24, 25].

After E. Lawrence and D. Sloan (USA) created a linear accelerator in 1930 and the betatron was invented by D. Kerst (USA) in 1940, and synchrotron was produced by V. I. Wexler (USSR) and E. McMillan (USA), radiation therapy received a new impulse for further improvement.

The progress of radiation therapy accelerated sharply in 1950s-1960s. As early as in 1956, H. Kaplan treated patients at Stanford University with 6 MeV photons [26]. In the early 1960s, compact linear accelerators with the possibility of rotational irradiation were created. However, the development of radiation therapy during this period was mainly associated with the use of remote gamma therapy with cobalt-60 (^{60}Co) sources [27].

The next stage in the development of radiation therapy (early 1990s) is associated with the widespread use of high-energy linear accelerators, normally up to 20 MeV [28, 29]. The introduction of this technique significantly improved the technical parameters of radiation therapy and its tolerance by patients.

Further optimization of radiation therapy is associated with the improvement of diagnostic equipment, the widespread use of computerized (CT), magnetic resonance (MRI), positron emission (PET) tomographs, which allowed to develop the systems of three-dimensional planning of conformal radiation therapy [30]. At the same time, improvements were made to some additional options accompanying radiation therapy: fixing devices, systems forming irradiation fields with a complex configuration, etc. have appeared. The use of optimized conformal planning systems for radiation therapy, which implies maximum dose uniformity in the target and minimal radiation load on the tissues surrounding the tumor, was a qualitatively new step in the improvement of radiation therapy.

In 1978, it became possible, for the first time, to vary the intensity of the beams over the area of exposure, which provided more opportunities for further optimization of the spatial distribution of the dose during the implementation of intensity-modulated radiation therapy (IMRT). In the recent years (2000–2018), it became possible to perform radiation therapy with due account for the changes in the position of the tumor during ir-

radiation, the so-called image-guided radiation therapy (IGRT) [31, 32]

The main sources of radiation in modern radiation therapy are still the photon and electron radiation of accelerators. Today, the most interesting area, from the scientific and practical points of view and the perspectives of the method development, is hadron therapy (proton, ion, neutron) [33]. Protons, carbon ions, due to the presence of the Bragg peak, have better possibilities than photon radiation for optimizing the spatial distribution of the dose, which is especially important when the tumor is close to structures which are critical in terms of radiosensitivity [34].

Ion and neutron radiation have numerous radiobiological advantages compared with sparsely ionizing (photon, electron) radiation as it makes it possible to target more effectively slow-growing, hypoxic, recurrent and radioresistant tumors.

R. Stone (USA), who began his research in 1938, six years after the discovery of neutrons, became a pioneer in the use of a fast neutron beam for the treatment of malignant neoplasms [35]. At that time, it was not known that the same absorbed doses of different types of radiation create significantly different effects. Traditional regimes of neutron irradiation of patients resulted in severe radiation damage, and after a series of failures in 1942, the use of neutron radiation was discontinued for a long time.

The revival of interest in neutron therapy occurred after the research performed by the radiologist M. Catterall (UK), who, in cooperation with the physicist D. Bewley (USA) in the 1970s in Hammersmith, performed clinical trials on a cyclotron with an energy of fast neutrons of 8 MeV; the outcome of this work was a manual on the use of fast neutrons in oncology therapy [36]. At the end of the twentieth century, neutron therapy began to develop in our country [37]. It was proved that it is most effective in the treatment of tumors that are resistant to sparsely ionizing radiation.

The first positive experience of neutron capture therapy (NCT) is associated with the name of H. Hatanaka (Japan), who received very promising results in the treatment of brain gliomas in 1968 [38].

R. Wilson (USA) reported the possibility of using protons for radiation therapy for the first time in an article published in 1946 [39], and proton therapy was carried out on accelerators in the Berkeley Radiation Laboratory in 1954 and at Uppsala University (Sweden) in 1957.

Practical development of radiation therapy applications began in Japan in 1994, in the city of Chiba. The first hospital in the world specialized in ionic therapy was created at the National Institute of Radiological Sciences (NIRS) [40].

It should be noted that the main factor restricting wider clinical use of these technologies was their high cost and a limited number of specialized medical sources of hadrons.

The history of the development of radiation therapy in our country is inextricably linked with the history of this discipline in the rest of the world.

An important role in the development of Russian radiology was played by P. A. Herzen MORC [41], where, as it has been already mentioned, the first specialized subdivision of this type in Russia, the department of radiation therapy of oncological diseases, was opened in 1903. That was the beginning of the first official research in this field in Russia. The department was headed by D. F. Reshetillo, a prominent scientist who was at the beginning of the research on the possibilities of radiation therapy for the treatment of malignant tumors. Under the leadership of D. F. Reshetillo, as early as in the very first stages of the development of the radiation therapy method in oncology, the effectiveness of the fractional irradiation method was studied [15].

The radiologists of the institute were at the origin of the creation of the first gamma-therapeutic units with radium and radium-mesothorium sources and took an active part in the development and testing of new models of these devices.

In the 1920s-1930s, radiologists investigated the effectiveness of extensive fractional method of radiation therapy, various aspects of the overall effect of radiation on the patient's body during local irradiation of a tumor, dose distribution over time, the best options for combining radiation of different energies with different tumor localizations (M. P. Astrakhan, M. P. Domshlak, D. B. Nevorozhkin, S. R .Frenkel and others).

P. A. Herzen MORC began the development of methods of concomitant and combined radiation treatment of breast and cervix cancer, as well as cancer with other localisations (P. A. Herzen, M. P. Domshlak, L. M. Nisnevich , A.I. Savitsky, S. R. Frenkel).

In 1939, the first teleradium unit in the USSR was installed at the institute; the source used in the unit was 4 g of radium. In that time, there were no installations with a greater activity in other countries.

After the war, P. A. Herzen MORC resumed its research aimed at the development and enhancement of radiation therapy. Special attention was paid to the development of the concomitant method with the use of various sources, dose levels and volumes of exposure. The combination of close-focus radiotherapy and remote radiotherapy was tested for the treatment of cancer of the oral cavity, vulva, and cervix (Astrakhan, D. B., Volkova, M. A., Kiseleva, E. S.).

In the 1960s – 1970s, studies were conducted at the institute with the use of ^{198}Au, ^{90}Y, ^{32}P, ^{131}I, as well as testing of brachytherapy devices of AGAT series, ROKUS series remote radiation therapy devices, the first domestic

MICROTRONE type spiral accelerator (V. A. Kvasov, Yu. A. Rakhmanin and others.). A significant contribution to the soultion of the problem of tumor radioresistance during radiation therapy was made by the research conducted by A. V. Boyko, S. L. Daryalova, A. V. Chernichenko.

In the years that followed, the areas of work of P. A. Herzen MORC in the field of radiation therapy were the following:

- the development and introduction into a wide clinical practice of a complex of automated methods and means of radical radiation therapy;
- development of radiomodifiers to increase the effectiveness of radiotherapy of malignant tumors;
- development and introduction into clinical practice of laser facilities for the treatment of cancer patients.

In 2014, P. A. Herzen MORC became a part of FSBI of the National Medical Radiology Research Center of the Ministry of Health of the Russian Federation, and Academician A. D. Caprin was appointed as the head of the institution.

The Roentgenologic and Radiologic Institute founded in St. Petersburg in 1918 (later known as the State Roentgenologic and Radiologic Institute and CRIRRI; and now called FSBI Russian Scientific Center of Radiology and Surgical Technologies named after Academician A. M Granov) of the Ministry of Health of the Russian Federation was the world's first institution of this kind [42]. Later, it became a model for roentgen radiological institutes established in Kharkov (1920), Moscow (1924) and other cities of the USSR.

The founder of the world's first Roentgenologic and Radiologic Institute was professor M. I. Nemenov. In the beginning of the activities of the institute, some of its specialists were the most significant representatives of Russian physics, clinical and theoretical medicine: I. V. Kurchatov, N. N. Anichkov, V. G. Garshin, A. A. Zavarzin, N. S. Kupalov, E. S. London, G. V. Mor, G. A. Nadson, V. A. Oppel, N. N. Petrov, P. V. Troitsky, N. Ya. Chistovich and others, whose works laid the foundations of Russian X-ray radiology.

For the first time in our country, treatment methods based on the use of X-rays and radium for various tumors and non-neoplastic diseases were developed in the Roentgenology and Radiology Institute, and in 1937 the first Russian manual on the clinical use of radium for therapeutic purposes was published.

In this period, as well as later on, the achievements of the Institute in the field of radiation therapy were also associated with the names of I. N. Grekov, F. S. Grossmann, L. I. Korytova, B. A. Konov, N. N. Petrov, A. S. Strashinin, L. P. Simbirtseva, V. A. Shaak, A. M. Yugenbyrg and many others.

In 1966, the medical and biological department was created at the phasotron of A. F. Ioffe Physicotechnical Institute for the purpose of developing methods of hadron (proton) therapy of tumor and non-tumor diseases that cannot be cured with traditional methods of radiation therapy. The successful introduction of this method into clinical is associated with the name of Professor B. A. Konov.

As mentioned above, in January 1924, by the decision of the Council of People's Commissars, Roentgen Institute was established (later, Moscow Research Institute of Roentgenology and Radiology; Moscow Research Institute of Diagnostics and Surgery), which is now the Federal State Institution «Russian Research Center of Roentgenology and Radiology» of the Ministry of Health of the Russian Federation (RRCRR) [43].

The first director of the institute was academician P. P. Lazarev, the founder of domestic biophysics, a pioneer in the study of the biological effects of ionizing radiation and the creator of the world's first rotational x-ray machines.

Since the establishment of the institution, a significant place in its work has belonged to the issues of improving radiation therapy for tumor and non-tumor diseases, including gynecological diseases. (Ivanitskaya, E.P., Karlin, M.I., Kolosov, M.A., Shaposhnikova, N.E., and others), thoracic and abdominal diseases (Kornev, N.I., Panshin, G.A., Pavlov, A.S., Podlyaschuk, L.D., Pereslegin, I.A., Ruderman, A.I., Sarkisyan, Y. K., Tsybulsky, I. B., and others).

Much attention was paid to the development of rational methods of radiation therapy, evaluation of the effectiveness of radiation treatment and the development of measures to prevent complications after radiation therapy (Panshin, G.A., Titova, V.A., Khmelevsky, E.V. and others).

The Institute is one of the pioneers in the development of modern methods of combined and complex treatment of malignant tumors of the main localizations, which have a significant economic effect.

At the Research Institute of Oncology opened on the basis of I. I. Mechnikov Leningrad Multidisciplinary Hospital, now FSBI N. N. Petrov National Medical Research Center of Oncology of the Ministry of Health of Russia (N. N. Petrov NMRC for Oncology), [44] radiation therapy of malignant tumors has been used since its foundation in 1927, when professor N.N. Petrov ordered radium preparations and needles to be made in Paris.

During the establishment of the institute, radiation treatment was carried out by the employees of one X-ray department which had two, and later three, radiotherapy devices.

In 1945, a special radium laboratory was organized at the institute, which was headed by N. D. Perumov. Under her leadership, a method of photodosimetry of radium gamma rays was developed and the suitability of this

method for photodosimetry of ^{60}Co rays was tested. This technique made it possible to measure doses and investigate the homogeneity of radiation in any planes of the irradiated tissue volume.

In 1967, a high-energy laboratory was opened, with powerful megavolt installations for remote radiation therapy; its head was A.P. Kozlov. The laboratory has developed computer programs for optimal dosimetry planning of megavolt radiotherapy, which are used in all Russian-made radiotherapy units (gamma devices like ROKUS, Agat C, Agat R, accelerators of B5M-25, LUE-25 types, etc., AGAT-B, AGAT-VU devices for intracavitary radiation).

In the late 1960s, the personnel of the former Radium Laboratory worked in the Radiology Department: L. E. Pakulina, N. D. Perumova, A. A. Stankevich, V. M. Uglova and others. The main scientific direction of the radiological department was the improvement and development of remote and contact radiation therapy for malignant tumors. In 1965–1966, a device for autoloading intracavitary gamma therapy was developed.

Currently, the department has a 40-bed in-patient ward, where intensive research is successfully conducted aimed at improving the treatment of common tumors of the esophagus, trachea and bronchi with the use of the methods of endoscopic surgery, argon plasma coagulation and intraluminal brachytherapy. A new medical technology has been created for the treatment of locally advanced malignant tumors of the central bronchi and trachea, and various types of intensive, large-scale preoperative irradiation in breast, lung, esophagus, cardiac stomach and rectum cancers are undergoing intensive testing.

Due to the creation of new specialized institutes and departments and oncological dispensaries in the USSR, there was a rapid development of technical, radiobiological and methodological aspects of radiation therapy.

Significant contribution to the development of radiation therapy in our country in the previous and the subsequent years was made by N. N. Azhigaliev, B.M. Aliev, S. B. Balmukhanov, L. M. Goldstein, Ya. G. Dillon, M. P. Domshlak, K. I. Zholkiver, A. N. Kishkovsky, A. V. Kozlova, G. V. Muravskaya, M.P. Pobedinsky, A.D. Podliashchuk, A. S. Pavlov, I. A. Pereslegin, A. I. Ruderman, S. F. Frenkel and many other scientists.

Successes in the development of domestic radiotherapy are also associated with the activities of the FSBI N.N. Blokhin National Medical Research Center of Oncology of the Ministry of Health of the Russian Federation [45, 46].

In 1959, it was decided to build the Institute of Experimental and Clinical Oncology of the Academy of Medical Sciences of the USSR (IE&CO of MSA of the USSR), which later became N.N. Blokhin Russian Oncological Reseach Center (N.N. Blokhin RORC). The first head of the entire radiotherapy section was A. I. Ruderman, and the specialists who worked under his leadership included B. M. Aliyev, E. M. Ivanova, M. M. Nevinskaya, M. S. Starichikov and others.

An important contribution to the successful development of radiation therapy in N. N. Blokhin RORC was the creation of the Department of Medical Physics and the Radiobiology Laboratory headed by professor S. P. Yarmonenko.

From 1980 to 1995, the Department of Clinical Radiation Therapy was headed by Professor B. M. Aliyev. His students became heads of radiotherapy departments in various parts of the USSR: in N. N. Blokhin RORC, S. I. Tkachev, T. V. Yuriev, in Lithuania, E. A. Aleknavichus, in Kyrgyzstan, R. A. Aralbayev.

From 1982 to 2001, the Radiation Therapy Department of N. N. Blokhin RORC was headed by Professor G. V. Goldobenko, the first President of the Russian Association of Therapeutic Radiation Oncologists (RATRO), an enthusiastic and talented scientist, an excellent doctor and teacher. Under his leadership, research in the field of optimization of dose fractionation modes was greatly expanded, as well as research related to the use of radioprotectors (hypoxic gas mixtures) and radiosensitizers (local hyperthermia, artificial hyperglycemia, and cryo-radiation therapy), and much broader opportunities were provided for the use of radiation therapy in pediatric oncology.

In 2001, professor S. I. Tkachev was appointed to the position of the head of the department.

The department of radiation therapy included the section of proton radiation therapy headed by professor A. I. Ruderman (1976–1984), where B.V. Astrakhan, G. D. Monzul, G. V. Makarova and others worked. The core assets of the department were the technical proton accelerators of A. I. Alikhanov Institute of Theoretical and Experimental Physics in Moscow and the Joint Institute for Nuclear Research in Dubna, Moscow Region, where proton radiation therapy was administered to more than 3,000 cancer patients.

As early as in 2001, the department of radiation therapy of N. N. Blokhin RORC became the first center in Russia to use 3D volumetric planning and conformal (3D CRT) radiation therapy and its more advanced options: intensity-modulated radiation therapy (IMRT), Volumetric Intensity Modulated Arc Therapy (VIMAT), image-guided radiation therapy (IGRT), radiation therapy with tumor movement control, stereotactic radiosurgery (SRS) and stereotactic radiotherapy (SRT). The study of the effectiveness of the use of radioprotectors and radiosensitizers continued, and the use of various types of the sequences of radiation and pharmaceutical treatment of cancer was enhanced and expanded.

The department of radiosurgery, established in 1980 and led by N.S. Androsov until 1995, and then by M. I.

Nechushkin, improved the methods of contact and concomitant radiation therapy in gynecological oncology (O. A. Kravets), oncoproctology (I. A. Gladilina), oncourology (A. V. Petrovsky), hematology (E. S. Makarov).

Since 2003, ESTRO educational schools for radiologists from Russia and the CIS countries have been held regularly on the basis of the Department of Radiotherapy of N.N. Blokhin RORC.

Since 2006, the Department of Radiotherapy and the Association of Medical Physicists of Russia (whose president is professor V. A. Kostylev) have organized and conducted educational courses for radiologists and medical physicists in Russia and the CIS countries. V. A. Kostylev and G. V. Goldobenko also organized the Russian Association of Therapeutic Radiation Oncologists (RATRO) and led it in the early stages of its formation. In the following years, RATRO presidents were Yu. S. Mardynsky, A. V. Chernichenko, and now it is led by A. D. Caprin.

Well-known scientists S. B. Aliyev, T. N. Borisova, S. M. Ivanov, S. V. Medvedev, O.P. Trofimova work in the radiation department. In 2015, the department of radiation therapy was headed by A.V. Nazarenko, and it continued to develop and improve the use of radiotherapy in the complex treatment of cancer patients.

An active part in the development of new methods of radiation, combination and complex therapy of malignant neoplasms and the improvement of existing ones is taken by oncology institutes and large oncological dispensaries in Arkhangelsk, Volgograd, Irkutsk, Kazan, Rostov-on-Don, Tomsk, Ufa, Chelyabinsk, Chita, etc.

As it is well-known, the foundation of radiation therapy is physical/technical, radiobiological and medical knowledge. Therefore, the main specialists in this field are, respectively, medical physicists, radiobiologists, radiotherapists, as well as representatives of engineering and technical field, without whose participation the creation and operation of modern radiotherapy equipment would be unthinkable.

When we recall the scientists and engineers who developed and improved the equipment for radiation therapy, we have to mention, first of all, three main organizations: Leningrad Research Institute of Electrophysical Equipment named after D.V. Efremov, now AO RIEPE (creation and production of accelerator technology and LUE-15, LUER 20, LUER 20M), Snezhin All-Union Research Institute of Instrument Engineering, now FSUE Russian Federal Nuclear Center E. I. Zababakhin All-Russian Scientific Research Institute of Technical Physics (creation and production of gamma-therapeutic equipment based on ^{60}Co and other radioactive elements), and RPA Agat (production of Rokus gamma-therapeutic units and Microtron accelerator).

Well-known researchers who worked in these institutions made a significant contribution to the development and production of Russian radiation therapy units. They include V. M. Aleshin, E. A. Zhukovsky, S.P. Kapitsa, V. A. Komar, A.R. Mirzoyan, A.F. Rimman, A. G. Sulkin, A. S. Shtan, M. V. Kheteev and many others.

Modern radiation therapy is also impossible without medical physicists. The contribution of Soviet and Russian physicists to ensuring the quality of radiation therapy in the 2nd half of the twentieth century is in no way inferior to the achievements of their American and European colleagues. This applies primarily to the emergence and implementation of mathematical methods for optimizing the distribution of the absorbed dose, multileaf collimation, matrix detectors for analyzing the dose distribution of photon and electron radiation, conformal radiation therapy, physico-technical substantiation and improvement of hadron (proton and neutron) therapy [47].

A significant contribution to the development of Soviet/Russian medical physics was made by S. M. Vatnitsky, I. A. Ermakov, R. V. Sinitsyn, A. M. Chervyakov, O. A. Shtukovsky (TsRRRI); A. I. Krongauz, R. S. Milstein, E. G. Chikirdin (MRRRI); E. B. Bozhanov, A. P. Kozlov (N. N. Petrov Institute of Oncology); V. A. Kvasov (P. A. Herzen Research Institure); O. N. Denisenko (MRRC, Obninsk); M. A. Weinberg, V.A. Kostylev, N. A. Lutova, N. N. Lebedenko, T. G. Ratner (N. N. Blokhin RORC); I. G. Tarutin, A. G. Strakh (N. N. Alexandrov Institute of Oncology, Belarus); B. K. Nikishin (KRRROI, Ukraine) and many others.

It was these specialists who suggested most of the technical solutions and provided their implementation, and their developments corresponded to the advanced trends in the development of therapeutic techniques. Unfortunately, for objective reasons, Russian manufacturers failed to maintain a high level and scope of radiotherapy equipment production.

We are currently witnessing a revival of attention to the Russian medical instrument-making industry and a rapidly reviving interest in the use of ionizing and non-ionizing radiation in various branches of science and technology, and especially in medicine.

The unique experience of cooperation of A. F. Tsyb MRRC and AO Research Institute for Technical Physics with leading physico-technical institutions of Russia served as the basis for the implementation of a pilot project on the creation and conduct of clinical trials of the first sample of a domestic specialized medical import-substituting radiotherapy complex based on innovative equipment, 6 MeV accelerator and a cone-beam tomograph, in Obninsk.

The work is implemented in the framework of the agreement between the Ministry of Education and Science of the Russian Federation and AO Recearch Institute of Technical Physics and Automation on the provision

of a subsidy dated 03.10.2017 No. 14.582.21.0011 "The Creation and Transfer for Clinical Trials of a Sample of an Import-Substituting Radiotherapy Complex Based on Innovative Eequipment (6 MeV accelerator and a cone-beam tomograph)". The unique identifier of the agreement is RFMEFI58217X0011.

The results of the work of A. F. Tsyb MRRC, a branch of the NMRC of Radiology of the Ministry of Health of the Russian Federation and AO Recearch Institute of Technical Physics and Automation confirm the relevance and practical significance of the research conducted in the institution. They are the evidence of the effective use of the synthesis of fundamental and applied research for the development of new medical radiological technologies and their introduction into medical practice.

The Institute of Medical Radiology of the Academy of Medical Sciences of the USSR, the largest institute of radiological profile, was established in Obninsk in 1962, and, with its powerful experimental base and clinic, it became the country's leading institution for the development of high-tech medical radiological methods for diagnosing and treating patients and the basic institution for the research on the problems of Medical Radiology and Radiation Medicine. Its founder and first director was academician G. A. Zedgenidze [48, 49]. Today it is A. F. Tsyb Medical Radiological Research Center (director: professor of RAS S. A. Ivanov), which since 2014 has been a branch of FSBI «National Medical Research Center of Radiology» of the Ministry of Health of the Russian Federation (Director General: Academician of RAS A. D. Kaprin), including also P. A. Herzen Moscow Research Institute of Oncology. (director: Academician of RAS A. D. Kaprin) and N. A. Lopatkin Research Institute of Urology and Interventional Radiology (director: corr. member of RAS O. I. Apolikhin).

The inclusion of the MRRC into the united Center, the Federal Research Center for Radiology of the Ministry of Health of the Russian Federation, provided broader opportunities for introducing the results of the center's own basic research into clinical practice, opening up new ways to successfully solve current development problems and create high-quality practical applications of therapeutic radiology [50].

Continuing research in the field of medical radiology, radiation biology and radiation epidemiology will undoubtedly contribute to the reinforcement of national security in the field of public health and improve the health of Russian citizens.

Part II of this article will present a more detailed review of the achievements of the A.F. Tsyb MRRC and its place in the history of the development of radiation therapy.

REFERENCES

1. L'Annunziata M.F. *Radioactivity: Introduction and History*. Amsterdam, Elsevier, 2007. 632 p.
2. Vlasov P.V. Otkrytie rentgenovskih luchej [Discovery of X-Rays], *Vestnik Rentgenologii i Radiologii*, 1995, no. 5, pp. 55–57. (In Russian)
3. Hellman S. Roentgen centennial lecture: discovering the past, inventing the future, *Int. J. Rad. Oncol. Biol. Phys.*, 1996, vol. 35, no. 1, pp. 15–20.
4. Röntgen W. On a new kind of rays, *Proceedings of the Wűrzburg Physico-Medical Society*, 1895.
5. Becquerel H. Sur les radiations invisibles émises par les sels d'uranium, *CR Acad Sci (Paris)*, 1896, 122, pp. 689–694. (In French)
6. Tarkhanov I.R. Opyt nad dejstviem Rentgenovskih X-luchej na zhivotnyj organism [Experience on the effect of X-rays on animal organism]. *Izvestiya. St.-Petersb. Biol. Lab.*, 1896, vol.1, no.3, pp. 47–52. (In Russian)
7. Despeignes V. Observation concernant un cas de cancer de l'estomac traité par les rayons Röntgen, *Lyon médical: Gazette médicale et Journal de médecine réunis Société médicale des hôpitaux de Lyon*, 1896, pp. 428–430. (in French)
8. Freund L. Ein mit Röntgen-strahlen behandelter Fall von Naevus pigmentosis piliferus, *Wien Med Wochensch*, 1897, no. 10, 428–33. (in German)
9. Connell P., Hellman S. Advances in radiotherapy and implications for the next century: A historical perspective, *Cancer. Res.*, 2009, vol. 69, no. 2, pp. 383–392.
10. *Osnovy luchevoy diagnostiki i terapii: natsional'noye rukovodstvo* [Fundamentals of radiation diagnosis and therapy: national manual], by acad. S.K. Ternovoy as eds. Moscow, GEOTAR-Media Publ., 2012. 992 p. (in Russian).

ЛИТЕРАТУРА

1. L'Annunziata M.F. Radioactivity: Introduction and History. – Amsterdam: Elsevier, 2007. – 632 p.
2. Власов П.В. Открытие рентгеновских лучей // Вестник рентгенологии и радиологии. – 1995. – № 5. – С. 55–57.
3. Hellman S. Roentgen centennial lecture: discovering the past, inventing the future // Int. J. Rad. Oncol. Biol. Phys. – 1996. – Vol. 35, No. 1. – P.15–20.
4. Röntgen W. On a new kind of rays // Proceedings of the Wűrzburg Physico-Medical Society. – 1895.
5. Becquerel H. Sur les radiations invisibles émises par les sels d'uranium // CR Acad Sci (Paris). – 1896. – 122. – P. 689–694.
6. Тарханов И.Р. Опыт над действием Рентгеновских Х-лучей на животный организм // Известия С.-Петербургской биологической лаборатории. – 1896. – Т. 1, № 3. – С. 47–52.
7. Despeignes V. Observation concernant un cas de cancer de l'estomac traité par les rayons Röntgen. Lyon médical // Gazette médicale et Journal de médecine réunis Société médicale des hôpitaux de Lyon. – 1896. – P. 428–430.
8. Freund L. Ein mit Röntgen-strahlen behandelter Fall von Naevus pigmentosis piliferus // Wien Med Wochensch. – 1897. – 10. – P. 428–33.
9. Connell P., Hellman S. Advances in radiotherapy and implications for the next century: a historical perspective // Cancer Res. – 2009. – Vol. 69, No. 2. – P. 383–392.
10. Основы лучевой диагностики и терапии: национальное руководство / Под ред. акад. С.К. Терновой. – М.: ГЭОТАР-Медиа, 2012. – 992 с.
11. Терапевтическая радиология: руководство для врачей / Под ред. А.Ф. Цыба, Ю.С. Мардынского. – М.: ООО «МК», 2010. – 552 с.
12. Curie P., Curie M. Les nouvelles substances radioactives et les rayons qu'elles émettent // Rapports présentés au Congrès

11. *Terapevticheskaya radiologiya: rukovodstvo dlya vrachey* [Therapeutic radiology: a guide for physicians], by Tsyb A.F., Mardynsky Yu.S. as eds. Moscow, OOO "MK" Publ., 2010. 552 p. (in Russian)
12. Curie P., Curie M. Les nouvelles substances radioactives et les rayons qu'elles émettent, *Rapports présentés au Congrès international de Physique*, Gauthier-Villars, Paris, 1900, vol. III, pp. 79–114. (in French)
13. Wickham L., Degrais P. *Radium as employed in the treatment of cancer, angiomata, keloids, local tuberculosis and other affectations*. New York, Paul B. Hoeber, 1913.
14. Mould R.F. Priority for radium therapy of benign conditions and cancer, *Curr. Oncol.*, 2007, vol. 14, no. 3, pp. 118–122.
15. Reshetillo D.F. *Lecheniye luchami rentgena* [Treatment with X-rays]. Moscow, 1906. (in Russian)
16. Regaud Cl. Influence de la duree d'irradiation sur les effets determines dans le testicule par le radium, *Compt. rend. Soc. biol.*, 1922, no. 86, pp. 787–790. (in French)
17. Pasteau O., Degrais P. De L'emploi du radium dans le traitement des cancers de la prostate, *J. Urol. Med. Chir.*, 1913, no. 4, pp. 341–366. (in French)
18. Ash D., Bottomley D.M., Carey B.M. Prostate brachytherapy, *Prostate Cancer and Prostatic Diseases*, 1998, no. 1, pp. 185–188.
19. Ferroux R., Monod O., Regaud Cl. Treatment of cancer of the neck of the uterus by radium at a distance; technique and first results, *J. de radiol. et d'électrol.*, 1926, X, 21–23 (also publ. in the *American Journal of Surgery*, 1927, vol. 2, no. 1, pp. 96.).
20. Coutard H. Principles of X-ray therapy of malignant diseases, *Lancet*, 1934, no. 2, pp. 1–12.
21. Quimby E.H. Achievement in Radiation Dosimetry, 1937–1950, *Br J Radiol*, 1951, vol. 24, no. 277, pp. 2–5.
22. Strandquist M. Studies of the Cumulative Effects of Fractionated X-Ray Treatment, *Acta Radiol*, 1944, Suppl. 55, pp. 1–300.
23. Ellis F. Dose, time and fractionation: a clinical hypothesis, *Clin. Radiol.*, 1969, no. 20, pp. 1–7.
24. Busch U. 100 years of the Coolidge tube, *Rofo*, 2014, vol. 86, no.1, pp. 85–86. (in German)
25. Coolidge W.D. The development of modern roentgen-ray generating apparatus, *Am. J. Roentgenology*, 1930, no. 24, pp. 605–620.
26. Kaplan H.S., Bagshaw M.A. The Stanford medical linear accelerator. III. Application to clinical problems of radiation therapy, *Stanford Med. Bull.*, 1957, vol. 15, no. 3, pp. 141–151.
27. Ginzton E.L., Craig S. Nunan History of microwave electron linear accelerators for radiotherapy, *J. Radiation Oncology Eml. Phys*, 1985, vol. 11, pp. 205–216.
28. Baker M. Medical linear accelerator celebrates 50 years of treating cancer, *Stanford Report*, 2007. Available at: https://news.stanford.edu/news/2007/april18/med-accelerator-041807.html (accessed 22.05.2018)
29. Chernyaev A.P. Nuclear-physical technologies in medicine, *Fizika ehlementarnyh chastic i atomnogo yadra*, 2012, vol. 43, no. 2, pp. 499–518. (in Russian)
30. Marusina M.Ya., Kaznacheeva A.O. Current state and prospects of tomography, *Nauchno-Tehnicheskii Vestnik Informatsionnykh Tekhnologii, Mekhaniki i Optiki*, 2007, no. 42, pp. 3–13. (In Russian)
31. Taylor A., Powell M.E.B. Intensity-modulated radiotherapy–what is it? *Cancer Imaging*, 2004, vol. 4, no. 2, pp. 68–73.
32. Matjakin G.G., Chuprik-Malinovskaya T.P., Nasnikova I.Yu., Yemeljanov I.V. Modern possibilities of radiation therapy in oncology, *Kremlevskaya Medicina*, 2011, no. 1, pp. 47–51. (In Russian)
33. Gulidov I.A., Mardinskiy Yu.S. Hadron radiation therapy of malignant tumors, *Vmeste protiv raka: Vracham vsekh spetsial'nostey*, 2005, no. 3, pp. 33–37.
34. Brown A., Suit H. The centenary of the Bragg peak, *Radiother. Oncol.*, 2004, no. 73, pp. 265–268.
35. Stone R., Laurence J., Aebersold P. Preliminary report on use of international de Physique, Gauthier-Villars, Paris. – 1900. – Vol. III. – P. 79–114.
13. Wickham L, Degrais P. Radium as employed in the treatment of cancer, angiomata, keloids, local tuberculosis and other affectations. – New York: Paul B. Hoeber, 1913.
14. Mould R.F. Priority for radium therapy of benign conditions and cancer // Curr. Oncol. – 2007. – Vol. 14, No. 3. – P.118–122.
15. Решетилло Д.Ф. Лечение лучами рентгена. – М., 1906.
16. Regaud Cl. Influence de la duree d'irradiation sur les effets determines dans le testicule par le radium // Compt. rend. Soc. biol. – 1922. – No. 86. – P. 787–790.
17. Pasteau O., Degrais P. De L'emploi du radium dans le traitement des cancers de la prostate // J. Urol. Med. Chir. – 1913. – No. 4. – P. 341–366.
18. Ash D., Bottomley D.M., Carey B.M. Prostate brachytherapy // Prostate Cancer and Prostatic Diseases. – 1998. – No. 1. – P. 185–188.
19. Ferroux R., Monod O., Regaud Cl. Treatment of cancer of the neck of the uterus by radium at a distance; technique and first results // J. de radiol. et d'électrol. – 1926. – Vol. X. – P. 21–23 (also publ. in the American Journal of Surgery. – 1927. – Vol.2, No. 1. – P. 96.)
20. Coutard H. Principles of X-ray therapy of malignant diseases // Lancet. – 1934. – No. 2. – P. 1–12.
21. Quimby E.H. Achievement in Radiation Dosimetry, 1937–1950 // Br J Radiol. – 1951. – Vol. 24, No. 277. – P. 2–5.
22. Strandquist M. Studies of the Cumulative Effects of Fractionated X-Ray Treatment // Acta Radiol. – 1944. – Suppl. 55. – P. 1–300.
23. Ellis F. Dose, time and fractionation: a clinical hypothesis // Clin. Radiol. – 1969. – No. 20. – P. 1–7.
24. Busch U. 100 years of the Coolidge tube // Rofo. – 2014. – Vol. 86, No. 1. – P. 85–86.
25. Coolidge W.D. The development of modern roentgen-ray generating apparatus // Am. J. Roentgenology. – 1930. – No. 24. – P. 605–620.
26. Kaplan H.S., Bagshaw M.A. The Stanford medical linear accelerator. III. Application to clinical problems of radiation therapy // Stanford Med. Bull. – 1957. – Vol. 15, No. 3. – P. 141–151.
27. Ginzton E.L., Nunan C.S. History of microwave electron linear accelerators for radiotherapy // J. Radiation Oncology Eml. Phys. – 1985. – Vol. 11. – P. 205–216
28. Baker M. Medical linear accelerator celebrates 50 years of treating cancer // Stanford Report. – 2007. Available at: https://news.stanford.edu/news/2007/april18/med-accelerator-041807.html (accessed 22.05.2018)
29. Черняев А.П. Ядерно-физические технологии в медицине // Физика элементарных частиц и атомного ядра. – 2012. – Т. 43, № 2. – С. 499–518.
30. Марусина М.Я., Казначеева А.О. Современное состояние и перспективы развития томографии // Научно-технический вестник информационных технологий, механики и оптики. – 2007. – № 42. – С. 3–13.
31. Taylor A., Powell M.E.B. Intensity-modulated radiotherapy–what is it? // Cancer Imaging. – 2004. – Vol. 4, No. 2. – P. 68–73.
32. Матякин Г.Г., Чуприк-Малиновская Т.П., Насникова И.Ю., Емельянов И.В. Современные возможности лучевой терапии в онкологии // Кремлевская медицина. Клинический вестник. – 2011. – № 1. – С. 47–51.
33. Гулидов И.А., Мардынский Ю.С. Адронная лучевая терапия злокачественных новообразований // Вместе против рака: Врачам всех специальностей. – 2005. – № 3. – С. 33–37.
34. Brown A., Suit H. The centenary of the Bragg peak // Radiother. Oncol. – 2004. – No. 73. – P. 265–268.
35. Stone R., Laurence J., Aebersold P. Preliminary report on use of fast neutrons in treatment of malignant disease // Radiology. – 1940. – No. 35. – P. 322–327.

fast neutrons in treatment of malignant disease, *Radiology*, 1940, no. 35, pp. 322–327.
36. Catterall M., Bewley D. *Fast neutrons in the treatment of cancer. London*, Academic Press and New York, Grune and Stratton, 1979, p. 39
37. Mardinskiy Yu.S., Gulidov I.A. Application of neutrons for remote radiation therapy of malignant tumor, *Voprosy onkologii*, 1993, vol. 39, no. 4–6, pp. 153–161. (in Russian)
38. Hatanaka H. Boron-neutron capture therapy for tumors, *Glioma*, 1991, pp. 233–249.
39. Wilson R. R. Radiological use of fast protons, *Radiology*, 1946, vol. 47, no. 5, pp. 487–491.
40. Kamada T., Tsujii H., Blakely E.A., Debus J., De Neve W., Durante M., Jäkel O., Mayer R., Orecchia R., Pötter R., Vatnitsky S., Chu W.T. Carbon ion radiotherapy in Japan: an assessment of 20 years of clinical experience, *Lancet Oncol.*, 2015, vol. 16, no. 2, pp. e93-e100.
41. Kaprin A.D., Alekseev B.Ya., Boiko A.V., Droshneva I.V. P.A. Herzen Moscow oncology institute: of XX century – in the XXI century, *Luchevaya diagnostika i terapiya*, 2013, no. 3, pp. 6-11. (in Russian)
42. *50 let deyatel'nosti tsentral'nogo nauchno-issledovatel'skogo rentgenoradiologicheskogo instituta MZ SSSR* [50 years of activities of the Central Scientific Research Roentgenoradiological Institute of the MH USSR], by K.B. Tikhonov as ed. Leningrad, 1970. 66 p.
43. *80 let Rossiyskomu nauchnomu tsentru rentgenoradiologii Minzdrava RF* [80 years of the Russian Scientific Center of Roentgeno-Radiology, MH RF]. by V.N. Kharchenko and N.I. Rozhkova as eds. Moscow, 2004. 323 p.
44. *«N.N. Petrov National Medical Research Centre of Oncology» Ministry of public health of Russian Federation. About centre.* [site]. Available at: https://www.niioncologii.ru/institute (Date of access: 22 May 2018)
45. *«N.N.Blokhin Russian Cancer Research Center» of the Ministry of Health of the Russian Federation. About center.* [site]. Available at: http://www.ronc.ru/ (Date of access: 22 May 2018)
46. Monzul G.D., Gladilina I.A. The use of protons in oncology (35-Year Practice of N.N. Blokhin Cancer Research Centre), *Radiatsionnaia biologiia, radioecologiia*. 2005, vol. 45, no. 6, pp. 670–674. (in Russian)
47. Tarutin I.G. My friends – medical physicists, *Meditsinskaya fizika*, 2016, no. 1, pp. 97–117. (In Russian)
48. *Gosudarstvennoye Uchrezhdeniye Meditsinskiy Radiologicheskiy Nauchnyy Tsentr Rossiyskoy Akademii Meditsinskikh Nauk* [Medical Radiological Research Center of the Russian Academy of Medical Sciences]. Obninsk, MRRC RAMS Publ., 2008. 33 p. (in Russian)
49. Zedgenidze G.A. *Ternistyy put' v nauku (avtobiograficheskiye ocherki)* [The thorny way to the science (autobiographical sketches)]. Obninsk, NIIMR Publ., 1992. 282 p. (in Russian)
50. Kaprin A.D., Galkin V.N., Zhavoronkov L.P., Ivanov V.K., Ivanov S.A., Romanko Yu.S. Synthesis of basic and applied research is the basis of obtaining high-quality findings and translating them into clinical practice, *Radiatsiya i risk*, 2017, vol. 26, no. 2, pp. 26–40. (In Russian)

36. Catterall M., Bewley D. Fast neutrons in the treatment of cancer. – London: Academic Press and New York: Grune and Stratton, 1979. – P. 39.
37. Мардынский Ю.С., Гулидов И.А. Нейтроны в дистанционной лучевой терапии злокачественных новообразований // Вопросы онкологии. – 1993. – Т. 39, № 4–6. – С. 153–161.
38. Hatanaka H. Boron-neutron capture therapy for tumors // Glioma. – 1991. – P. 233–249.
39. Wilson R.R. Radiological use of fast protons // Radiology. – 1946. – Vol. 47, No. 5. – P. 487–491.
40. Kamada T., Tsujii H., Blakely E.A. et al. Carbon ion radiotherapy in Japan: an assessment of 20 years of clinical experience // Lancet Oncol. – 2015. – Vol. 16, No. 2. – P. e93-e100.
41. Каприн А.Д., Алексеев Б.Я., Бойко А.В., Дрошнева И.В. Московский научно-исследовательский онкологический институт им. П.А. Герцена: Из XX века – в век XXI // Лучевая диагностика и терапия. – 2013. – № 3. – С. 6–11.
42. 50 лет деятельности Центрального научно-исследовательского рентгенорадиологического института МЗ СССР / Под ред. К.Б. Тихонова. – Ленинград, 1970. – 66 с.
43. 80 лет Российскому научному центру рентгенорадиологии Минздрава РФ / Под ред. В.Н. Харченко, Н.И. Рожковой. – М., 2004. – 323 с.
44. Федеральное государственное бюджетное учреждение "Национальный медицинский исследовательский центр онкологии имени Н.Н. Петрова" Министерства здравоохранения Российской Федерации (ФГБУ "НМИЦ онкологии им. Н.Н Петрова" Минздрава России). О Центре: [сайт]. URL: https://www.niioncologii.ru/institute (дата обращения: 22.05.2018)
45. Федеральное государственное бюджетное учреждение «Национальный медицинский исследовательский центр онкологии им. Н.Н. Блохина» Министерства здравоохранения Российской Федерации (ФГБУ «НМИЦ онкологии им. Н.Н. Блохина» Минздрава России). О Центре: [сайт]. URL: http://www.ronc.ru/ (дата обращения: 22.05.2018)
46. Монзуль Г.Д., Гладилина И.А. Использование протонов в онкологии (35-летний клинический опыт ГУ РОНЦ им. Н.Н. Блохина РАМН) // Радиационная биология. Радиоэкология. – 2005. – Т. 45, № 6. – С. 670–674.
47. Тарутин И.Г. Мои друзья – медицинские физики // Медицинская физика. – 2016. – № 1. – С. 97–117.
48. Государственное учреждение медицинский радиологический научный центр Российской Академии медицинских наук. – Обнинск: МРНЦ РАМН, 2008. – 33 с.
49. Зедгенидзе Г.А. Тернистый путь в науку (автобиографические очерки). – Обнинск: НИИМР, 1992. – 282 с.
50. Каприн А.Д., Галкин В.Н., Жаворонков Л.П. и др. Синтез фундаментальных и прикладных исследований – основа обеспечения высокого уровня научных результатов и внедрения их в медицинскую практику // Радиация и риск. – 2017. – Т. 26, № 2. – С. 26–40.